12-2004

Oxidation of Titanium in Alpha-Calf Serum Solution

Ali Stait Ismailoglu
Western Michigan University

OXIDATION OF TITANIUM IN ALPHA-CALF SERUM SOLUTION

by

Ali Sait Ismailoglu

A Thesis
Submitted to the
Faculty of The Graduate College
in partial fulfillment of the
requirements for the
Degree of Master of Science
Department of Materials Science and Engineering

Western Michigan University
Kalamazoo, Michigan
December 2004

ACKNOWLEDGMENTS

First and foremost, I would like to acknowledge Dr. Pnina Ari-Gur, my professor at Western Michigan University. She has been both my counselor and mentor during my enrollment at the University. Without her help and knowledge it would have been impossible to accomplish the goals I have achieved.

Secondly, I would like to thank Panjian Li, PhD for giving me the privilege and opportunity to work at DePuy Orthopedics with him. Further, I would like to thank Xiofian Yang, PhD, a great scientist, for spending her precious time with me. She taught me most of what I learned while at DePuy. Her teachings played the biggest role in my learning how to use the lab and how best to apply this knowledge. Also I would like to thank other key people who helped me throughout my thesis, Kai Sun, PhD. who showed me how to use the XPS. Also I would like to thank to Dr. John B. Miller for spending time with me in analyzing my results and answering my questions. And to my cousin Osman Yilmaz, who spent long hours with me while at the XPS lab. Also I would like to thank to my uncle, Dr. Mehmet B. Ismailoglu for everything that he did for me.

At last I would like to thank my graduate committee members for spending their precious time in reading my thesis and giving remarkable comments. Finally, I would like to extend my appreciation to all the support staff and other individuals who helped me during the period of my thesis.

Ali Sait Ismailoglu

OXIDATION OF TITANIUM IN ALPHA-CALF SERUM SOLUTION

Ali Sait Ismailoglu, M.S.

Western Michigan University, 2004

Titanium and its alloys have been used extensively in orthopedic implants mainly because of its excellent biocompatibility. This biocompatibility is attributed to its surface oxide film (3-7 nm thickness) that forms immediately upon exposure of titanium to air. In the research, the oxidation of Ti-6Al-4V in alpha-calf serum solution was studied. Four different immersion times were tested. Characterization of surface topography and its chemical composition was examined using Atomic force microscopy (AFM), Fourier transform-infrared radiation (FT-IR), and X-ray photoelectron spectroscopy (XPS). The *AFM* results clearly show the gradual change that occurred in the samples topography which is associated with more-rounded surface topography that is caused by the hydration of titanium surfaces. Finally, after three months in the serum solution, hydrated titanium oxide surface is visible. *XPS* results, for the as-polished sample after thirty seconds of surface sputtering, shows TiO_2 and Ti_2O_3 through out of its surface. With the increased immersion time, surface is predominantly composed of TiO_2 and sub-oxides of Ti_2O_3 and TiO which is associated with the further oxidation of Ti_2O_3 to TiO_2. As a result, XPS results showed that, immersion of Ti-6Al-4V in alpha calf serum solution changes the topography of the surface and the oxidation level of titanium.

TABLE OF CONTENTS

LIST OF TABLES

LIST OF FIGURES

CHAPTER I

INTRODUCTION

Biocompatibility

The aim of an implant material is to replace a part of the body. In order to be an implant material, all implant materials should show satisfactory mechanical, chemical and physical properties [1]. For example, most of the materials that are used as medical devices have to be biocompatible. Biocompatibility is the property of an implant material, where it performs this ability in the host tissue, for an acceptable period of time without causing any side effects [1, 2]. Therefore materials that are being used as a biomaterial have to biocompatible. Depending on the application of the material, there are some degrees of biocompatibility (for example required biocompatibility of an orthopedic implant is different than the temporary skin contacts). Therefore because of the importance of this issue, there are many regulations and rules for acceptable biocompatibility, which come from ISO standards of 10993-1 and all the biomaterial manufacturers should meet the minimum requirements that are listed by ISO, FDA, MDA and other standard organizations [2-4]. For example, the United Kingdom Medical Device Agency (MDA) provides assistance to medical device manufacturers by issuing rules on the acceptability of medical devices and their required biocompatibility [2, 4].

Material properties that are related to biocompatibility should include chemical inertness, lack of toxicity and adhesion [2, 3]. Table 1 represents the series of tests for medical devices according to ISO-10993-1, for example the test for "*local effects after implantation*" is for observing the foreign body reactions. After

implantation for one month, if the implant material is protected in a tough, thin surface layer, then it can be concluded that the implant material is biocompatible [3].

Table 1. Evaluation of Medical Devices According to ISO 10993-1, reference [3]

- Interaction with blood
- Tests for carcinogenicity
- Degradation of materials
- Reproductive toxicity
- Local effects after implantation
- Systemic toxicity

The surface properties of the implant material are important for biocompatibility, and its surface properties can be different from the bulk material's properties. This is significant because the biological environment is in contact with the material's surface. Of course, the bulk properties are important for the functioning of the material; for example, in titanium-based orthopedic implants low modulus of elasticity, strength-to-weight ratio, fatigue strength and the toughness of the implant are important [1, 5-7].

Corrosion of Implant Materials

Corrosion is the degradation of metals and their alloys by chemical reactions with their surrounding environments which starts on the surface of the material [2, 3, 6]. These environments can be strong acids or alkalis. Titanium and its alloys belong to a group of metals which form a passivated oxide surface layer, in a similar way to stainless steel, aluminum alloys, and cobalt- and nickel-based alloys. In this group of metals, titanium has a special place due its corrosion resistivity property and depending on the corrosive environment titanium either can get corroded very fast or very slowly [3, 6]. For example titanium is very corrosion resistive in nitric acid solutions; on the other hand it can get corroded in hydrofluoric acid spontaneously [3]. Every material has a different corrosion resistivity in different environments [3]. Therefore, regarding to materials chemical composition such as alloying elements, impurities or surrounding environments properties (pH of the solution, temperature, chloride concentration) or surface conditions of the material will determine the corrosion resistivity properties [3, 6].

The corrosion process in metal-aqueous solutions can happen in two ways which starts on surface of material. First one is called uniform corrosion, where the corrosion takes place uniformly on surface. Second one is called localized corrosion where corrosion happens locally and acts into the depth of the surface [6]. These corrosion effects in aqueous solutions are based on two conditions which happens either under aerobic conditions or anaerobic conditions. Under aerobic condition oxygen is the oxidizing compound where metal oxides and hydrated oxides can be formed; and this reaction happens in physiological environments. In anaerobic

condition water is the oxidative media. Under this condition metal oxides and hydroxides can be formed [3, 6].

While maintaining the desired bulk properties of a material, modifying the surface properties of an implant material by surface treatment methods can be a way of increasing the corrosion resistivity of implant materials [2]. Also another reason for applied surface modification is either to protect the implant material from damages that can be caused by the host or to protect the host from getting damaged by the implant material [2]. Secondly surface treatment methods can be applied in order to increase the corrosion resistivity of implant material. There are many different surface treatments, the selection of which depends on the application. These surface treatment methods can be ion implantation, plating, coating, deposition techniques or heat treatment [2, 3]. As a conclusion selection of the implant material and surface treatments play a key role in preventing the corrosion of the material, because by applying the appropriate material it is possible to protect and to prevent the corrosion of the implant material [2, 3].

Bioacceptability of Implant Materials

Bioacceptability is the effect of the organism on the implant material such as tissue regeneration, bone formation on the implants surface [8]. Bioacceptability and biocompatibility properties of implant materials are achieved or increased by surface modification techniques. One of the most common surface modification technique is surface coatings such as hydroxyapatite (HA) coatings on orthopedic implants [3]. These hydroxyapatite coatings have received great attention due to their bioactivity

and increased bone formation around the implant material [9-11]. The formation of bone-like apatite layer on implant materials is necessary, for example by coating the implant materials with certain coatings it is possible to increase and improve the bioacceptability of the implant material [12, 13]. Therefore, coatings on implant materials surfaces are essential, because it is possible to optimize the surface properties by increasing and improving the bioacceptability of the implant material as well as shorten the time period of bone formation on implant surfaces [12-15].

Properties and Applications of Titanium as a Biomaterial

Titanium and its alloys are well-known and important biomaterials, which have been successfully used in the fabrication of dental and orthopedic implants [3, 16, 17]. The success of titanium which is being used in orthopedic and dental field is due to their high biocompatibility and corrosion resistance in the biological environments [3, 18-20]. Also the bulk properties of titanium and its alloys such as low elastic modulus, high tensile strength and low weight properties make titanium suitable material as an implant material [1-3, 5-7].

The biocompatibility of titanium is due to its surface oxides which are spontaneously formed in air and which has a thickness of 3-10nm [21-23]. This air-formed oxide layer is dense and stable, which results in the high corrosion resistance of titanium [3, 21-23] as a result when titanium is inserted into body this dense oxide layer allows a good corrosion resistance of the implant material which stops the interactions of the implant material's surface with the environment by releasing metal ions and compounds [24]. For example, the corrosion-resistant oxide film of titanium

is similar to high grade 316 stainless steel commonly used as an implant material. However stainless steel shows higher reactivity than titanium in the host after implantation and sometimes implants made from 316 stainless steel fails due to corrosion and ferreting fatigue [25, 26]. The surface morphology, roughness and composition of the oxide layer will play an important role for biocompatibility of the titanium implants [23, 24, 27, 28].

It can be said that material selection is a key role in biomaterials, and in order for a material to be considered as a useful biomaterial it must [8, 29]:

- Show minimum change in the host tissue, bone and fluid environment due to chemical reactions that may occur between the implant material and the surrounding environment.
- Show minimum wear, tear and dimensional shape change in the host body.
- Posses the required mechanical properties.
- Be able to be sterilized.

Hypothesis

Immersion of Ti-6Al-4V polished disks in α-calf serum solution at a controlled temperature, 37^0C, and a controlled pH, 7.2, may cause the oxidation and the hydration of the surfaces which may change the surface chemistry.

In order to investigate and see this change and to prove this prediction, for each sample AFM, FT-IR and XPS analysis were done. During the experiments, samples were immersed into α–calf serum solution for different time periods. Also an as-polished sample was kept in order to compare with the immersed samples.

CHAPTER II

LITERATURE REVIEW

Titanium and Its Alloys

Titanium was discovered in the beginning of the 18th century [30]. Until the second half of the 20th century, it was not widely used [30]. It has been approximately fifty years since titanium and its alloys became widely used in the industry [30].

Titanium is the ninth most common element on the earth's crusts [3]. It became popular for the military applications of aircrafts and gas turbine engines in the second half of the 20th century because titanium is light, strong and corrosion resistant [5, 31] . For example because of the good anti-corrosive properties titanium is suitable for use in aggressive environments such as in heat-exchangers, food and chemical processing and as a biomaterial [31]. Also titanium and its alloys are widely being used in golf clubs, bicycles and automotive industry which is due to its low density and relative strength advantages over other candidate materials [2, 3, 5].

There are many reasons why titanium is widely being used in the today's industry, first of all the density of titanium is approximately 60% of steel and nickel based super alloys, which is a great advantage where weight reduction is needed [30]. Titanium's strength to weight ratio is greater than the any other structural metal [30]. Also titanium is available in a wide variety of types and it can be cast, forged and wrought [30]. Also, because of being a biocompatible material, and due to its corrosion resistance, titanium and its alloys are widely being used in the orthopedic and dental fields [1, 32-34]. The corrosion of an implant material is related to ion

release from the material into the biological environment [35]. With increased corrosion resistance, this ion release is minimized (an example of this is given further in the text) [35]. When titanium and its alloys are compared to stainless steel, cobalt-nickel-chromium or to cobalt-chromium-molybdenum alloys, titanium shows higher corrosion resistance (less foreign ion release) in corrosive environments [35], because of this cobalt-chromium alloys as an implant material is challenged by titanium and its alloys [22]. This corrosion resistivity of titanium is attributed to its protective surface oxide layer [21-23, 35, 36]. As a result, materials that are being used as biomaterials, such as, stainless steel, cobalt-chromium alloys and titanium alloys must have to be biocompatible, corrosion resistant and must be available when they are needed. Also biofunctionality, bioadhesion and processability properties of materials are important [6].

With the increased number of old people population, the need for more dependable materials for replacing broken or damaged parts of the human body is increasing too [35]. Therefore, there is a great need for materials that are chemically inert and that have adequate mechanical strength. Because of the reasons that were listed previously (biocompatibility, corrosion resistance and etc.) titanium is the choice of an implant material [1-3, 31-35]. Titanium and its alloys do not cause any allergic reactions within the host tissue, and also possesses no thrombotic reaction with the blood [35].

Chemistry and Structure of Titanium

Pure titanium has two crystalline structures (it is an allotropic element). One is body centered cubic (BCC); the other is hexagonal closed packed (HCP). The HCP structure is in equilibrium at room temperature and is also known as α *phase*. The BCC structure is stable at elevated temperatures and is known as β *phase* [37]. Titanium and its alloys are divided in to three classes according to the phases that are present in the microstructure, the α and the β structures are the basis for this group [35-37]. These alloys are α, α–β, β [30, 35–38].

By alloying elements that are listed in table 2, such as Al, V, Sn, Mo, Zr it is possible to manufacture different crystalline structures [30]. The crystal structure can be stabilized by alloying the titanium metal with certain elements; as a result, it is possible to intentionally create the so-called α, α–β and β alloys [22, 30, 35, 36]. The alloying elements for stabilizing α phase can be oxygen, tin and aluminum [20, 35]. Beta phase stabilizers include molybdenum, tantalum, iron, vanadium, niobium and chromium [30]. These alloying elements and their effect on the alloy properties are listed in table 2.

α (titanium) and α–β (Ti-6Al-4V) alloys are widely being used in the orthopedic and dental fields [5, 35, 39]. For example in skeletal devices, Ti-6Al-4V has a great advantage over pure titanium because of the better mechanical properties of Ti-6Al-4V [35], values for tensile strength and other mechanical properties are listed in table 3.

Table 2. Effects of Alloying Elements on Titanium, Adapted from [30]

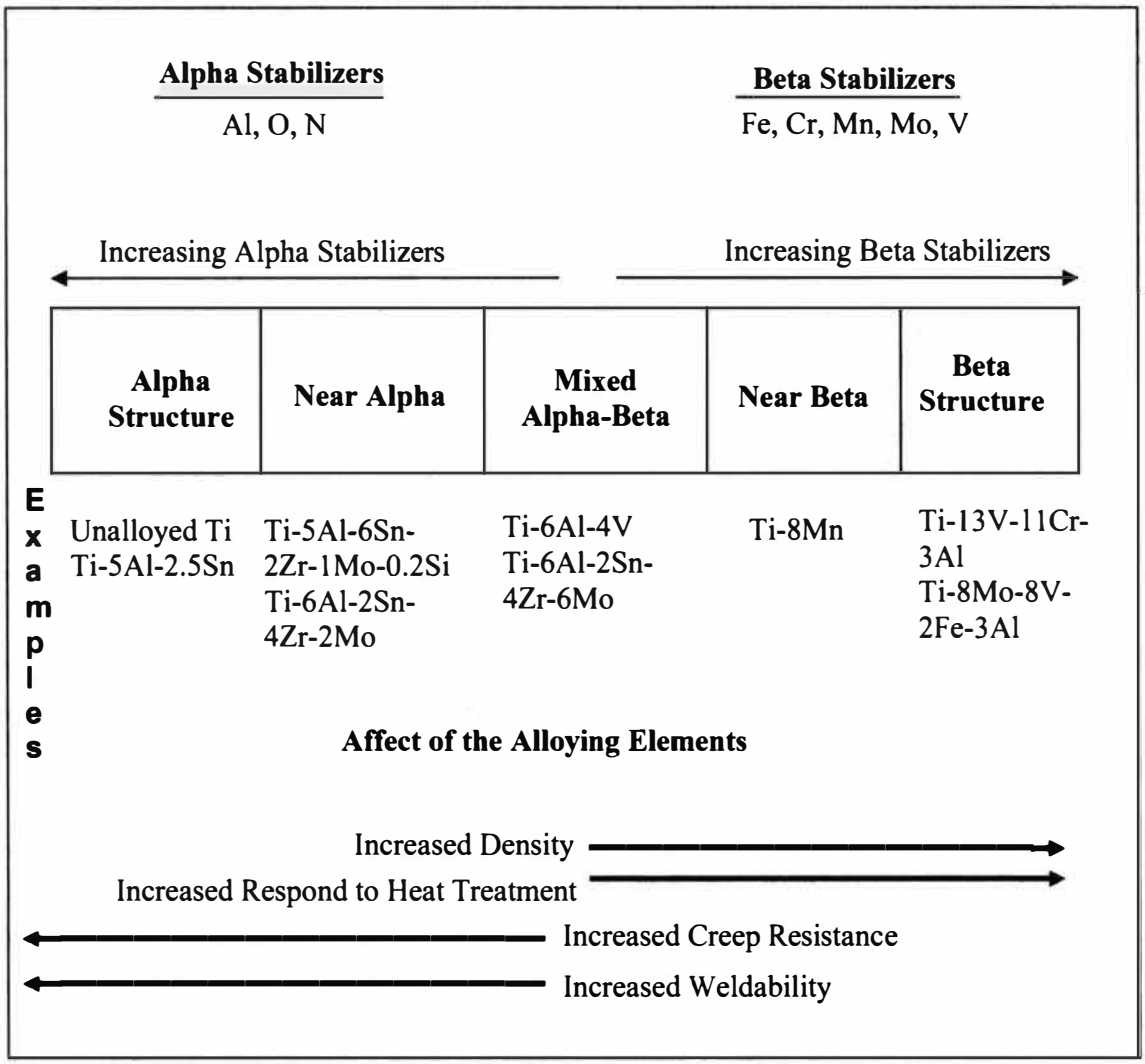

Alpha Titanium Alloys

At room temperature, these alloys have a hexagonal closed packed microstructure [37]. α titanium alloys are weldable and have very good creep resistance at elevated temperatures [30]. Because of their hexagonal closed packed crystalline structure they do not undergo a ductile-brittle transformation at low temperatures typical of BCC alloys [28], this makes them attractive for use in

cryogenic applications [3]. These alloys are not heat treatable because they are stable single-phased alloys; therefore their mechanical properties cannot be improved by heat treatment [30]. With α stabilizing elements such as oxygen, tin and aluminum, at room temperature, it is possible for the α phase to keep its structure in the hexagonal closed packed state because these alloying elements are soluble in the HCP structure [22, 30, 35, 37].

Alpha-Beta Titanium Alloys

These alloys have the combination of alloying elements that are α–stabilizers and β–stabilizers where the properties and the characteristics of both structures are needed [30]. As a result, both HCP α phase and the BCC β phase can co-exist at room temperature [37]. The excellent combination of strength and ductility of α-β alloys are created by heat treatment which is due to the alteration of the amounts of α–β phases and the phase composition [37]. For example when aluminum and vanadium are added as an alloying element, this alloys tensile strength can be increased from 242MPa to 1000MPa [22, 30]. Also their good creep resistance under cyclic loadings makes them suitable in the applications of orthopedic implants [30].

Beta Titanium Alloys

Beta titanium alloys are metastable alloys [30]. For example, elevated temperatures or cold working at ambient temperatures can cause partial transformation of the β phase into α phase. This metastable characteristic of β alloys can produce special properties such as, increased cold formability, excellent

forgeability and increased hardness [30]. The major alloying elements such as, tantalum, niobium and molybdenum are considered to be biocompatible [30].

Table 3. Mechanical Properties of Titanium Implants, reference [30]

Grade Type	Metallurgical Condition	Tensile Strength MPa	Yield Strength MPa	Elongation %	Reduction in Area %	Hardness (Rockwell)
Ti CP-1	700^{0}C	241	172	24	30	70 HRB
Ti CP-4	700^{0}C	552	483	15	25	100 HRB
Ti-6Al-4V	700^{0}C	931	862	15	30	36 HRB
Ti-12Mo-6Zr-2Fe	760^{0}C	1000	965	15	40	33 HRB
Ti-15Mo-2.8Nb-0.2Si	800^{0}C	793	655	22	60	24 HRB

In table 3, the mechanical properties of selected titanium implants are characterized. As can be seen from the values in the table, the tensile strength of α phases can change from 241MPa to 552MPa; this is due to the addition of different alloying elements like aluminum, molybdenum. Also α–β alloys such as Ti-6Al-4V can exhibit a tensile strength up to 931MPa [30, 35].

Processing and Microstructure of Titanium and Its Alloys

The microstructure of a material plays an important role in determining the mechanical properties of titanium implants [3]. The microstructures are obtained by thermo-mechanical processes and heat treatment. This thermo-mechanical process will produce either a structure that has grains elongated in the working direction, or a dynamically-recrystallized equiaxed structures. The heat treatment applied structures will transform from elongated structure to an equiaxed structure [3]. The microstructures of titanium will depend on several criteria's such as, prior work, alloying elements, cooling temperature, cooling rate and several other factors [30]. Figure 1 represents different microstructures of titanium and its alloys. For example image c, shows the microstructure of equiaxed α after 1 hour annealing at 699^0C [30]. As a result with different types of processing methods, coarse and/or fine grain structures can be formed [30, 37]. For example, for the α–β alloys, the transformed β and retained β constituents can exist in different forms such equiaxed, acicular or both. The equiaxed structure is formed by deforming the material in the α–β state and heat-treating at low temperatures. The acicular structures are formed by deforming the material in the β phase or heat- treating above the β phase followed by quenching [30]. With these micro structural manipulations for acicular structures, it is possible to increase the fracture toughness and the creep properties. For equiaxed structures, higher strength, higher ductility, and increased formability can be achieved also low cyclic fatigue properties can be improved too [30].

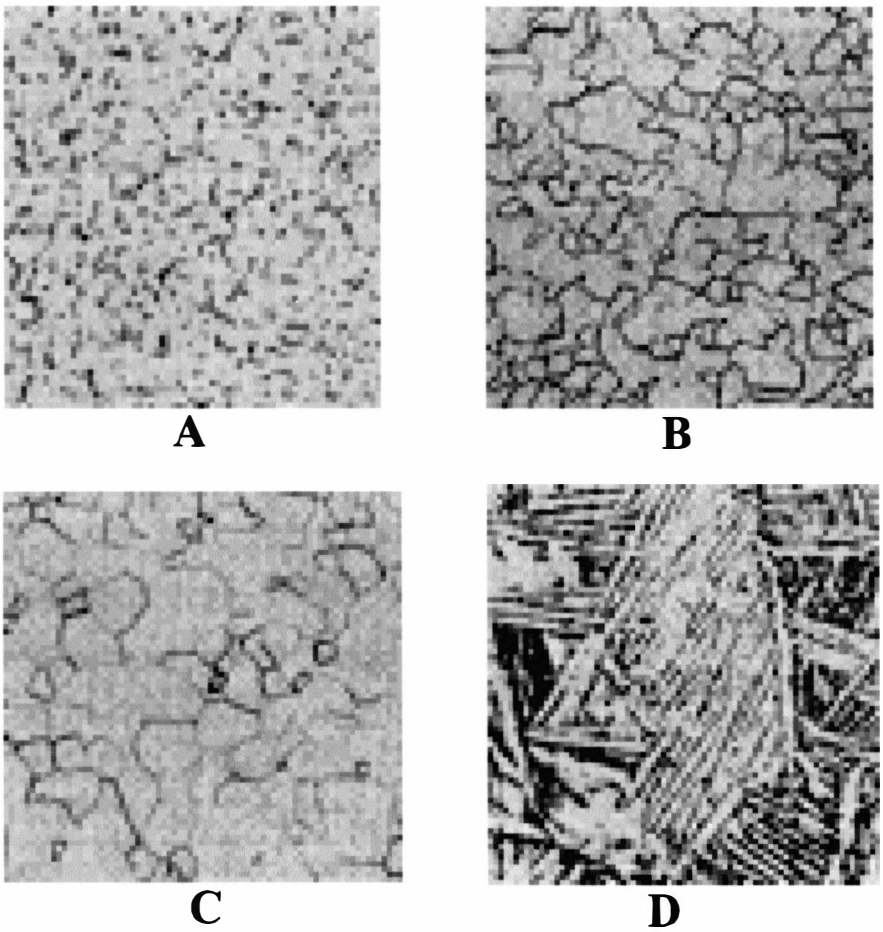

Figure 1. Microstructures of α, β and α–β Titanium Alloys, reference [30]. (a) Equiaxed α–β Structure. (b) Equiaxed β. (c) Equiaxed α Structure. (d) Acicular α–β Structure.

Properties of Ti-6Al-4V

Since the 1960s, the usage of titanium metal and its alloys as biomaterials have increased [20, 40]. Bothe *et al.* [40] used titanium implants in the femurs of cats. The major reasons for this increase is being biocompatible, having high corrosion resistance and better mechanical properties over other implantable materials [21-23, 25-26, 35]. Currently commercially pure titanium and Ti-6Al-4V have

successfully been applied in more complex applications such as shoulder prostheses, hip joints and dental implants [2, 3, 7, 32-34].

The use of CP titanium metal came first in the orthopedic industry and Ti-6Al-4V alloy followed it [19]. Ti-6Al-4V is a α–β alloy, which contains 6 wt% of aluminum and 4 wt% of vanadium [1, 5, 29, 32]. Ti-6Al-4V has higher yield strength, moderate ductility and ultimate tensile strength than the titanium metal [5]. Also Ti-6Al-4V has a better combination of mechanical properties compared to the other implant materials [5]. The comparison of the tensile strength of Ti-6Al-4V with other potential implant materials is represented in table 4.

Table 4. Tensile Strength of Ti-6Al-4V Compared to Other Potential Implant Materials, reference [2]

Material	Tensile Strength (MPa)
Ti-6Al-4V	895-1250
Titanium Alloys	240-1500
Stainless Steel	400-1500
Aluminum	70-700
Alloyed Steel	100-2300

The superior properties of this alloy are developed by refining the grains by cooling either from β region or from α–β region or by low temperature aging, or by decomposing martensite structure during quenching [30]. This process is illustrated in figure 2. When Ti-6Al-4V alloy is slowly cooled from the β phase, around 980^0C, α

phase starts to form. When this happens, it starts with the formation of α from the β phase in the shape of plates. These plates grow parallel to the {110} plane in the β phase. With slow cooling process, this α plate grows very rapidly along the plane, but it thickens very slowly on the perpendicular direction to this plane [30].

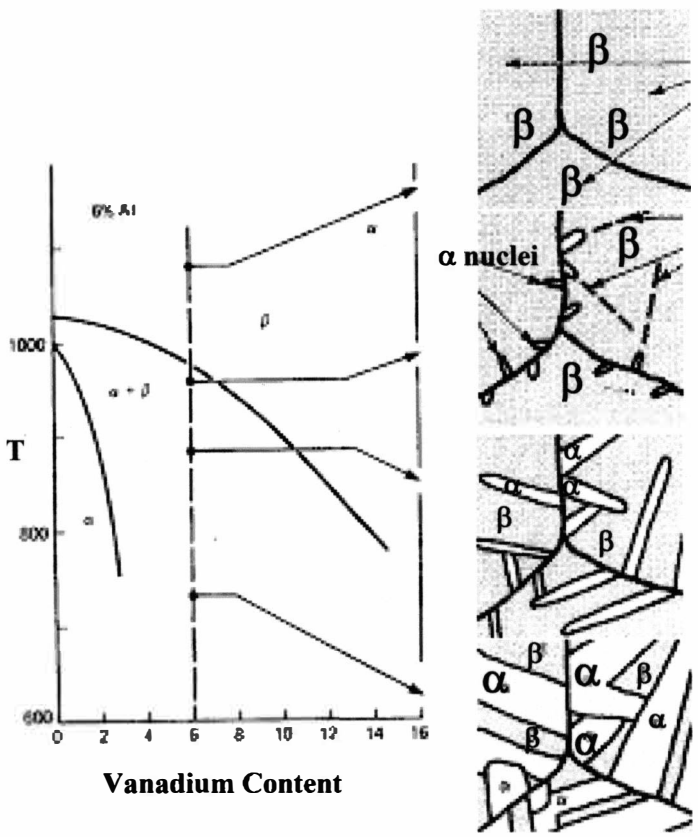

Figure 2. Schematic Development of Ti-6Al-4V Alloy, reference [30]

Surface Properties of Biomaterials

In biomaterials one of the major issue is how the implant material responses to the biological environment and how the biological environment responses to the implant, because the surface of the implant in the host tissue is directly in contact with the biological environment [41]. Therefore the surface of the implant material plays a key role in biocompatibility; because biocompatibility of biomaterials is achieved by the interactions between the surface of the material and the tissues with which it interacts [42-45]. For example when titanium implants are inserted into a biological environment first the implant material surface adsorbs ions and water molecules [3, 6, 41, 42, 46]. Then a protein layer is adsorbed on the implanted surface. After the adsorption of protein, the cells in the environment recognize the protein film and the host tissue interacts with this film [41, 42, 46]. Finally, according to the properties of the cell layers and the protein on the surface, a bone tissue is being structured [3, 6, 42, 43]. As result of this, the original surface property of the implant material plays an important role.

Need for Surface Processing for Biomaterials

There are a couple of different reasons why medical devices should be subjected to specific surface treatment methods, because the biological response between the host tissue and the implant material depends on the surface properties of the implant [22]. Variety of processing and manufacturing methods are being applied to implant materials, such as casting, forging, rolling and machining, the surface properties can change in a desired or undesired way. For example, in machining that

is used for cutting the material, the newly created surface is exposed to the atmosphere that will cause oxidation of the titanium. Also coolants and lubricants used in the machining process can cause or change the oxidation nature of the surface [3]. Manufactured surfaces can contain contaminants in the form of residues and/or particulates from processing agents. Therefore, with the traditional manufacturing methods, the surface of the titanium material can be contaminated and such a surface is not acceptable for medical applications. Because of these unwanted properties, additional surface treatments must be performed in order to achieve a uniform and acceptable surface finishing. Depending on the state of the original surface, contaminants, structural defects, undesired reaction films, deformed surface layers and residual stresses must be removed from the surface [2, 3, 17], because the surface morphology, roughness and composition surface determines the biocompatibility of the titanium implants [23, 24, 27, 28].

Oxidation of Titanium and Its Alloys

Biomaterials that are made from titanium and its alloys, possesses good biocompatibility when inserted into a biological environment, which is attributed to their corrosion resistive thin passive oxide film [42-44]. Because of titanium and its alloys wide range applications, titanium oxides are currently a research interest in the biomedical applications, and also these oxide surfaces are one of the best biocompatible surfaces in the applications of biomaterials [41, 47].

When titanium metal is exposed to an oxidizing environment, titanium metal surface nucleates oxide in few nanoseconds [23, 48]. Because the titanium oxides are

thermodynamically stable and the formation of the oxide has a very high negative Gibbs free energy, titanium can get oxidized very easily in oxidative media [2].

Generally the oxide layer that covers the titanium surface consists of the most stable titanium oxide, which is titanium dioxide (TiO_2) [41, 48-50] with oxidation state of the titanium is +4. There are other titanium oxides, which are TiO and Ti_2O_3 [47, 48, 50-52].

Table 5. Standard Free Gibbs Energies of Different Metals, Adapted from [53]

Metal	Most stable oxide	ΔG_0^{298} per mol of metal [kJ/mol]
Titanium	TiO_2	-888.8
Vanadium	V_2O_5	-1419.5
Aluminum	Al_2O_3	-1582.3
Zirconium	ZrO_2	-1042

TiO_2 can exist in three different crystalline forms; rutile, anatase and brookite structures or can be amorphous [50]. Anatase and rutile have tetragonal structures, anatase has a lattice parameter of $c/a>1$, on the other hand rutile has a lattice parameter of $c/a<1$ [51]. In rutile and anatase structures, titanium atoms are coordinated to six oxygen atoms and these crystalline phases can form at high temperature (above room temperature) [50]. The oxide surface which is formed at room temperature, is amorphous and as mentioned before has a thickness of 3-10nm [48, 50]. For instance, TiO_2 films prepared by atomic layer deposition technique,

below 160^{0}C amorphous oxide are being formed. Above 350^{0}C rutile structure and between 160-350^{0}C anatase structures can be formed [45, 54].

The thickness of this room- temperature grown oxide layer depends on the history of the sample and also is affected by the exposure time, temperature and the humidity of the environment [55]. Room temperature grown oxide layer grows very fast in a short time because of reasons explained earlier, but this growing rate slows down after a certain period of time because the interactions between the substrate and atmosphere stops [55] and this trend is illustrated in figure 3. For example McCafferty *et al.* [49], and several other researchers [51, 52] have reported that the oxide surface which is formed on titanium surface is primarily consists of titanium dioxide, and closer to the substrate, sub-layers of Ti_2O_3 and TiO are present. This is illustrated in figure 4.

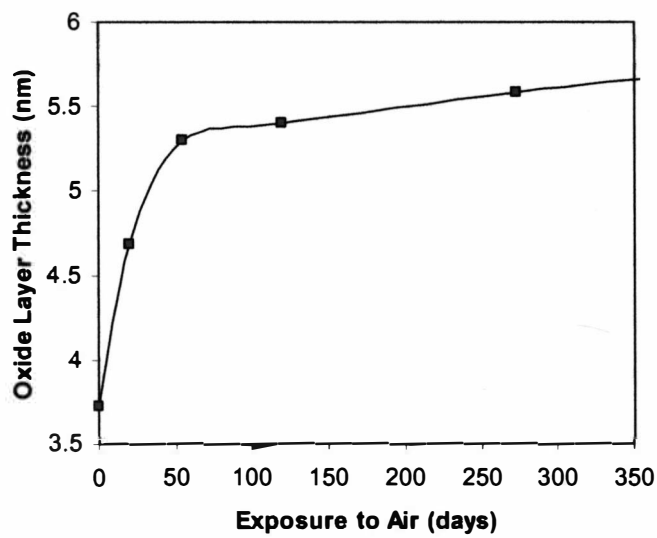

Figure 3. Growth of Room Temperature Formed Titanium Oxide Layer Dependence on Time, Adapted from [55]

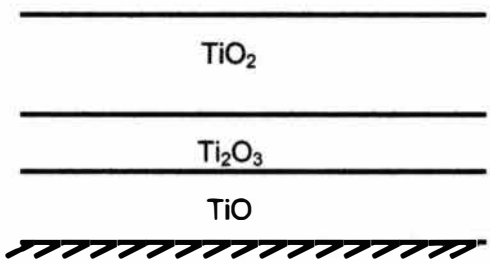

Figure 4. A Model of the Titanium Sub-Oxides Formed on Titanium, Adapted from [49]

According to figure 4, on the outer part of the oxide layer, is mainly composed of TiO_2. Deeper in the oxide layer sub-oxides of Ti_2O_3 and TiO are present. This data is from McCafferty *et al.* [49] and they report that for any time in the surface sputtering process, the oxide layer on titanium surface can be modeled by the layered structure [49] and the findings of this research proves this too.

For example, Lausmaa *et al.* [41] have reported that thermal treatment of room temperature grown oxide surface of titanium above 200^0C can change the microstructural properties of the oxide film and can increase the oxide thickness from few nanometers to 40 nanometers and they conclude that the thickness of the thermal oxides depends on time and temperature of oxidation. This relation is illustrated in figure 5. Also the thickening of the oxide surface increases the biocompatibility of implant by reducing ion release in to the environment, and Browne *et al.* [56] have reported that annealing Ti-6Al-4V alloy for 40 minutes at 400^0C reduces the titanium ion release from 0.14 to 0.03$\mu g/cm^3$.

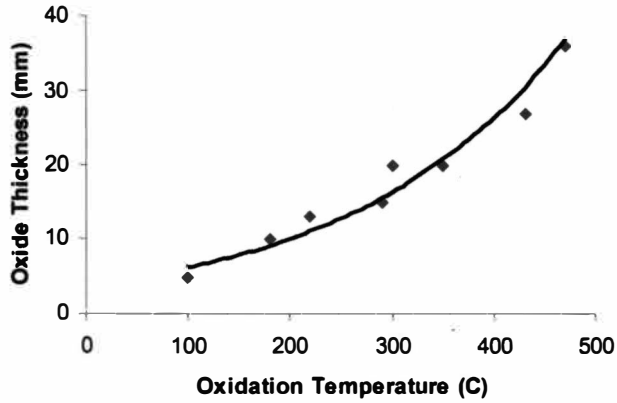

Figure 5. Oxide Thickness Change as a Function of Oxidation Temperature in air for 60 minutes, Adapted from [41]

Motte *et al.* [57] investigated oxidation of titanium and Ti-6Al-4V with water vapor, and they have reported that at low temperatures, below 950^0C, pure titanium gets oxidizes faster than Ti-6Al-4V alloy and this is due to existence of aluminum in the alloy. But above 950^0C oxidation rates of both metals are the same and they conclude that for both metal and alloy, at above 900^0C surface oxide mostly consist of rutile structure.

When titanium metal and its alloys are immersed in water or aqueous solutions, adsorption of hydroxide ions (OH^-) and H^+ ions will occur or it can be said that hydration of titanium oxide happens and oxygen from water act as electron traps that provide conductivity [58, 59]. With this conductivity, the electrostatic potential drops and with the resultant electric field, ion migration happens and will result in thickening of the oxide film [58, 59].

Titanium oxide surfaces in contact with aqueous solutions are highly hydroxylated and their surfaces are usually negatively charged. Bearinger *et al.* [59]

have studied the hydration of titanium surfaces under freely corroding and under potentiostatically held cathodic conditions and they report that hydrated titanium surfaces experiences oxide surface thickness and dome-like (swelled titanium oxide) hydrated oxide structures on surface of titanium with immersion in aqueous solutions. Another study on hydrated titanium oxides was done by Hawana *et al.* [61]. In their experiments they compared the oxidation and hydration of Ti-6Al-4V surfaces with water and Hanks' solution (is a solution that only contains inorganic ions, such as calcium, sodium, phosphate [42]). According to their results, immersion of Ti-6Al-4V alloy for 300 seconds in Hanks' solution will result in increased OH^- on the surface relative to samples immersed into water for 300 seconds. Also when titanium and its alloys are in contact with aqueous fluids Steinemann *et al.* [36] have reported that the growth of the oxide film is due to the oxygen diffusion through the oxide film to the titanium-metal interface and Tengvall *et al.* [62] showed that chemical reactions will occur on the titanium surface, such as enzymatically produced oxides (O^{-2}) and peroxides (H_2O_2). Lu *et al.* [63] have studied the oxidation of polycrystalline titanium with oxygen and water at -123 and 577^0C and they conclude that at -123^0C, oxygen can oxidize Ti to Ti^{+4}, Ti^{+3} and Ti^{+2}, on the other hand at the same temperature exposure to water will only produce Ti^{+2}. As a result oxidation is influenced by the samples temperature and oxidizing environment. As was previously mentioned, the major oxidation state of the air-formed oxide layer on titanium is +4, which corresponds to TiO_2. This oxidation state can be observed on Ti-6Al-4V alloy too, in air formed or in the simulated body fluids formed oxide layer. Ask *et al.* [5] and several other authors [52, 58] reported and from the results that

were obtained from tests performed in the current research, the aluminum in the Ti-6Al-4V alloy can also form an oxide in the form of Al_2O_3. The oxidation state of aluminum is +III.

Simulated Serum Environment

In order to investigate the oxidation of titanium in simulated environment, α-Calf Serum, which is a fraction of Bovine Serum, is used in the experiments of this thesis. Body fluids contain organic compounds such as serum albumin, amino acids, enzymes, fibrinogen and etc [64]. Also anions and cations are present, such as chloride, phosphate, sodium, potassium, calcium and other anions and cations [64]. Besides cations, anions and organic compounds, dissolved oxygen and carbon dioxide can be present [64]. Aragon *et al.* [64] reported that 316L stainless steel corrodes 176 times faster than Ti-6Al-4V alloy in isotonic solution at body temperature. Feng *et al.* [21] have reported that bovine serum albumin adsorbed on titanium surface increased the bioactivity of the implant and concludes that the amount of adsorption is related to the hydroxyl groups on the surface and depends on the surface energy of the implant. They report multiple carbon and oxygen species were present on titanium surfaces, which indicates protein adsorbed on titanium chemically instead of physically through the interactions of surface hydroxyl groups. Also they concluded that surface hydroxyl groups increases the reactivity of titanium with protein. Deligianni *et al.* [65] studied the protein adsorption of bovine serum albumin and fibronectin from single protein solution by XPS. They report that due to the existence of protein molecules on the surface, such as carbon singly bonded to nitrogen

(-C-N-), carbon doubly bonded to oxygen (-C=O-) and $-H_2-$ functional groups can be present.

Table 6 represents the biochemical assay of α-calf serum solution. As can be seen from the table, serum solution that is used in the experiment has a pH of 7.56 (which was measured during solution preparation too) and contains calcium, phosphate, protein, albumin and other constituents.

Table 6. Biochemical Assay of Alpha-Calf Serum Solution, reference [63]

Test	Value	Units
Gamma Globulin	0.1	% tp
Alkaline phosphates	176	mU/ml
Lactate dehydrogenase	3561	mU/ml
pH	7.56	
Total protein	4.6	gm%
Albumin	2.1	gm%
Total Bilirubin	0.5	mg/dl
Sodium	158	meq/L
Potassium	<1.0	meq/L
Calcium	<0.1	mg/dl
Chloride	137	meq/L

X-Ray Photoelectron Spectroscopy

Introduction

All materials interact with their surroundings through their surfaces, therefore the chemical and the physical compositions of the surfaces determine the interactions between the surface and the environment [67]. The surface chemistry of the materials will affect the corrosion resistance, adhesion property, wettability and other properties. Therefore surface properties can play an important role in the performance of materials [67]. X-ray photoelectron spectroscopy is very important technique, for surface characterization for the materials such as polymers, ceramics, metals, and so on [6].

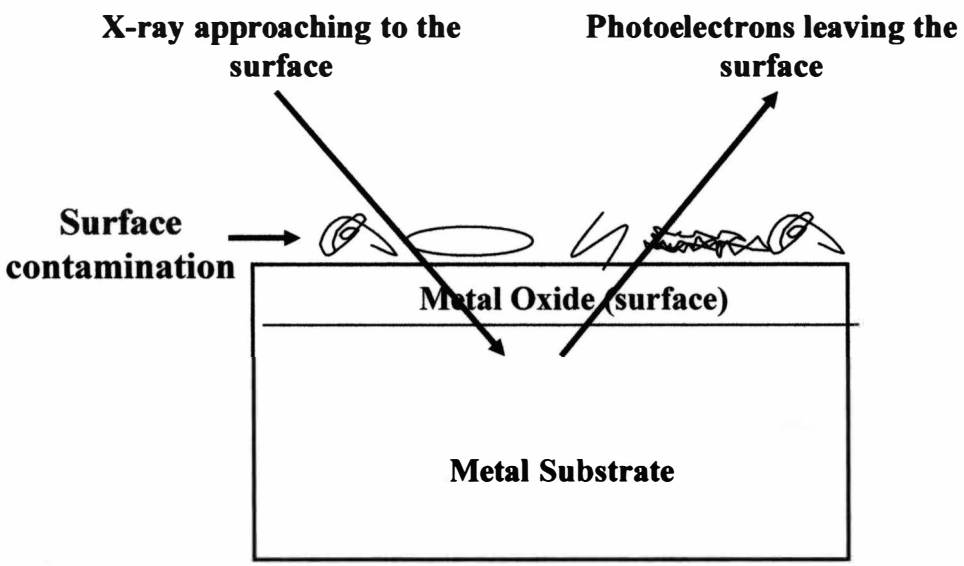

Figure 6. Schematic Representation of XPS Analysis on A Metal Substrate With the Oxide and Contamination Surfaces, Adapted from [3]

Photoelectron spectroscopy is a technique for surface characterization which has been widely being used to examine the chemical composition of solid surfaces [68]. Under ultra high vacuum (10^{-9}-10^{-8} Torr), the energy which is created by the photons (hυ) hitting the surface. As a result, energy is being absorbed by an electron with a binding energy of ''E_b'' where the electrons are ejected from the sample's surface with a kinetic energy of $\mathbf{E_k = h\upsilon - E_b - \phi}$, where "$\phi$" is the spectrometer's work function [67, 68]. This ejected electron will reserve its kinetic energy until it is detected by the electron detector. As a result, the energy distribution of photo-emitted electrons will be equal to the energy distribution of the electron states in the material's surface [67] and this is illustrated in figure 7. Also in order to irradiate the material's surface, two sources of anodes can be used. These anodes are usually Al and Mg (after monochromatization) with Kα energies of 1486.6eV and 1253.6eV respectively [67, 68].

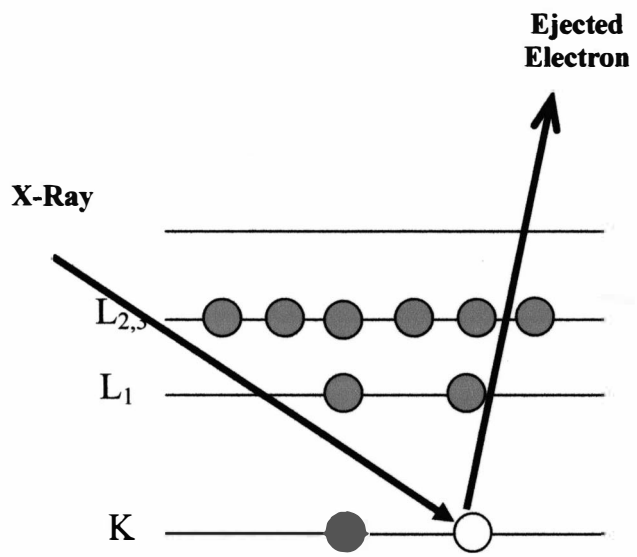

Figure 7. Schematic Representation of the XPS Process, Adapted from [67]

The X-ray Source

X-rays are generated by bombarding the anode target with high energy electrons [67] and the character of x-ray energy is determined by the x-ray source [68]. The quality of the X-ray emission from the anode is directly related to the electrons energy. For instance, if the electron's energy is increased from 4keV to 10keV, this will yield an increase of the photon flux, from an aluminum anode [67]. These high energy electrons are emitted from a thermal source, and this source is usually an electrically heated tungsten filament. In some cases where high current densities are required, lanthanum hexaboride emitters can be used [67, 69].

In the XPS analysis, the choice of the anode source is very critical. Without broadening the resultant spectrum the anode that is used must be able to excite an intense photoelectron peak from all the elements [67]. Anodes are usually supplied in a single X-ray gun with a twin-anode configuration, which allows separating the two overlapped radiations, such as Auger and photoelectron transitions [67, 68].

Table 7. Different Anode Materials for XPS, references [67, 68]

Element	Energy (eV)
Zr	151.4
Mg	1253.6
Al	1486.6
Ag	2984.4
Cr	5417.0

In table 7 several possible anodes with different energies are represented. In a twin mode arrangement any of these anodes can be used. By using higher energy anodes, it is possible to increase the analysis depth; this is because of the increased kinetic energy of the ejected photoelectrons [67]. And also another advantage is the ability to access energy levels which cannot be reached by lower energy anodes [67]. An example of an XPS instrument is shown in figure 8.

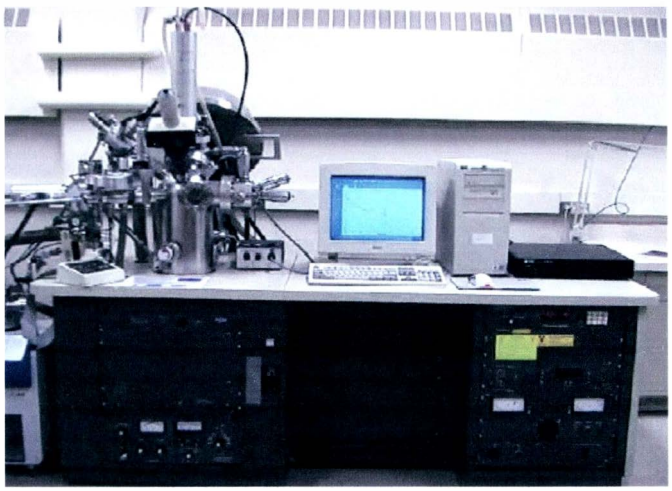

Figure 8. Image of PHI 5400, That was Used During the XPS Analysis, Image is Adapted from [70].

In conclusion, X-ray photoelectron spectroscopy is a sensitive surface characterization technique that has an information depth between 2 to 10nm. This information depth will depend on the angle of detection, anode that is used and also depends on the sample under examine [67, 68]. With depth profiling sample's surface can be etched up to several μm and with this instrument it is possible to detect chemical compositions of different element [67-69].

Atomic Force Microscopy

Introduction

In 450 BC, Greek philosophers Democritus and Leucippus introduced the concept of an atom [71]. Since that time, scientists and engineers have been trying to image and characterize individual atoms [71]. Atomic Force Microscopy (AFM) is a high resolution technique which is being used to study the surface topography of materials [72].

Scanning Tunneling Microscope (STM) was developed in 1982 by Binning, Rohrer, Gerber and Weibel at the laboratories of IBM in Zurich, Switzerland. Binning and Rohrer won the Nobel Prize in Physics for this invention [73, 74].

When the tip of the probe is very close to the surface, several different types of interactions can occur between the tip and atoms. One of these interactions, van der Waals forces, occurs when the tip of the probe is a few nanometers from the surface [71]. If an externally electrical potential is applied, electrostatic interactions will happen. The main difference between the two microscopes is that in STM the topography of the sample is imaged by electron conduction, but in AFM the topography and the morphology of the surface conducted by the mechanical forces

between the surface and the probe tip [71, 75].

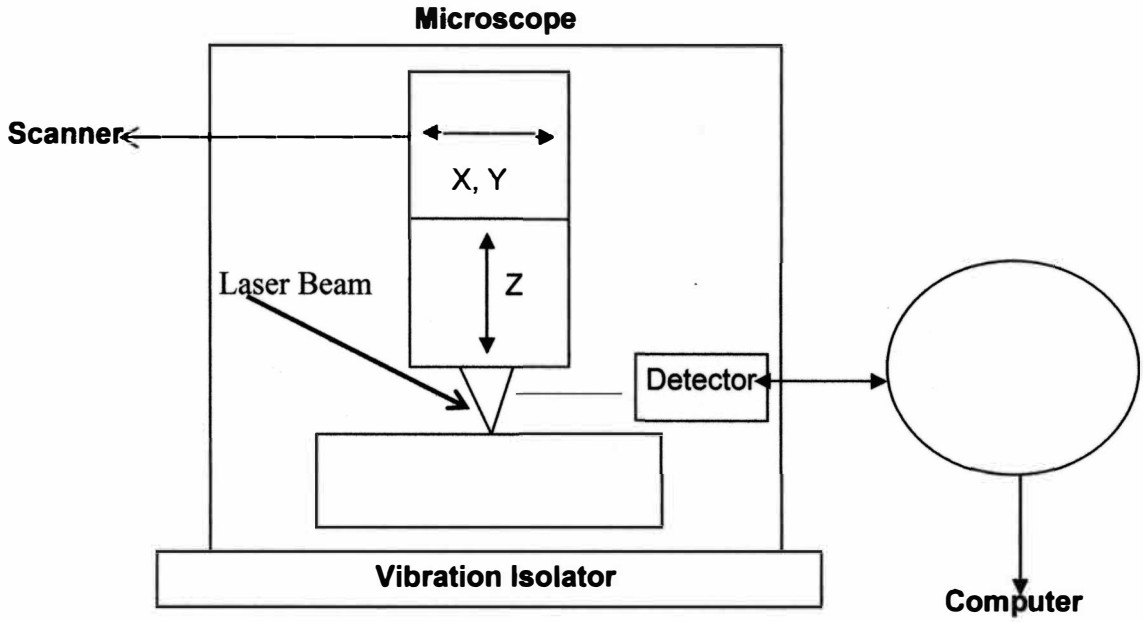

Figure 9. Schematic Representation of Scanning Probe Microscope Components, Adapted from [73]

Atomic force microscope is a very powerful instrument which is widely being used in surface science. And also it finds applications in the life and physical sciences and also in the nano technology applications [75].

Tapping Mode AFM

In this mode, the tip which is attached at the end of the oscillating cantilever scans the samples surface. This cantilever oscillates at or near its resonance frequency with amplitudes between 20nm to 100nm. During the scanning the tip taps the surface of the sample, and by maintaining constant oscillation amplitude and the interactions between the tip and surface, an image of the surface topography can be achieved. Also this mode can be achieved in the ambient and liquid environments [73].

Fourier Transform Infrared Spectrometer (FT-IR)

Introduction

Infrared spectroscopy measures the interactions between the infrared light and the matter [76]. Light is an electromagnetic radiation. As such it is composed two perpendicular waves -- magnetic and electric waves [76, 77]. The electric part of the light interacts with the molecules. Measurements obtained from infrared spectroscopy are called *infrared spectra*, which are measured infrared intensities versus wavelength of light [76].

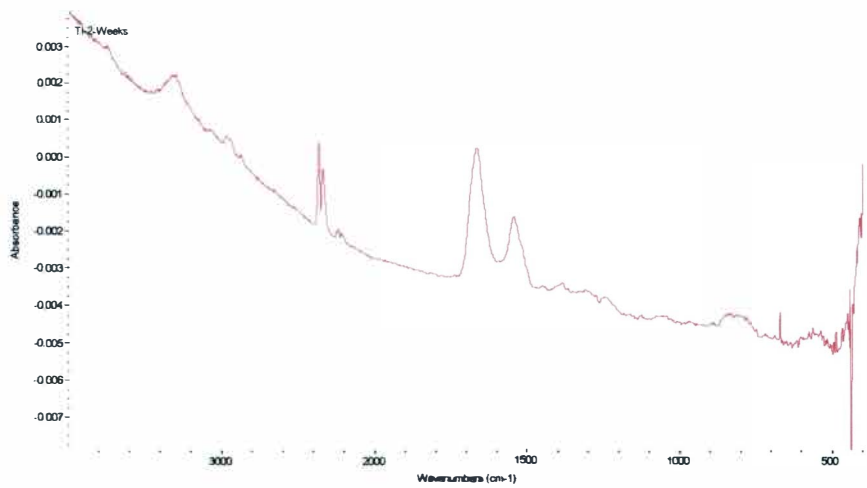

Figure 10. Representation of an Infrared Spectrum, From the Obtained Data From This Thesis

Infrared spectroscopy allows us to identify unknown chemical functional groups in a molecule, such as carbonyl group in acetone. Such functional groups sometimes show the same chemical properties from one molecule to another [76, 77]. These functional groups absorb the infrared radiation regardless of the structure of the rest of the molecule. Therefore, once the wave number of the bands of these

functional groups is known it is possible to classify the functional groups. And also the intensities of the peaks are proportional to the concentration of the molecule. Therefore infrared spectroscopy can be use to measure the concentrations. These properties of the infrared spectroscopy make it a very useful chemical analysis tool [76, 77].

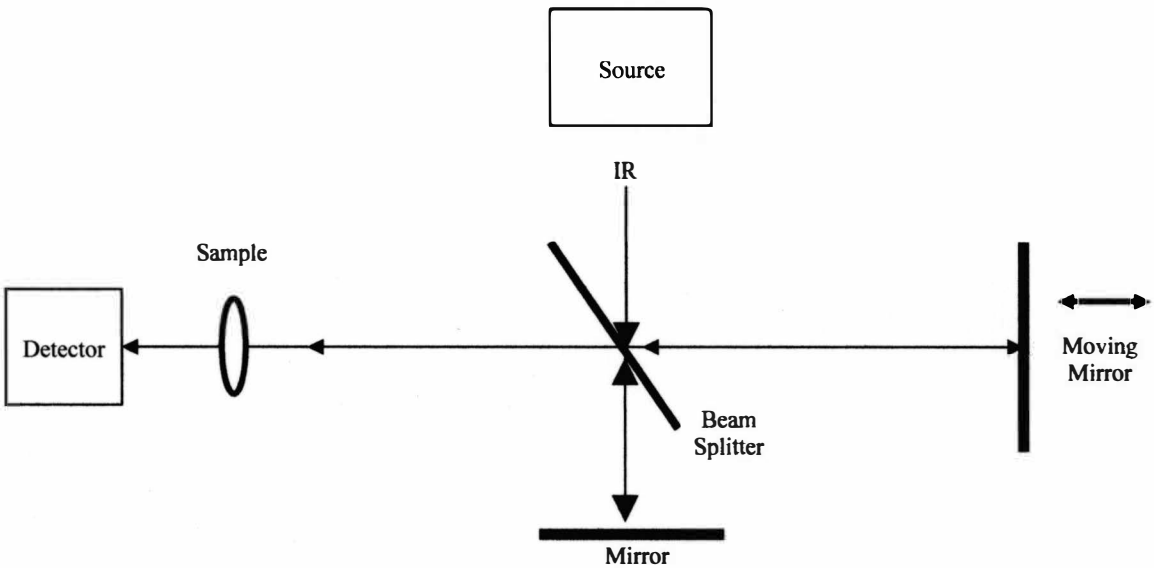

Figure 11. Schematic Representation of Infrared Spectrometer, Adapted from [77]

As a conclusion, FT-IR is an easy, sensitive and a fast technique for analyzing solids, liquids, gasses, polymers and powders. Although having advantages it can not identify samples that are containing individual atoms because they lack of chemical bonds [76, 77].

CHAPTER III

EXPERIMENT

Preparation of Ti-6Al-4V Disks

Ti-6Al-4V disk samples were provided by DePuy Orthopedics, Inc, Warsaw, IN. Sample and solution preparations, FT-IR and AFM tests were conducted at DePuy Orthopedic research and development laboratories. XPS tests were conducted at the University of Michigan's Electron Microbeam Analysis Laboratory (EMAL), Ann Arbor, MI.

Sample Preparation and Cleaning

Ti-6Al-4V pre-polished disks, with 16 mm diameter and 1.6 mm thick (samples are shown in figure 12), were ultrasonically cleaned with Liqui-Nox® detergent for 30 minutes. After this cleaning procedure, all samples were rinsed under running RO-Water to remove detergent residues. Then they were ultrasonically cleaned in alcohol for 30 minutes. After cleaning with alcohol, the disks were dried in air.

Alpha-Calf Serum Solution Preparation

To investigate the oxidation of Ti-6Al-4V samples in the simulated serum environment, one liter of Alpha-Calf serum solution was prepared. In the preparation procedure of the solution, 0.2g of sodium azide was added into the solution and mixed about 15 minutes to inhibit bacterial growth. After 15 minutes of mixing, according to solution preparation protocol, 0.174g of potassium phosphate, 0.3048g of magnesium chloride and 0.3676g of calcium chloride were also added to the solution. While adding calcium chloride to the solution, it was mixed with 2ml of 1N

hydrochloric acid, in order to avoid the precipitation of calcium chloride in the solution. During the preparation of the serum solution, the temperature was kept at 37^0C (± 0.01) and a pH of 7.2. When calcium chloride was mixed with HCl, the pH of the solution dropped to 6.8. Therefore, to return the pH at 7.2, approximately 2ml of sodium hydroxide was added to the serum solution. After treating the serum solution with these chemicals, the solution was mixed at these conditions about 20 minutes in a heating tank to maintain homogenous solution at 37^0C with a pH of 7.2.

Experimental Setup

After the solution preparation, four different immersion times were chosen:

2-Weeks

1-Month

2-Months

3-Months

Twelve cleaned Ti-6Al-4V disks were placed in different glass bottles with 50ml of the serum solution and 4 bottles were filled with the serum solution, only as a control group. Therefore, for each immersion time there were three samples, one sample for AFM, an other one for FT-IR and a third one for the XPS analysis, also one as-polished sample was kept as a baseline for comparison with the immersed samples to see the surface change. When the bottles were filled with the serum solution, all samples and the control bottles were kept in the CO_2 incubator at 37^0C (± 0.01) till the designated immersion times were over. During the experiment, every seven days these bottles were taken out from the incubator only for replenishing the

solution. Each time the serum solution was changed, the same solution preparation protocol was followed.

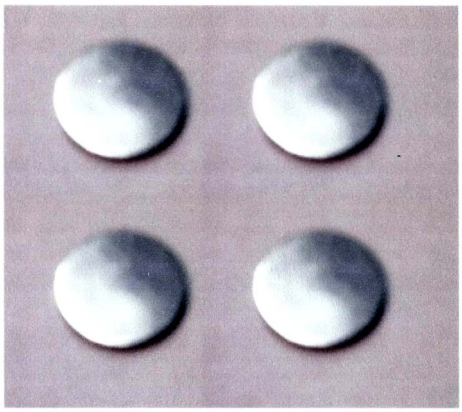

Figure 12. Photograph of Pre-Polished Ti-6Al-4V Samples Used For the Experiments

Sample Cleaning After the Serum Solution

When the designated immersion times were over, each sample was dipped in different beakers with RO-Water for 5 minutes and samples were dried at the room temperature. After cleaning, samples were ready for the AFM, FT-IR and XPS analyses.

Atomic Force Microscopy (AFM)

Atomic force microscopy was used to study the surface morphology. The AFM was Digital Instruments, model Dimension™ 3100 Series. AFM imaging for surface topography characterization was performed on Ti-Polished, Ti-2Weeks, Ti-1Month, Ti-2Months and Ti-3Months samples. AFM imaging was also performed on

the same samples after washing samples surfaces with BCA Total Protein Assaying. The AFM images were obtained with the Tapping Mode™ of the instrument at a scan rate of 2Hz and with 10μm, 5μm, 2μm and 1μm scans respectively.

In this thesis one of the major reasons for the AFM imaging was to compare the surface topography changes with the immersion time, comparing with the as-polish sample.

Fourier Transform Infrared Spectrometer (FT-IR)

Fourier Transform Infrared Spectroscopy (FT-IR) was used for surface characterization, was Nicolet, model number Magna-IR 550 Spectrometer Series II. FT-IR surface characterization was performed on Ti-2Weeks, Ti-1Month, Ti-2Months and Ti-3Months samples and compared with the scan obtained from the Ti-Polished sample. Also FT-IR characterization was done on the same samples after removing the adsorbed protein on the sample's surfaces. Every time, before acquiring data, the FT-IR bench was aligned according to the user's manual and samples were collected with 64 number of scans and with a resolution of 4. The data spacing was 1.928cm^{-1} and Happ-Genzel apodization was used.

X-ray Photoelectron Spectroscopy (XPS)

X-ray photoelectron spectroscopy (XPS) experiments were done at the University of Michigan's Electron Microbeam Analysis Laboratory (EMAL), image of the XPS instrument is shown in figure 8. As-Polished, Ti-2Weeks, Ti-1Month, Ti-

2Months and Ti-3Months samples were analyzed, to study the surface oxide changes with the immersion time, comparing with the As-polished sample.

The XPS was PHI 5400 with an X-ray source of Mg Kα, which has energy of 1253.6eV. The experimental conditions for the instrument are described in the table 8. Before introducing the samples into the analyzing chamber, silver paint was used as an adhesive between the sample and the holder, to prevent the charging of the surfaces.

The samples tested by XPS were first sputtered with an argon-ion beam to examine chemical changes below the surface (depth profiling). The ion gun conditions are listed in table 9. Sputtering time varied from thirty seconds to thirty minutes. All samples were first sputtered for 30 seconds, for surface cleaning purpose only. After this cleaning procedure, all sample's surfaces were further sputtered for 1 minute, 5 minutes, 10 minutes, 15 minutes, 20 minutes, 25 minutes and 30 minutes respectively. After each sputtering process, for every sample, the survey spectra were followed by a narrow scan acquisition for elemental peaks of interest.

Narrow energy scans were done for Ti 2p, Al 2p, O 1s, C 1s and V 2p levels, in order to see the correlation between oxygen, titanium, aluminum and vanadium. Carbon narrow energy scan were done to detect organic compounds on the surfaces.

Table 8. XPS Experimental Conditions, reference [70]

X-ray Source	Mg Kα (1253.6 eV)
Gun Power	300 Watts
Voltage	15 kv
Pass Energy	17.9 eV
Work Function	4 eV
Vacuum Pressure	10^{-8}-10^{-9} Torr
Step Size	0.1 eV

Table 9. Ion Gun Conditions, reference [70]

Ion Gun Beam Voltage	3000V
Gas	Argon gas
Emission Current	25mA
Sputter Area	8mm
Objective Focus	76%
Gun Pressure	15mPa

In order to see the chemical composition changes as a function of sputtering time, peak fitting was applied to Ti 2p, O 1s, and C 1s levels. Also for controlling the peak shifts, both C 1s and Ar 2p2/3 levels were taken as a reference [16, 17, 78].

BCA Total Protein Assay

BCA Protein Assaying is a detergent-compatible formulation, which is based on bicinchroninic acid (BCA) for the detection and analysis of total protein [79]. After immersion in the alpha-calf serum solution, Ti-2Weeks, Ti-1Month, Ti-2Months and Ti-3Months samples surfaces were dissolved with 2% of 5ml SDS solution. Each sample inserted in to a test tube with this amount of SDS solution. Each test tube then inserted into boiling water and samples surfaces were washed with this solution for approximately one hour. After this process, samples were kept overnight for examination the next day.

For the measurements of total protein amount BCA Total Protein Assay kit instructions were followed which is from Pierce Biotechnology Inc. [79].

For the standard sample preparation 2% of 5ml SDS solution was prepared and respectively 700, 400, 450, 400 and 400μL of SDS added to each microcentrifuge tube. Following this, 100μL of bovine serum albumin (BSA) was pipetted into the first standard sample (700μL) and from this solution other standard samples were diluted. The amount of dilution and final concentrations of each standard is given in table 10. Also another microcentrifuge tube was left blank, for control purpose. After preparing the standard solutions, 100μL of solutions from each tube were transferred to two sets of microcentrifuge tubes. Also 100μL of each sample solution were pipetted in to microcentrifuge tubes (2 replicates were prepared). After preparing each standard and sample solution, 500μL of Reagent 1 pipetted into each tube, vortexed and incubated at room temperature for 5 minutes.

Table 10. The Amount of Dilution and Final Concentration of Each Standard Sample, reference [79]

Vial	Vol. of Diluents	Vol. BSA	Final BSA Conc.
A	700 μL	100 μL of Stock	250 μg/mL
B	400 μL	400 μL of vial A dilution	125 μg/mL
C	450 μL	300 μL of vial B dilution	50 μg/mL
D	400 μL	400 μL of vial C dilution	25 μg/mL
E	400 μL	100 μL of vial D dilution	5 μg/mL
F	0	0	0 μg/mL

After this incubation 500μL of Reagent 2 was added into each tube and centrifuged at 10,000 g for 5 minutes. After centrifuging all microcentrifuge tubes, as much of the supernatants were poured off and a working reagent was prepared, which had 50 parts of BCA™ Reagent A and 1 part of BCA™ Reagent B. To each sample and standard tube 300μL of working reagent was pipetted and from each solution 225μL were taken and transferred to a 96-well microplate. Prior to readings from MicroPlate reader, samples were incubated at 60°C for 30 minutes. The major reason for this testing was to compare the surface topography change before and after immersion.

CHAPTER IV

RESULTS AND DISSCUSSIONS

X-ray Photoelectron Spectroscopy

Figure 13 shows the results of the as-polished sample (Ti-Polished) after 30 seconds of surface sputtering, which is approximately 0.1nm below the outer surface. The outer oxide layer which was formed on the surface had about 48% TiO_2, 46% Ti_2O_3, and 6% of TiO was found. These values are different from the more common oxide in the literature where TiO_2 is commonly reported as the major titanium oxide on titanium implant materials exposed to air. McCafferty *et al.* [49], Milosev *et al.* [52] and several other authors have reported that room-temperature formed native-oxide film on titanium contains mostly TiO_2, with sub-oxides of Ti_2O_3 and TiO. However Botha *et al.* [80] reported on titanium samples that were exposed to air and contained mostly Ti_2O_3. The formation of equal amounts of Ti_2O_3 and TiO_2 in our case is assumed to result from the sample oxidation in an environment short in oxygen supply when the titanium surface was being polished. No evidence of titanium metal was found after 30 seconds of surface sputtering.

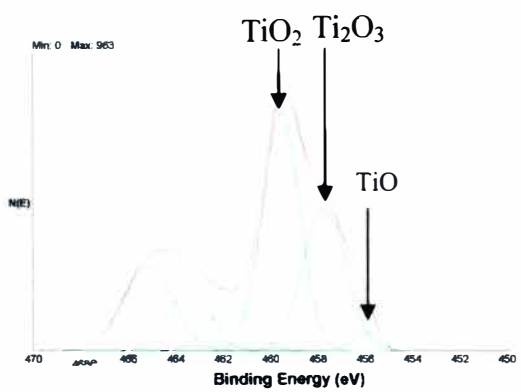

Figure 13. As-Polished Sample after 30 Seconds Sputtering, Ti 2p

The as-polished samples surface was sputtered up to 4 hours. After 30 minutes of surface sputtering process, the oxide concentration on the sample's surface did not show a significant change with comparison to that of 4 hours of sputtering. It was concluded that after 30 minutes of surface sputtering of the as-polished sample to the titanium metal surface was reached. The thickness of the oxide film on the as polished sample is assumed to be same in the literature, where it is said to be 6-7nm [21-23]. As a result every 1 minute 0.2nm of oxide layer was removed, and concluded that in 30 minutes approximately 6-7nm of oxide layer was removed. Even though XPS runs in ultra high vacuum, in one second it is possible for one monolayer of gas, which can be oxygen, to be adsorbed on the surface at 10^{-6} Torr [67], and oxygen is present in titanium bulk as an interstitial element too, therefore it is impossible to remove all the oxygen.

With increased sputtering time, the titanium metal peak becomes more dominant and oxide concentration of the as-polished sample on the surface drops. After 30 minutes of surface sputtering, where approximately 6-7nm of oxide layer is being removed, concentrations of TiO_2 and Ti_2O_3 drops to 34% and 28% respectively, on the other hand TiO concentration increases to 38%, which indicates that TiO is close to the interface metal-oxide, which was expected. Figure 14 represents the narrow scans that were obtained from as-polished sample for Ti 2p, O 1s, C 1s and Al 2p levels, after 30 seconds and after 30 minutes of sputtering its surface.

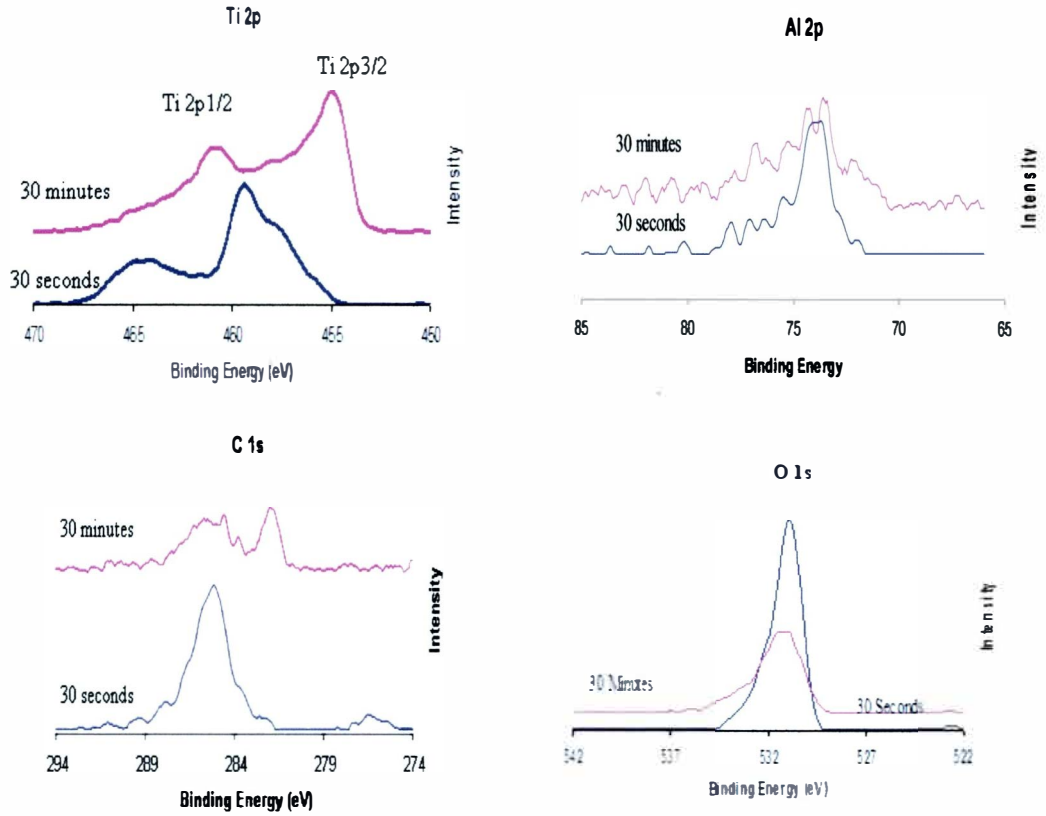

Figure 14. Comparison of the Ti 2p, O 1s, C 1s and Al 2p peaks for the As-Polished Sample, After 30 Seconds and 30 Minutes Sputtering the Surface.

As can be seen from Figure 14, as the surface oxide layer is being removed from the surface, the peak position of an air-formed oxide layer in titanium shifts from a higher binding energy, 459.4eV, to a lower binding energy, which is in agreement with the findings of Schniedgen *et al.* [58]. The peak position at 459.4eV represents the presence of the TiO_2. As the peak shifts from higher energy to lower energy, metallic titanium component becomes more evident, with peak position at 454.8eV.

Also aluminum was observed in the oxide surface. The peak position of Al_2O_3 is located at 73.87eV, and the metallic part of the aluminum is located at 72.3eV, the aluminum peak fitting is shown in figure 15.

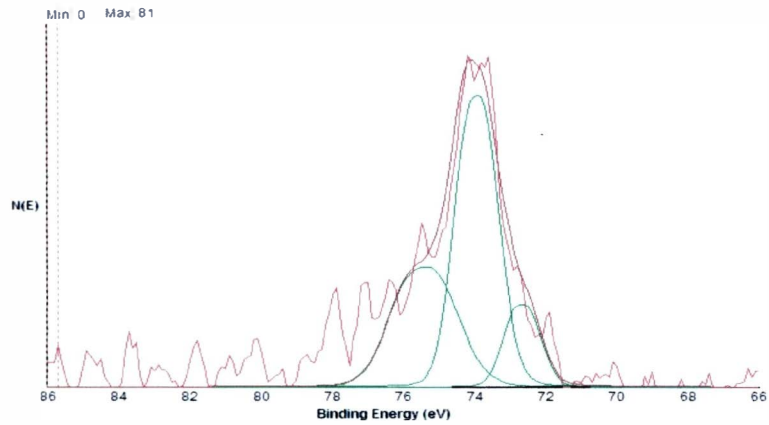

Figure 15. As-Polished Samples Al 2p Peak Fitting after 30 seconds Surface Sputtering

No evidence of vanadium oxide (V_2O_5) was found in the oxide layer, which indicates that vanadium did not complete its oxidation, which is in agreement with the findings of Milosev *et al.* [52] and Botha *et al.* [80].

For the same sample after 30 seconds of surface sputtering, predominantly O^{-2}, H_2O and OH^- groups existed on the surface (please refer to appendix B) and (OH^- species were verified by FT-IR too), with the binding energies of 530.7, 533.2 and 531.6eV respectively and these results are in agreement with Milosev *et al.* [52]. Binding energy of 530.7eV indicating the formation of TiO_2 on the surface. After 30 minutes of surface sputtering, the oxide concentration dropped from 55% to 30% where it is assumed that the oxide film on the as polished sample was removed and had a thickness of approximately 6-7nm, this trend is represented in the figure 16.

Carbon is always present on the surface of the as-polished sample, which can be due to a leakage in the chamber or environment conditions, and also in the bulk carbon is present as an interstitial impurity approximately 0.1% [80]. After 30 seconds of surface sputtering (for cleaning purpose), C-C, C-O and C=O species are present at binding energies of 285, 286.4 and 288.3eV respectively which is in agreement with McCafferty *et al.* [49]. After 30 minutes of surface sputtering, most of the carbon species were sputtered away, and at a binding energy of 281.8eV, titanium carbide peak became more dominant which is shown in figure 17.

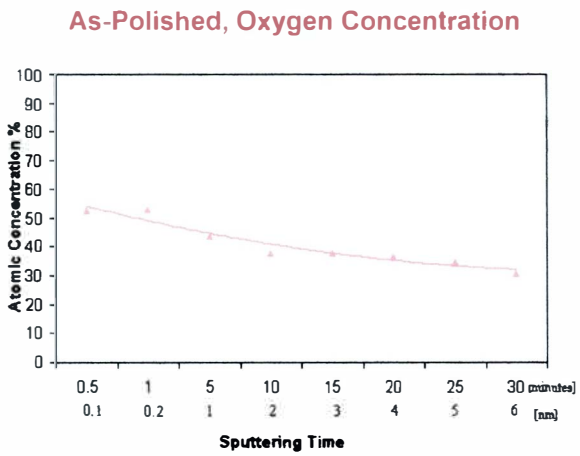

Figure 16. Change of Oxygen Atomic Concentration with Sputtering Time

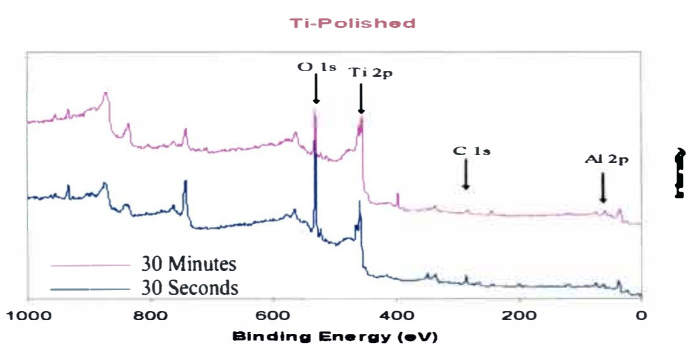

Figure 17. Representation of the Survey Scan of As-Polished Samples Surface, after 30 Seconds and 30 Minutes of Surface Sputtering

The results for the serum solution-treated samples, for example Ti-3Months, after 30 seconds of surface sputtering, in comparison with the as-polished sample, the oxide layer which was formed on the surface was 88% TiO_2 and 12% Ti_2O_3, with no evidences of either TiO or titanium metal. This trend was observed for the other immersed samples too. For example, Lu *et al.* [63] studied the oxidation of titanium with oxygen and water at temperatures between -123 and 577^{0}C and their findings show that, at 37^{0}C, oxygen can oxidize Ti to Ti^{+4}, Ti^{+3} and Ti^{+2}, but for the same sample at approximately the same temperature (37^{0}C), when titanium is exposed to water, they have reported that the oxidation of titanium is limited with water, and they reported that, at 37^{0}C no TiO_2 or Ti_2O_3 is present. In our findings the oxide layer, which is formed in α–calf serum solution at 37^{0}C, is a mixture of TiO_2, Ti_2O_3 and TiO as going deeper in the oxide layer. Another study by Motte *et al.* [57] on oxidation of Ti-6Al-4V with water vapor temperatures between 650 and 950^{0}C. The results of their findings showed that at temperatures above 900^{0}C surface oxide mostly consist of rutile TiO_2 structure which is partially in agreement with the findings of this current research.

This increased concentration of TiO_2 on the immersed samples surfaces is due to the further oxidation of Ti_2O_3, which is not a stable oxide, into TiO_2, which is the most desirable and most stable oxide for bio-acceptability [80]. Also temperature (samples were kept at 37^{0}C in the incubator) and the chemical reactions between the surface and serum solution caused this oxidation.

After 30 minutes of surface sputtering, oxide layer on the Ti-3Months sample is mostly composed of TiO, at a concentration of 33%. Also TiO_2, Ti_2O_3 and

titanium metal were found in concentrations of 27%, 15% and 25% respectively and the peak fitting results of titanium is represented in figure 19. When titanium metal and its alloys are immersed in water or aqueous solutions, adsorption of hydroxide ions (OH^-) and H^+ ions will occur or it can be said that hydration of titanium oxide happens [59, 60]. For immersed samples for example, Ti-3Months, hydroxyl species were being identified on the sample's surface, and this hydrated titanium surfaces, which is the combined effect of adsorption of water and formation of hydroxide, are being represented in figure 18, which is the peak fitting results of O 1s of Ti-3Months sample.

These peak fitting results provides evidences for the presence of titanium oxide, which is TiO_2, hydrated titanium, and adsorbed water and these results are similar to the findings of Lu et al. [58]. Also the presence of hydrated titanium species on the immersed samples is shown in the FT-IR results.

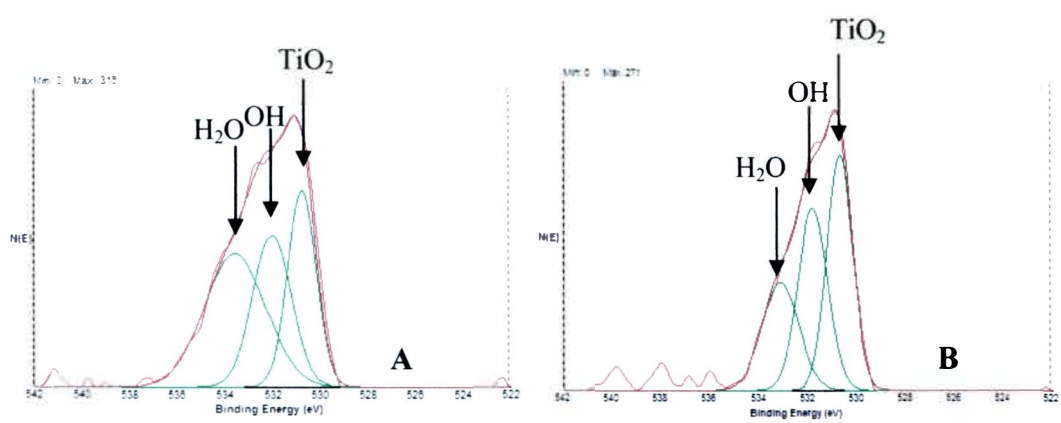

Figure 18. Oxygen Peak of Ti-3Months Samples Peak Fitting Results. A. After 30 Seconds of Surface Sputtering, B. After 30 Minutes of Surface Sputtering

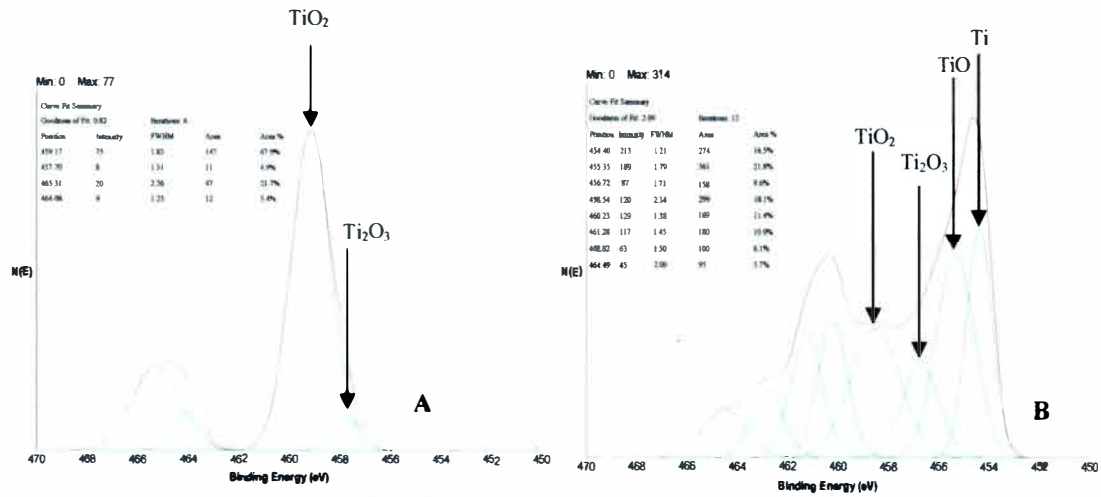

Figure 19. Ti-3Months Sample, Ti 2p Level Curve Fitting Results after, A. 30- Seconds and B. 30-Minutes of Surface Sputtering

For Ti-3Months sample, as the immersion time increases, the carbon concentration on the surface increases too. In comparison with the as-polished sample, with the increased immersion time C-O (organic adsorbates at 286.5eV) on the surface increases, where the same trend was seen and described in the FT-IR results. In addition to C-O, formation of C-C and COO organic adsorbents on the surface increases. These organic adsorbents have binding energies of 285 and 288.87eV respectively. Also no evidence of titanium carbide was found in Ti-3Months sample. An example of C 1s peak fitting after 30 seconds of surface sputtering is represented in Figure 20, other peak fitting results are given in Appendix B.

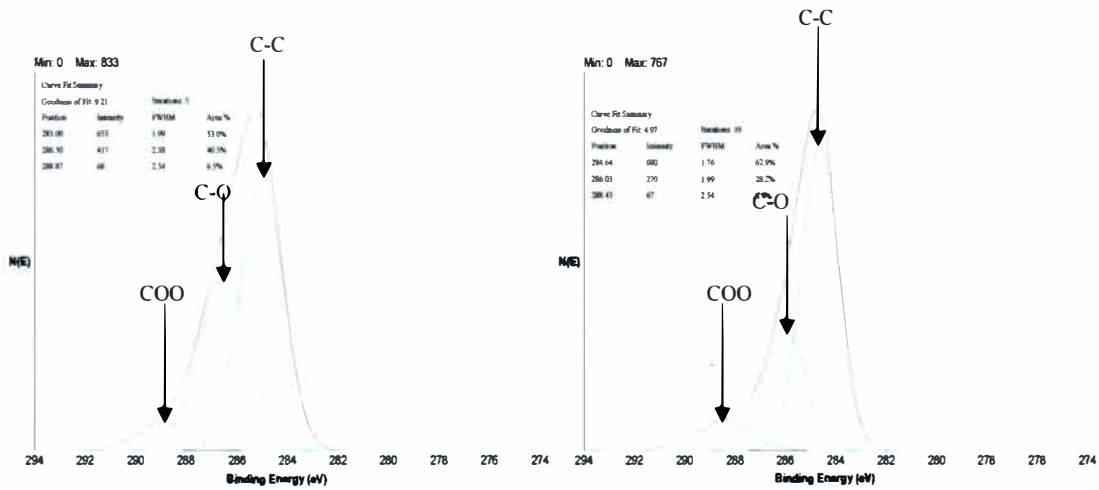

Figure 20. Representation of C 1s Narrow Scan for Ti-3Months Sample after 30 Seconds and 30 Minutes of Surface Sputtering

With increased immersion, the oxygen concentration on the samples surfaces increases and this increase is due to the oxidation of Ti_2O_3 to the TiO_2 state. After 30 seconds of surface sputtering for Ti-3Months sample with the ion-gun bombardment, carbon and oxygen species were removed from the surface and titanium metal peak started to become dominant on the surface. This titanium (Ti 2p), in comparison with the Ti-Polished sample, shows much more TiO_2 concentration than the as-polished sample because of the further oxidation of Ti_2O_3 to TiO_2, where Ti-Polished sample has lower TiO_2 concentration than the immersed sample, with relative atomic concentrations of 88% and 48% respectively.

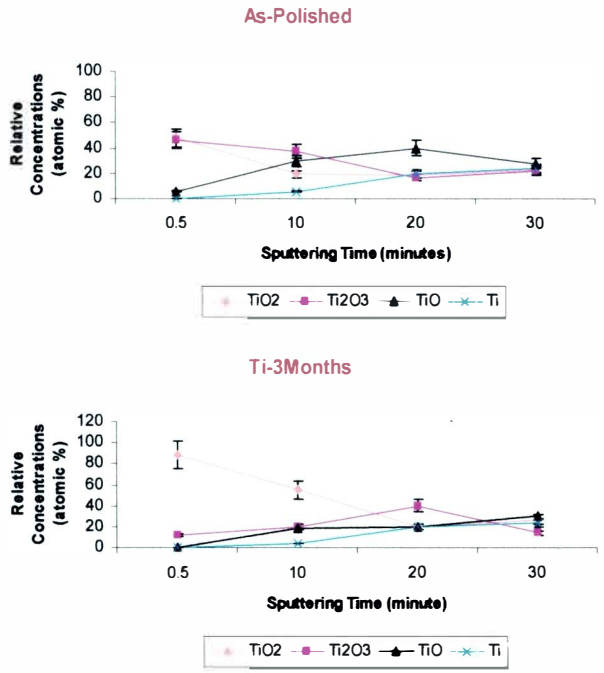

Figure 21. Comparisons of the Different Oxide Concentrations in As-Polished and Ti-3Months Samples with Sputtering

As mentioned earlier the outer surface oxide of the as-polished sample is composed of about 48% of TiO_2 and 46% of Ti_2O_3. From figure 21 we see that this changes after immersion in the serum solution. After immersion, the Ti_2O_3 further oxided into TiO_2. As a result the TiO_2 concentration in Ti-3Months sample increases, where it is shown in figure 21. The observed broadening of the Ti_2O_3 peak can be related to the non-stoichiometric nature of the oxide [58].

As a conclusion, with increased immersion time in comparison with the as-polished sample, Ti_2O_3 gets oxidized into the most desirable and most stable oxide surface for bio-acceptability, TiO_2. Under this layer, Ti_2O_3 and TiO oxides are present.

Atomic Force Microscopy

As can be seen from the figure 22, with increased immersion time, the surface morphology and the roughness of the Ti-6Al-4V samples surfaces have significantly changed. The as-polished sample had originally a smooth surface. After immersion in the α–calf serum solution the surface changed and became more-rounded. This change results from the hydration of titanium surfaces and forms dome-like hydrated oxide structures on surface of titanium, which is in agreement with Bearinger *et al* [59]. Figure 22 represent the surface topography changes of the samples, in comparison with the as-polished sample and images were taken at 2μm scale. The other surface topography images of the samples were taken at different magnification scales of 10 μm, 5 μm and 1 μm and are shown in Appendix A. As can be seen from the images in figure 22, with this continued oxidation in the serum solution causes the hydration of the surfaces and this increase was reported by Bearinger et al. [59] and Xiao et al. [78].

After the protein assaying, samples surfaces were washed away, and the hydrated titanium oxide surface became dominant, and visible, which is represented in figure 23 and these images are taken at 2μm scale, for other images please refer to appendix A.

As a result of AFM surface characterization, it is concluded that with immersion in the α–calf serum solution changes the surface topography which is caused by the hydration of titanium surfaces.

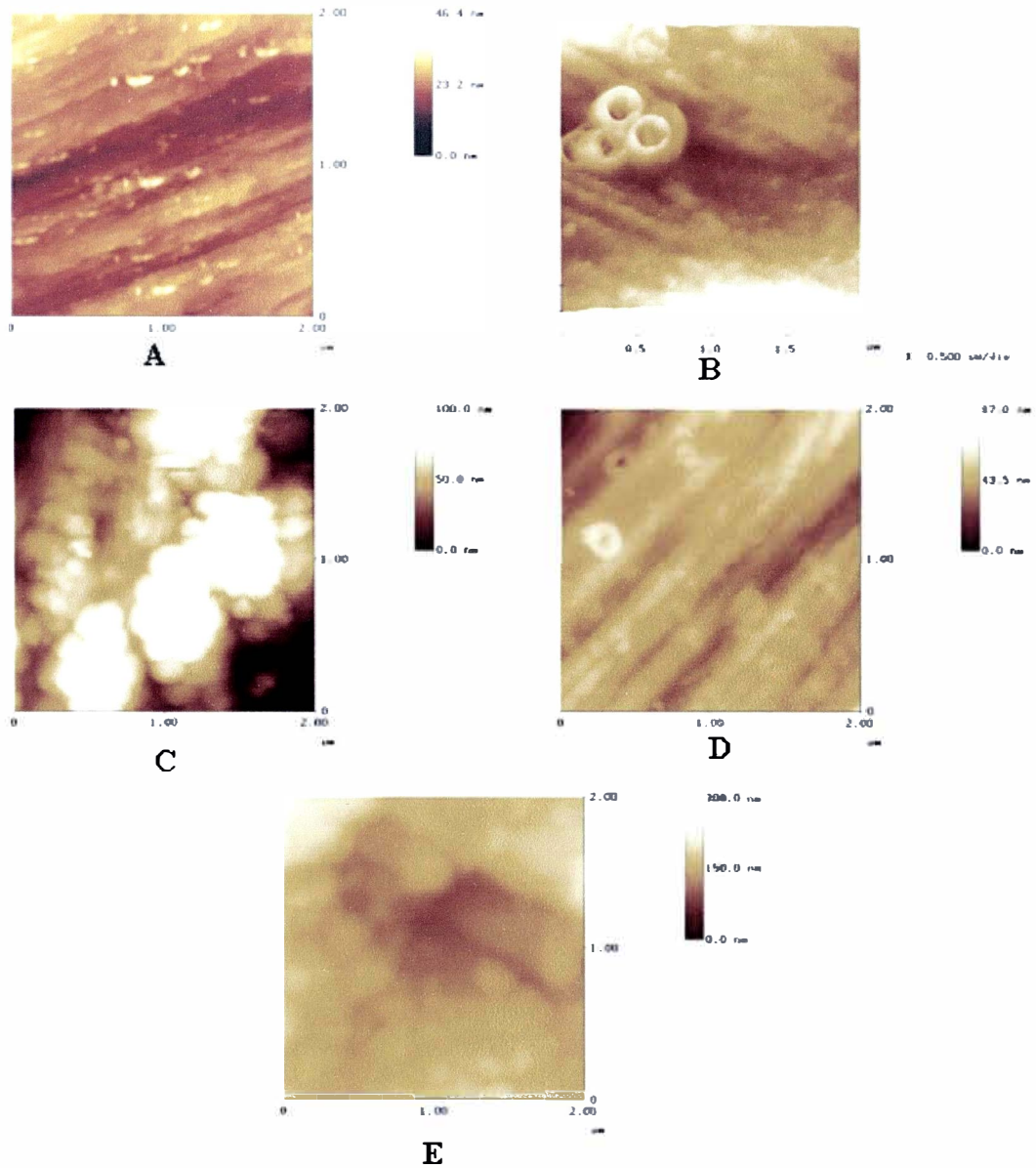

Figure 22. AFM Surface Topography of Different Duration of Immersed Samples. (A) As-Polished, (B) Ti-2Weeks sample, (C) Ti-1Month sample, (D) Ti-2Months sample and (E) Ti-3Months sample

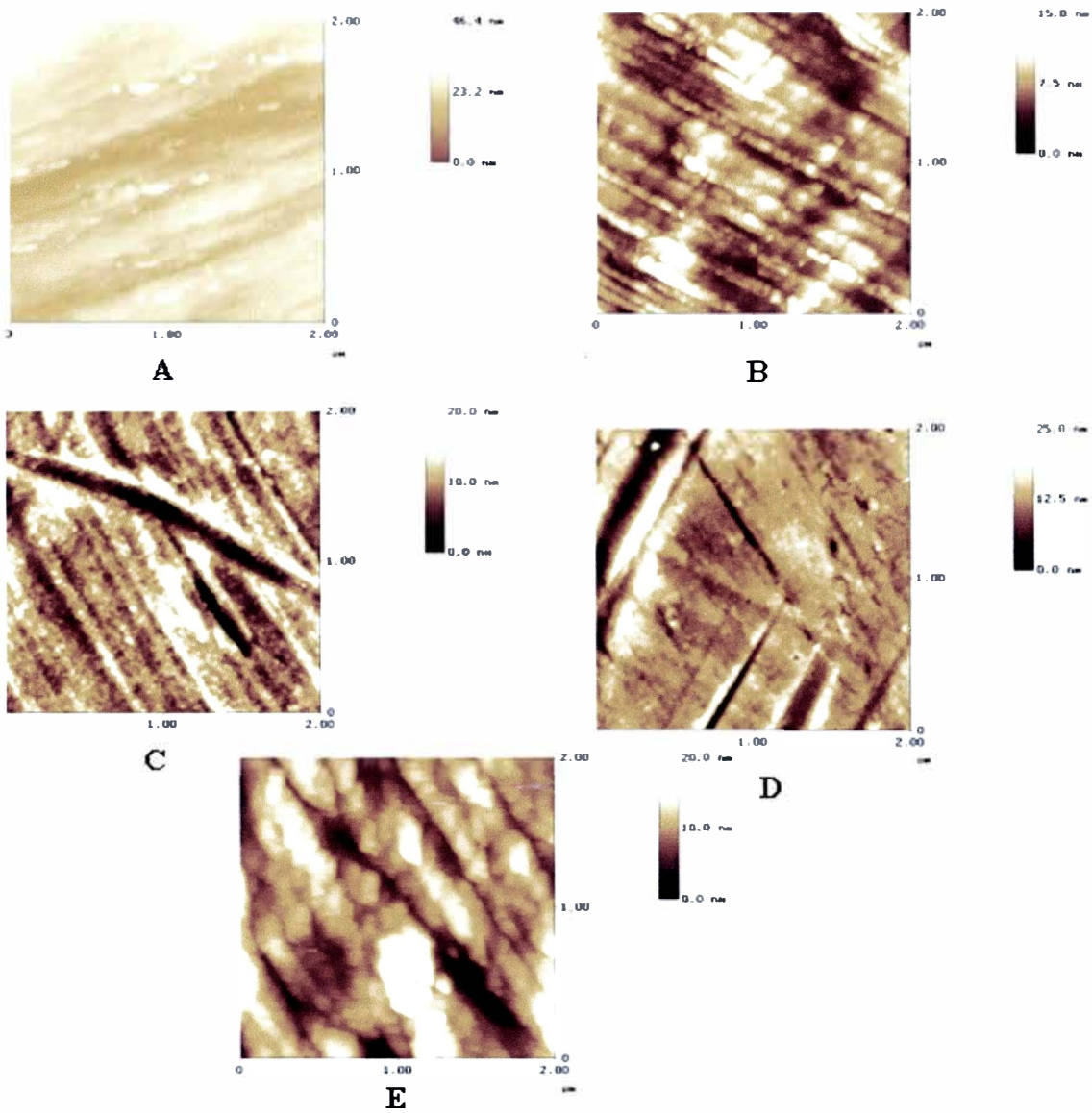

Figure 23. AFM Surface Topography of Different Duration of Immersed Samples after Washing off the Protein from the Surfaces. (A) As-Polished, (B) Ti-2Weeks sample, (C) Ti-1Month sample, (D) Ti-2Months Sample and (E) Ti-3Months sample

Fourier Transform Infrared Spectroscopy

FT-IR results show that, adsorption of O-H, C-N and C=O chemical constituents on the Ti-6Al-4V surfaces increases with the immersion time. Increase of these constituents is due to the protein adsorption on the surfaces and the hydration of the titanium surfaces in the serum solution. The as-polished sample was used only for background collection. For the samples Ti-2Weeks, Ti-1Month, Ti-2Months and Ti-3Months, the peak with wave number of ~3400cm^{-1}, which is the hydroxyl groups OH on the surfaces increases in intensity on the surface with the increased immersion time. Also around peaks at ~1650cm^{-1} and ~1550cm^{-1}, represent the C-N and C=O organic groups respectively and also adsorption of these organic compounds increases with the immersion time too. In the Figure 24 comparison of the different samples FT-IR spectra are presented.

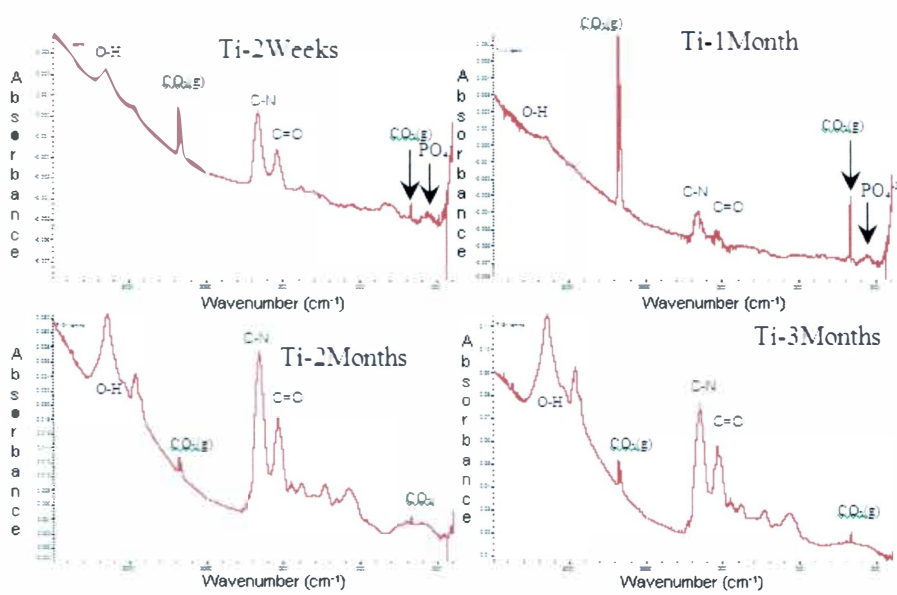

Figure 24. Comparisons of the Samples FT-IR Spectra of the Different Samples

It is also important to note from figure 24 in Ti-2Weeks and Ti-1Month sample's spectra, that a phosphate peak is present (~560cm^{-1}). This phosphate peak comes from the reagents that were added to the alpha-calf serum solution during preparation. But after two months of soaking samples in the solution, this phosphate peak disappears, which indicates that phosphate is present on the very surface of the sample.

After the protein assay, as can be seen from the result in figure 25, all the adsorbed protein on the samples surfaces have been removed and washed away, AFM results after washing away the surfaces proves this too.

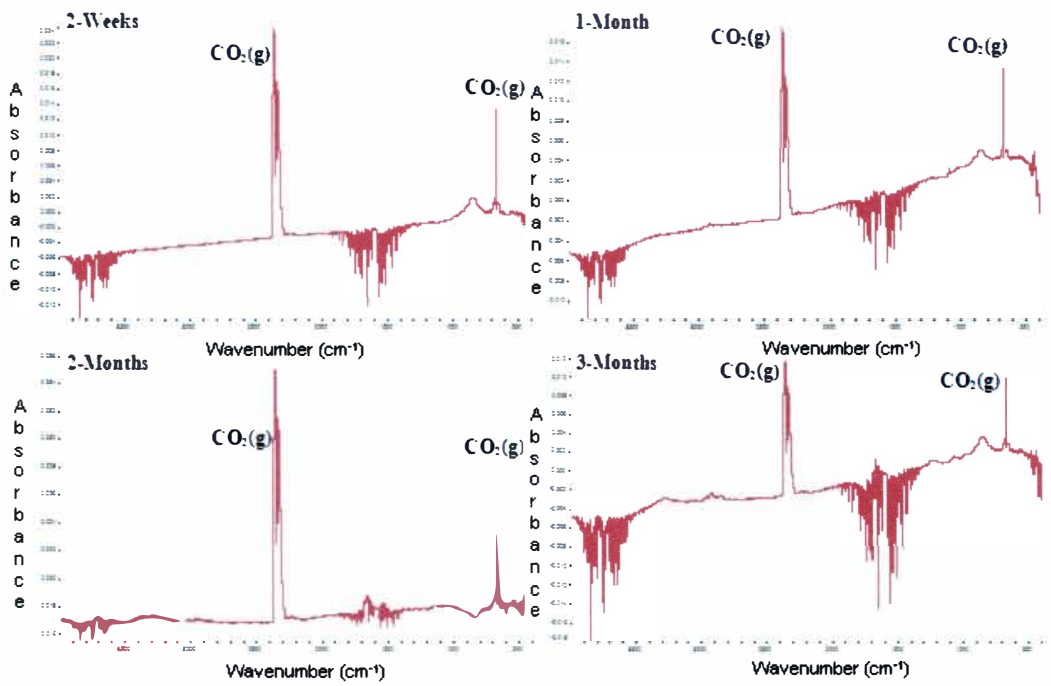

Figure 25. Comparisons of the Samples FT-IR Spectra of the Different Samples, After Performing Protein Assay

BCA Total Protein Assay

Protein assay was performed on samples Ti-2Weeks, Ti-1Month, Ti-2Months and Ti-3Months samples. During the test, BCA Total Protein Assay protocol [79] was followed. Before performing the assay, samples were inserted into 2% SDS solution and adsorbed proteins on the surfaces were dissolved. Figure 26 represents the standard curve that was gathered from the micro plate reader. The adsorbed protein amounts with the increased immersion time are listed in table 11.

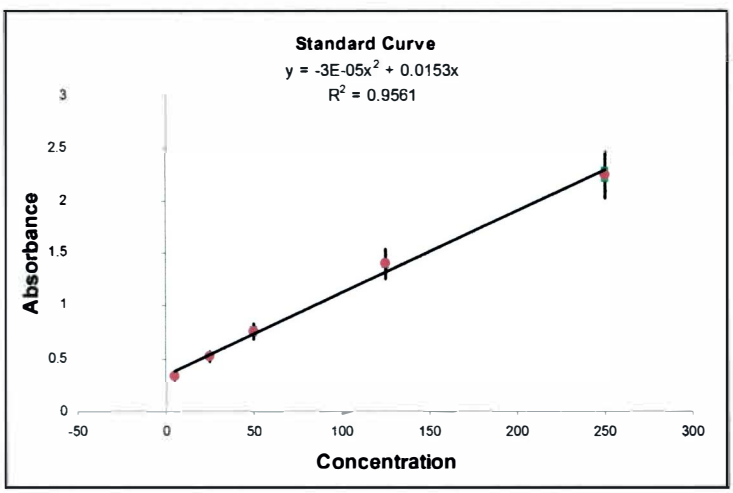

Figure 26. Standard Curve that was Gathered from Protein Assay

Sample	Adsorbed Protein (μm/mL)
Ti-2Weeks	5.31
Ti-1Month	5.556
Ti-2Months	6.60
Ti-3Months	7.04

Table 11. Amount of Protein Adsorbed on Titanium at Different Immersion Times

CHAPTER V

CONCLUSION

The AFM results show that, with increased immersion time, there is a gradual but very significant topographical change of the samples surfaces. After immersion in the α–calf serum solution, the surfaces of Ti-6Al-4V samples have become more rounded. The change results from the reactions that happened between the surfaces of the samples and serum solution. Formations of dome-like structures are due to the hydration of titanium surfaces.

The FT-IR results show that, with the increased immersion time in the solutions, formation of O-H, C-N and C-O constituent's increase. Also, phosphate is present on the surfaces of Ti-2Weeks and Ti-1Month samples. This phosphate is due to the chemicals, which were added to the alpha-calf serum solution during preparation. But after two months of soaking the samples in the solution, this phosphate peak disappears, which is due to the protein adsorption on the surface.

XPS results for the as-polished sample show that, the surface of the oxide layer is a mixture of desired TiO_2 and undesired Ti_2O_3. After immersion in the serum solution this Ti_2O_3, further oxidizes into TiO_2, and with increased immersion time, this bio-acceptable oxide layer covers the Ti-6Al-4V surface.

CHAPTER VI

FUTURE RECOMMENDATION

In order to increase the biocompatibility of the as-polished sample, it is recommended oxidizing it in air to improve the surface properties, to create a uniform TiO_2 surface.

It is also recommended to investigate the calcium and phosphate initiation on Ti-2Weeks and Ti-1Month samples. More than one month of immersion in the serum solution, because of increased protein adsorption on the surface makes it impossible to identify these elements.

Appendix A

Atomic Force Microscopy

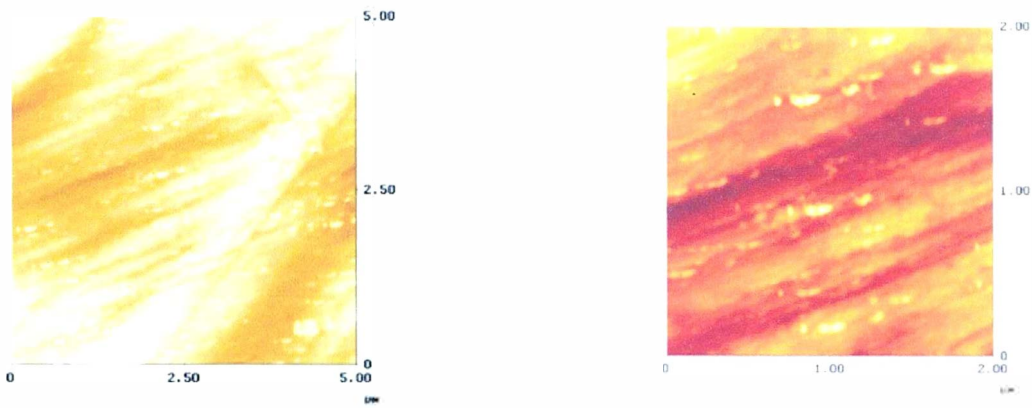

Figure A-1. AFM Images of As-Polished Sample

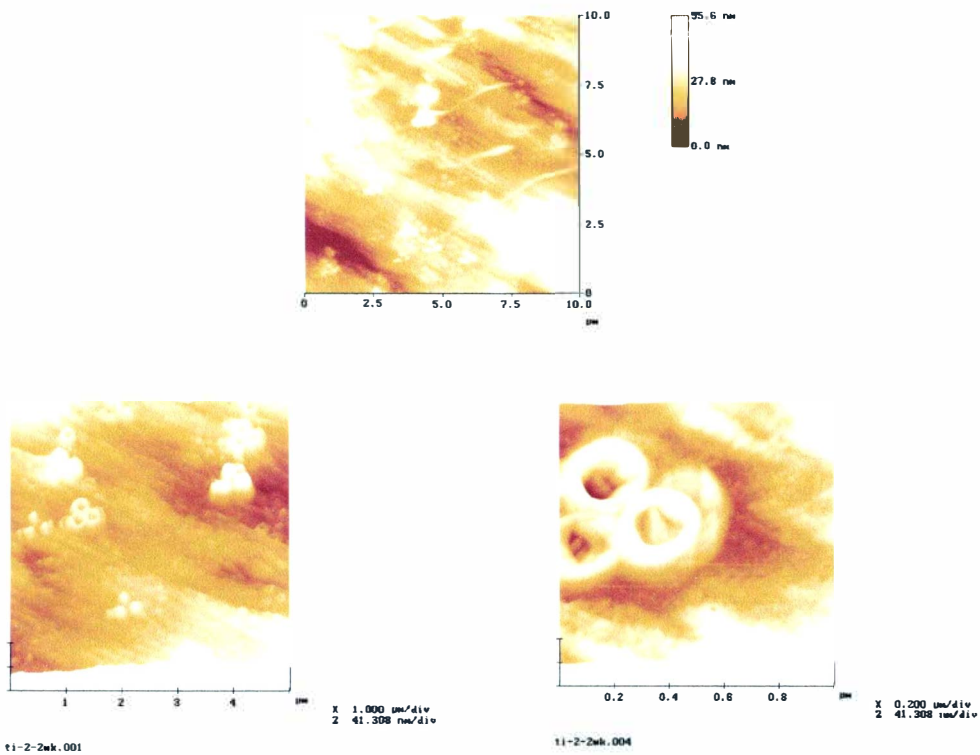

Figure A-2. AFM Images of Ti-2Weeks Sample

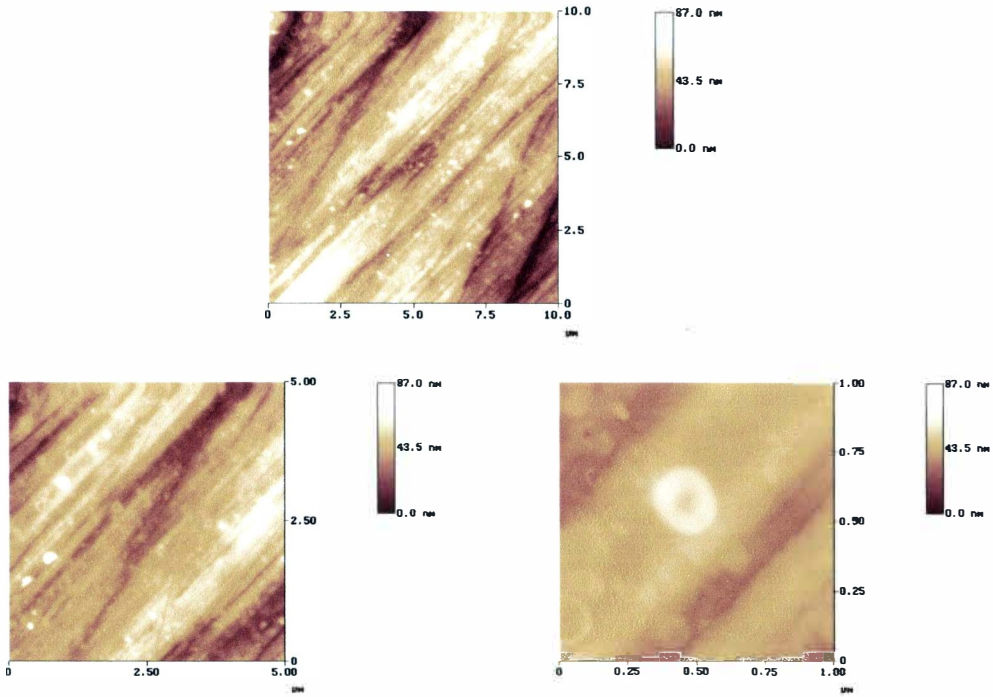

Figure A-3. AFM Images of Ti-1Month Sample

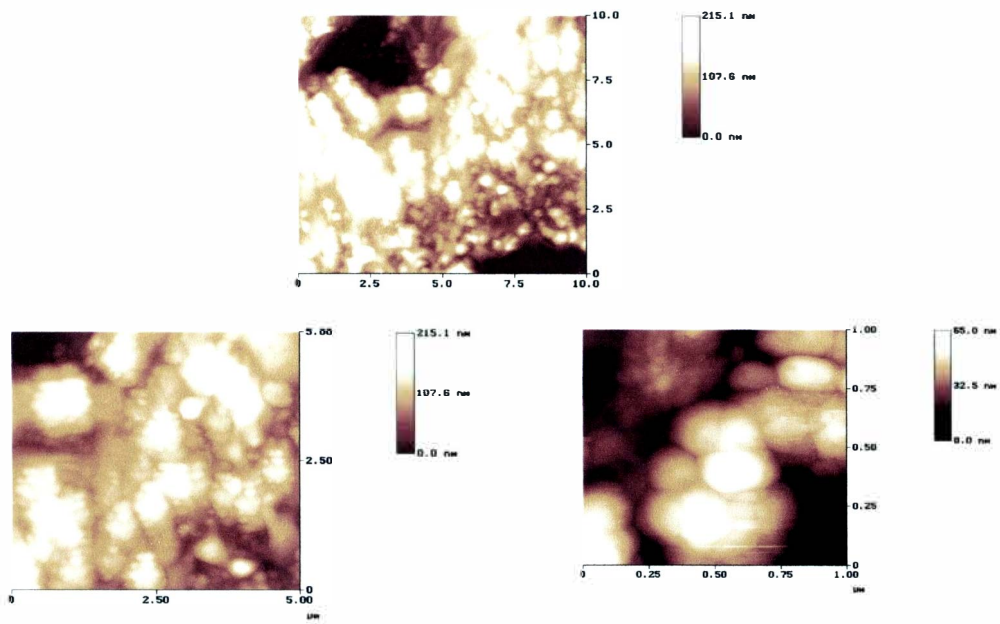

Figure A-4. AFM Images of Ti-2Months Sample

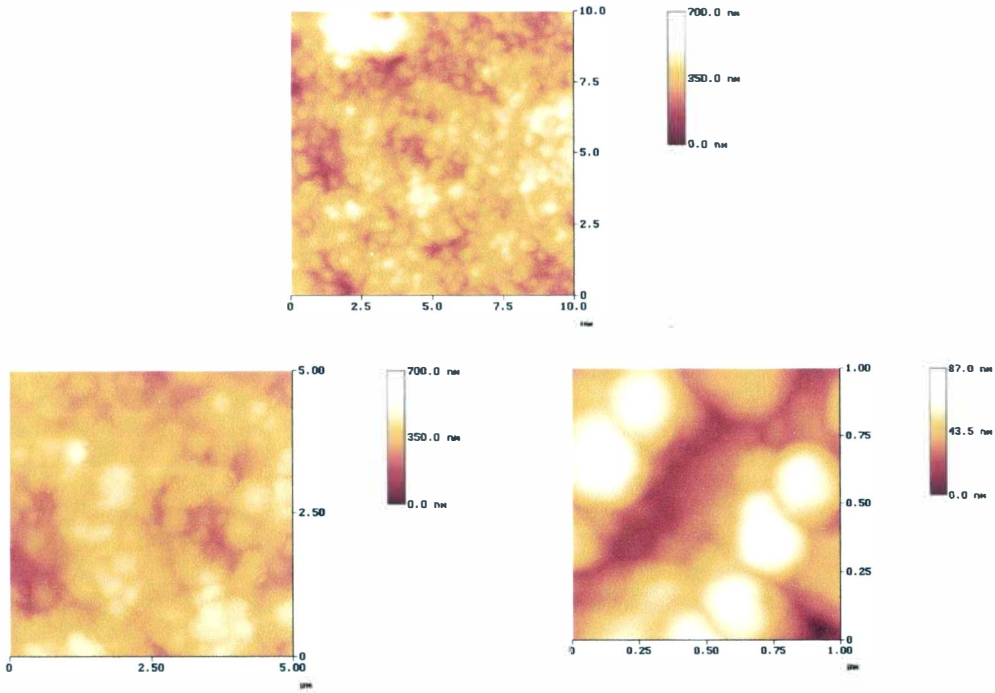

Figure A-5. AFM Images of Ti-3Months Sample

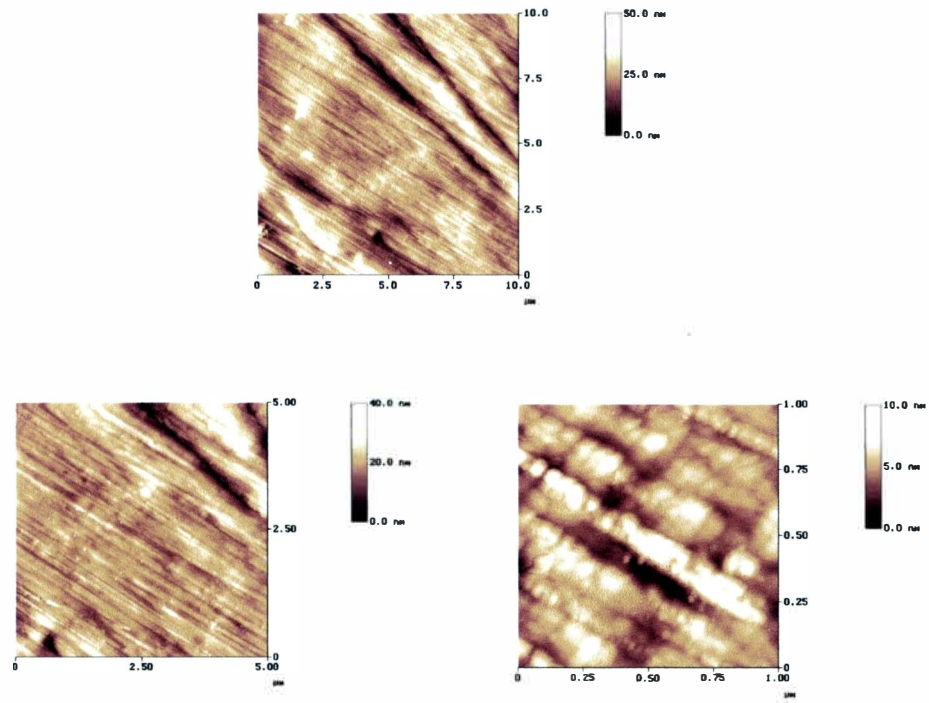

Figure A-6. AFM Images of Ti-2Weeks Sample After BCA Total Protein Assay

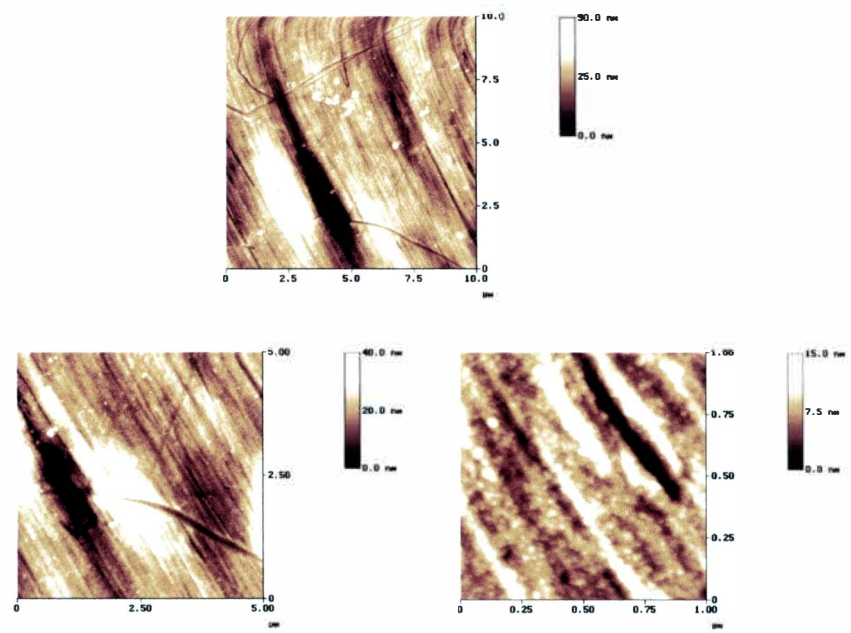

Figure A-7. AFM Images of Ti-1Month Sample After BCA Total Protein Assay

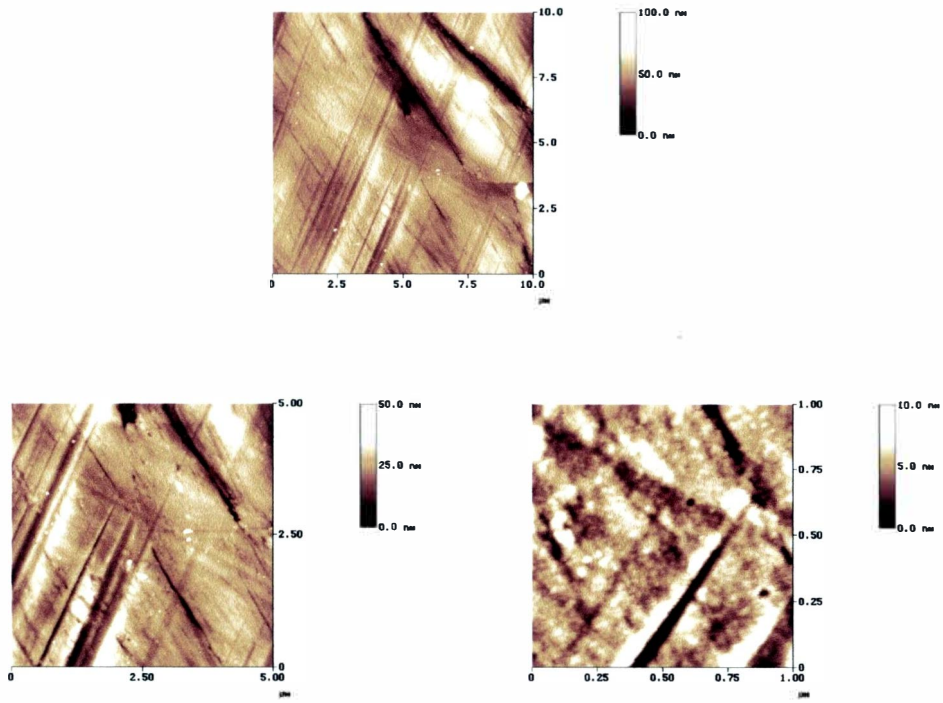

Figure A-8. AFM Images of Ti-2Months Sample After BCA Total Protein Assay

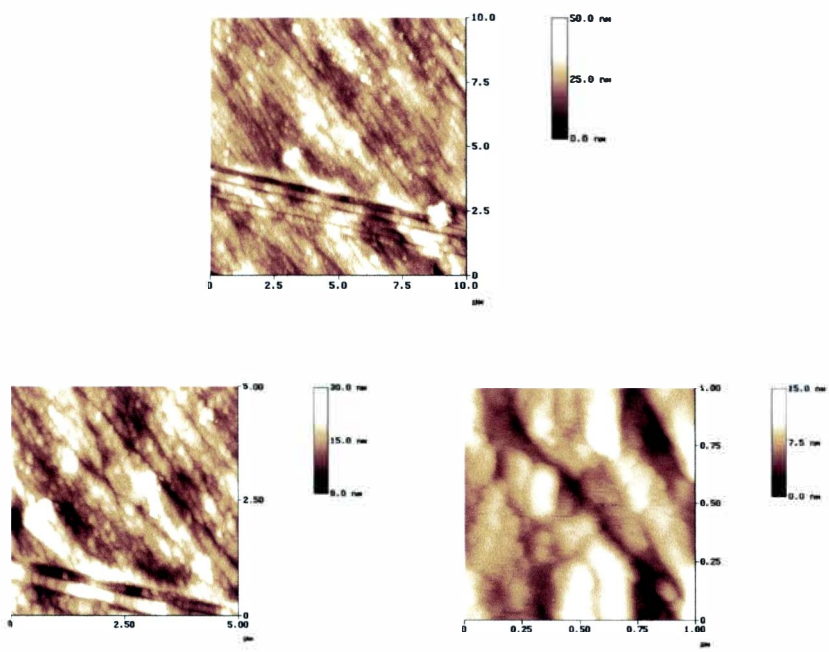

Figure A-9. AFM Images of Ti-3Months Sample After BCA Total Protein Assay

Appendix B

X-ray Photoelectron Spectroscopy Spectra

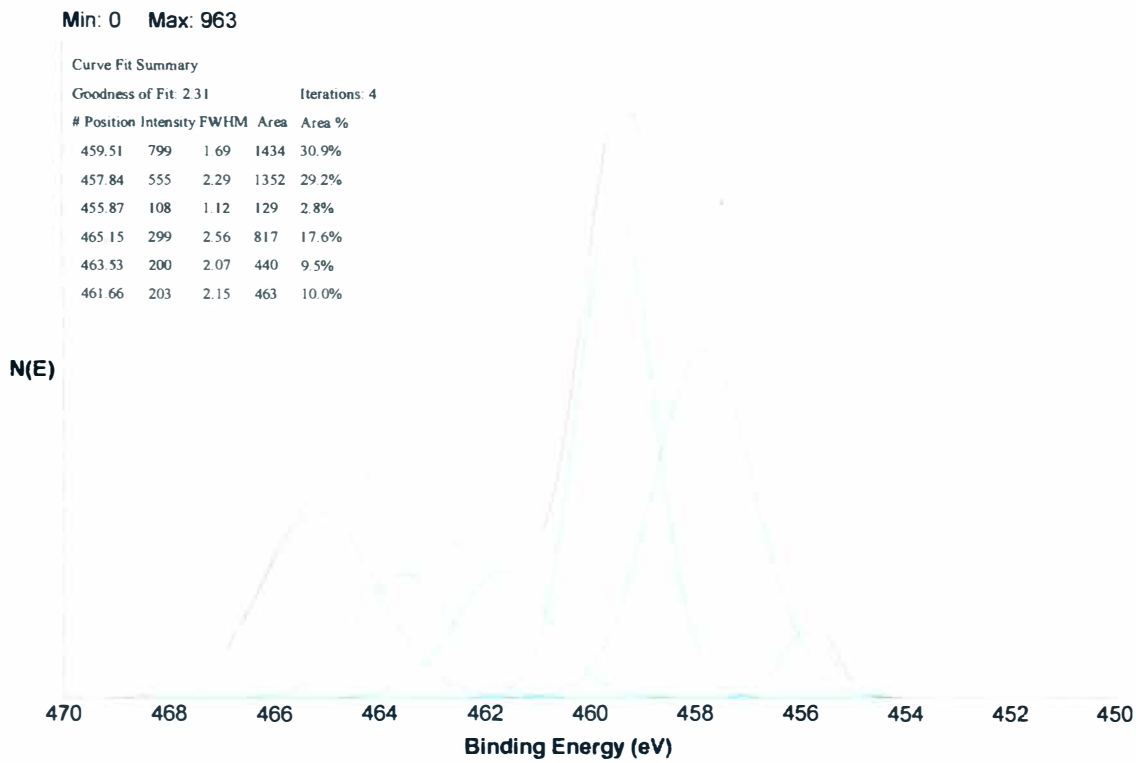

Figure B-1. Ti-Polished Sample after 30 Seconds Bombardment, Ti 2p

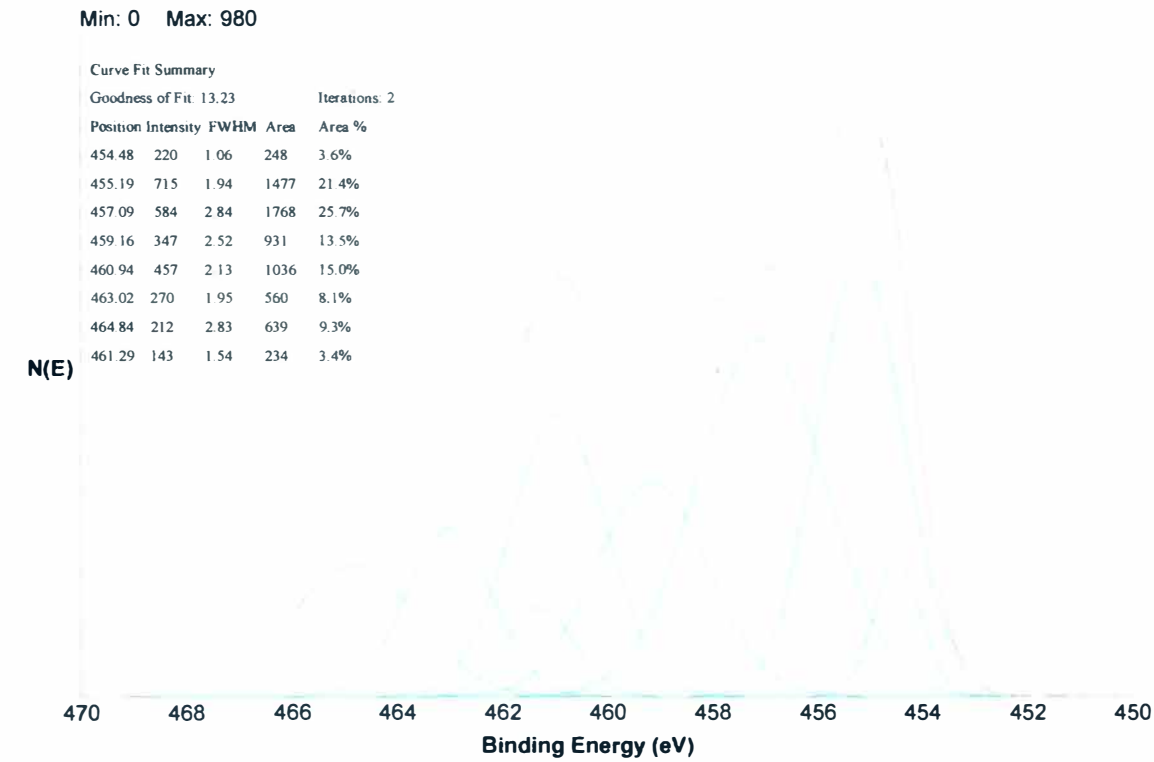

Figure B-2. Ti-Polished Sample after 10 Minutes Bombardment, Ti 2p

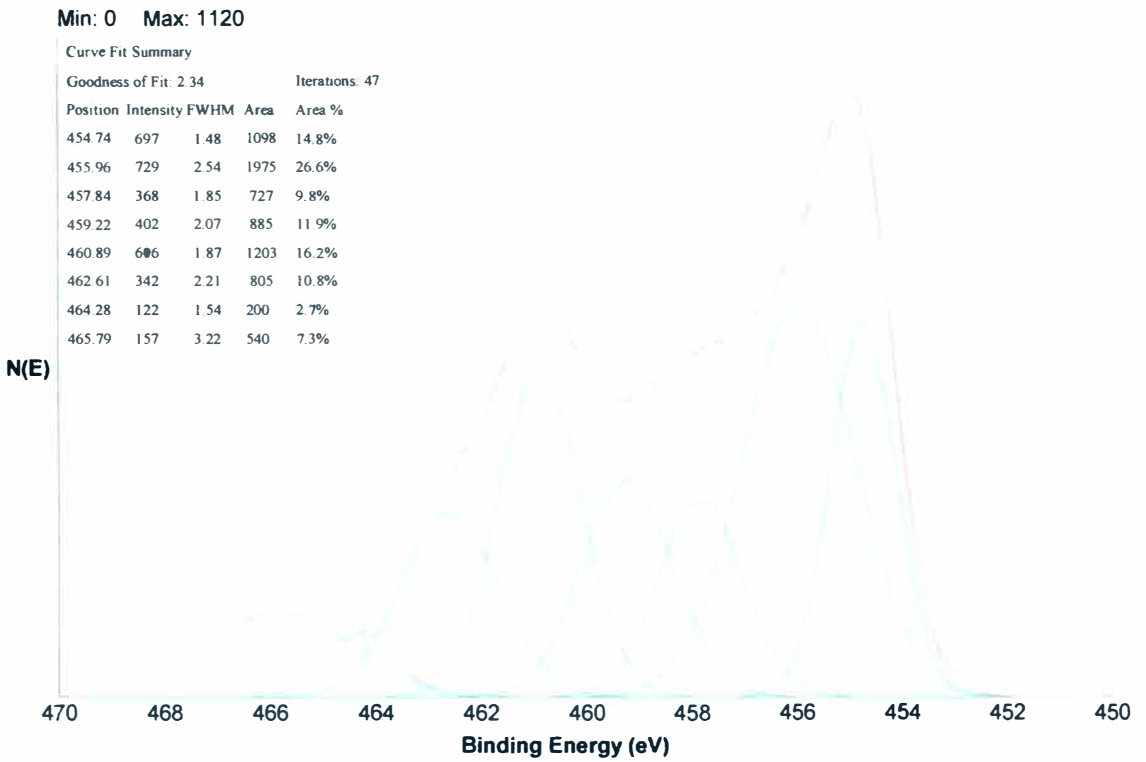

Figure B-3. Ti-Polished Sample after 20 Minutes Bombardment, Ti 2p

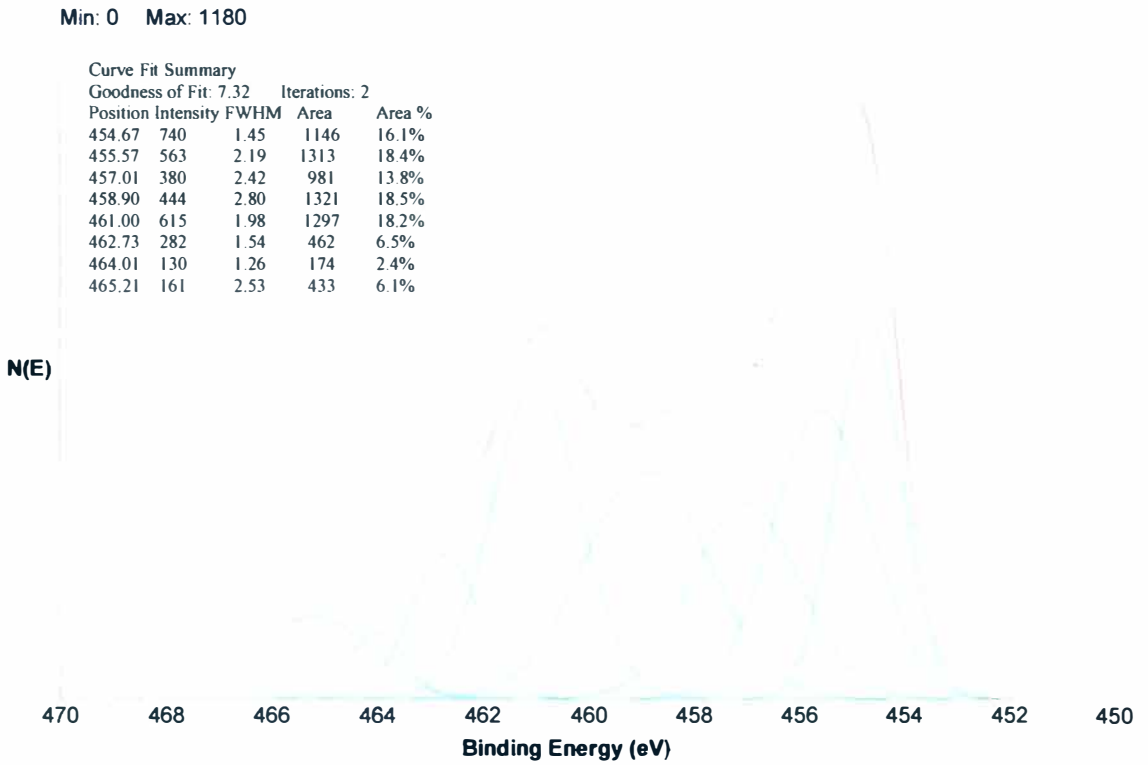

Figure B-4. Ti-Polished Sample after 30 Minutes Bombardment, Ti 2p

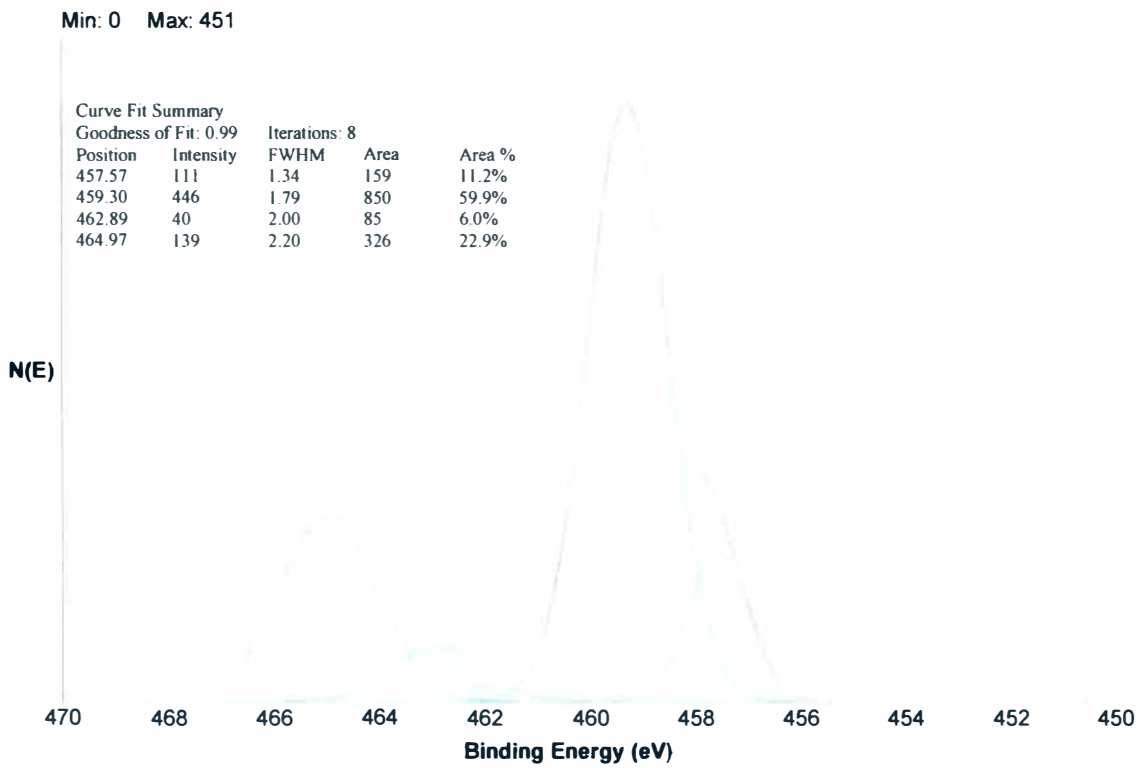

Figure B-5. Ti-2Weeks Sample after 30 Seconds Bombardment, Ti 2p

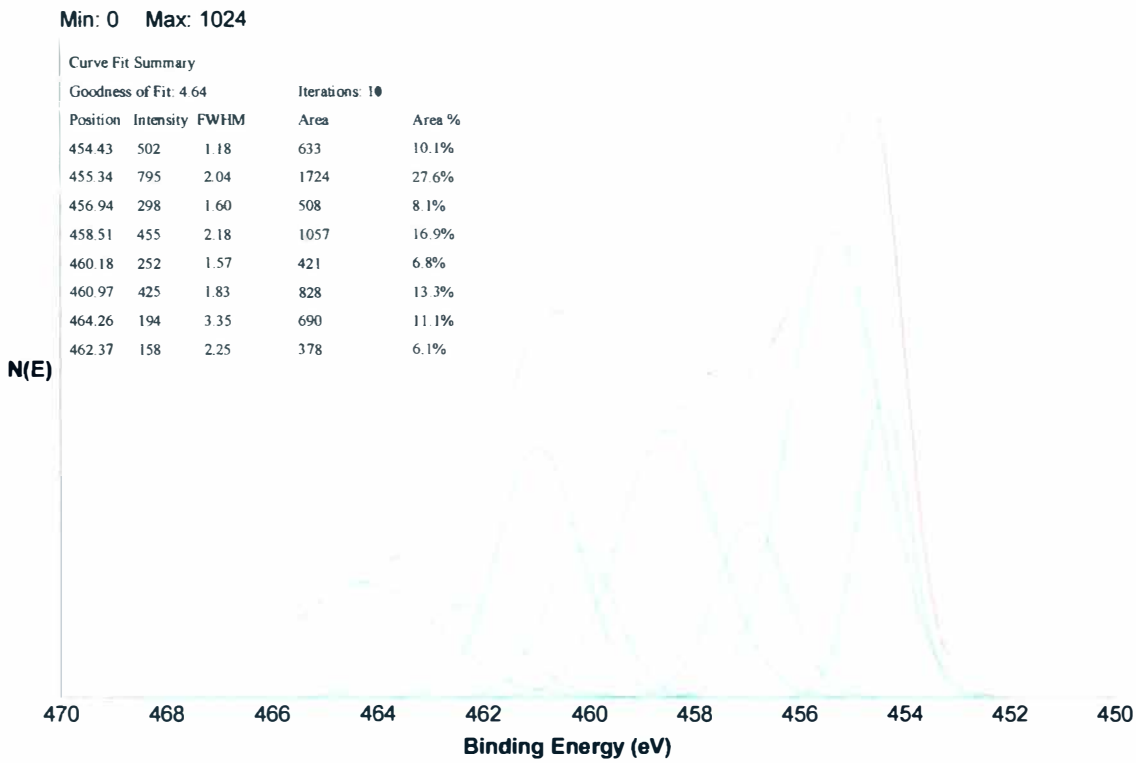

Figure B-6. Ti-2Weeks Sample after 10 Minutes Bombardment, Ti 2p

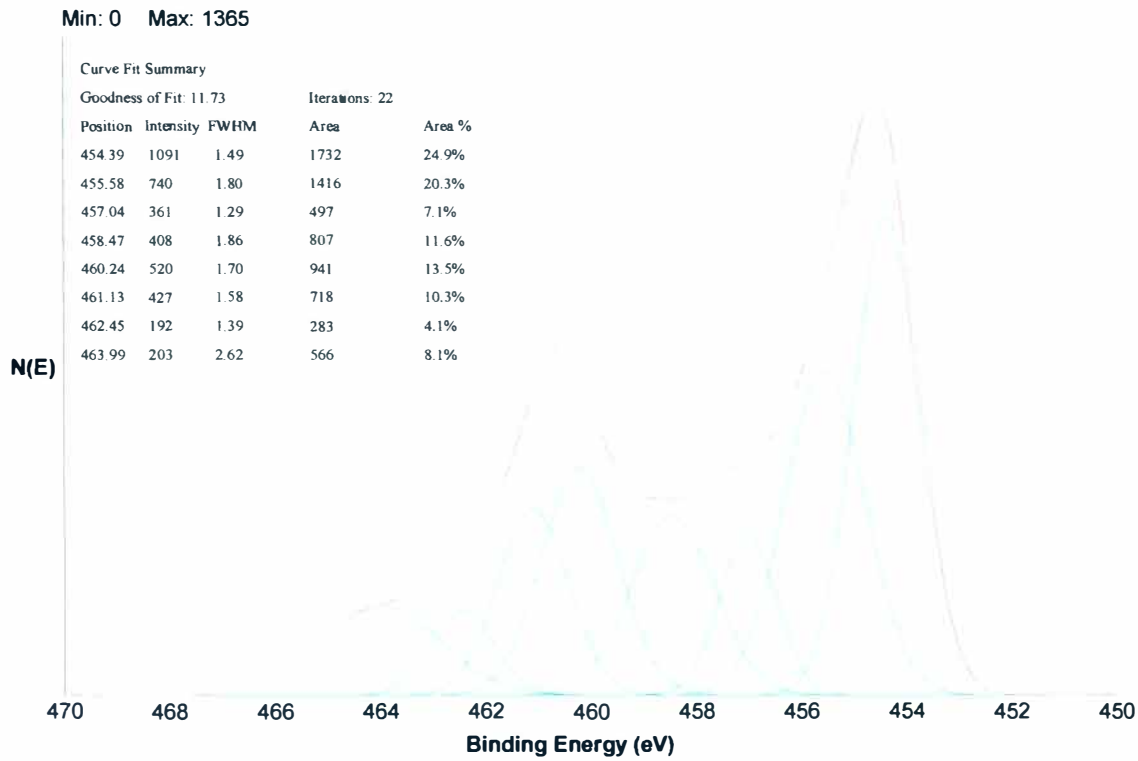

Figure B-7. Ti-2Weeks Sample after 20 Minutes Bombardment, Ti 2p

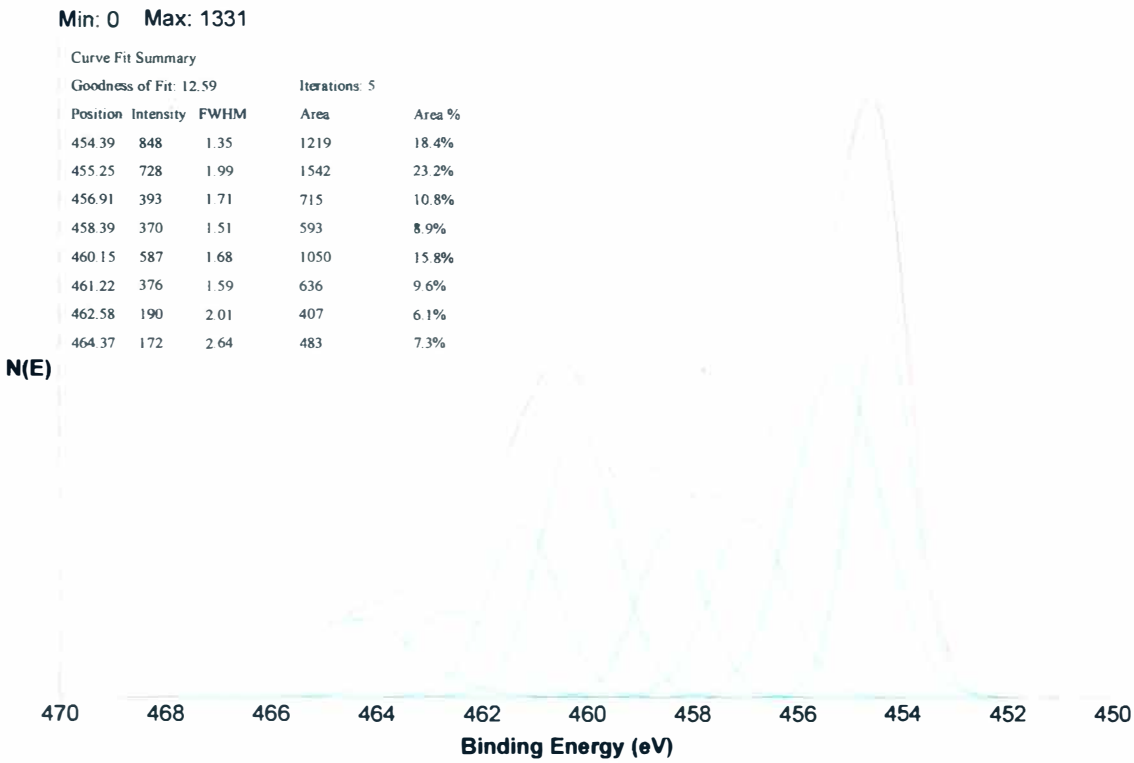

Figure B-8. Ti-2Weeks Sample after 30 Minutes Bombardment, Ti 2p

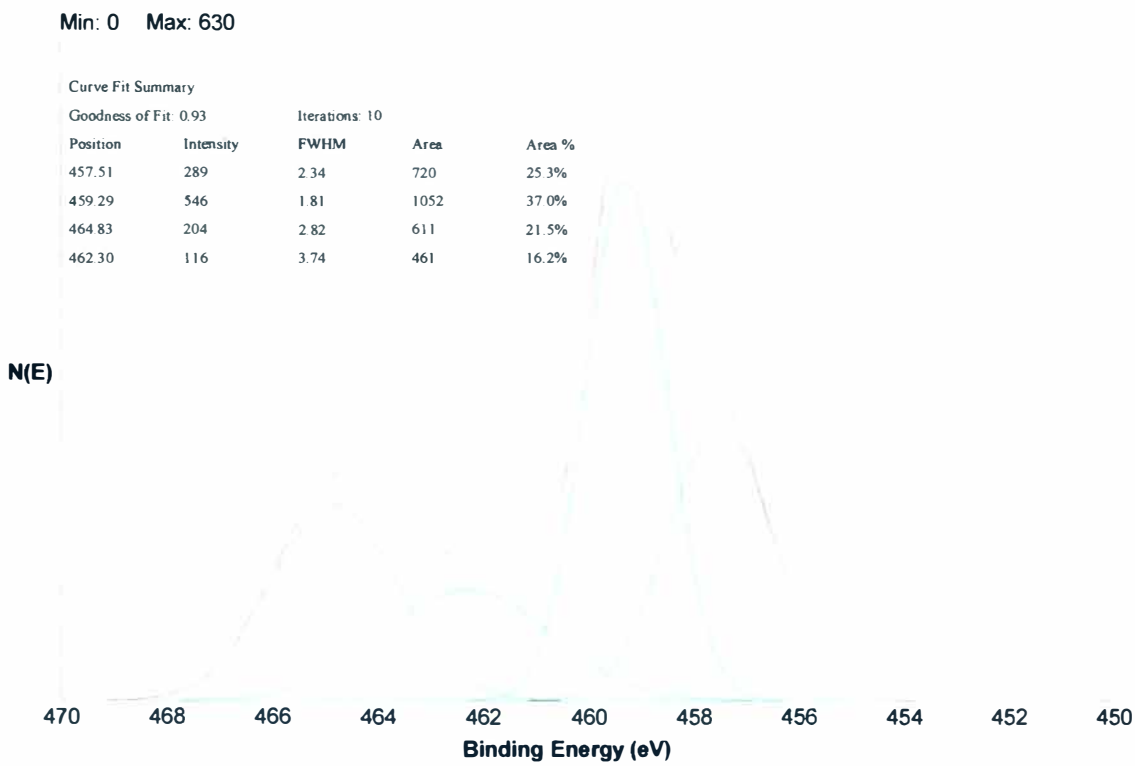

Figure B-9. Ti-1Month Sample after 30 Seconds Bombardment, Ti 2p

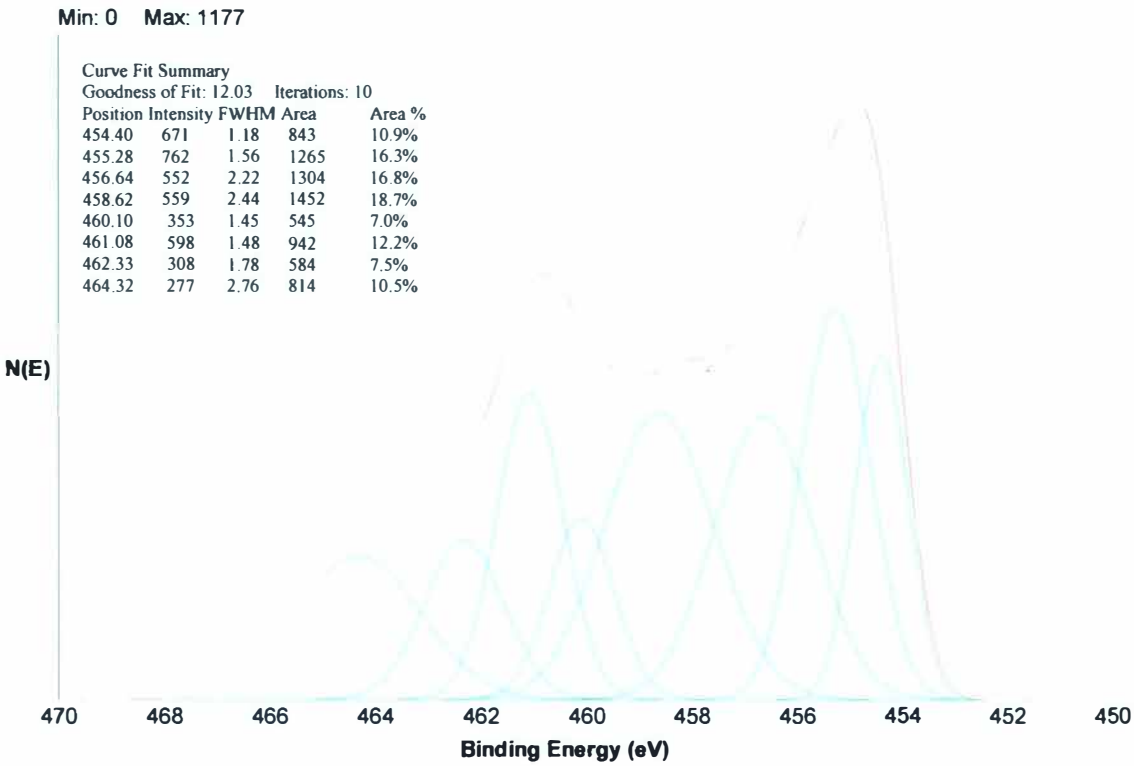

Figure B-10. Ti-1Month Sample after 10 Minutes Bombardment, Ti 2p

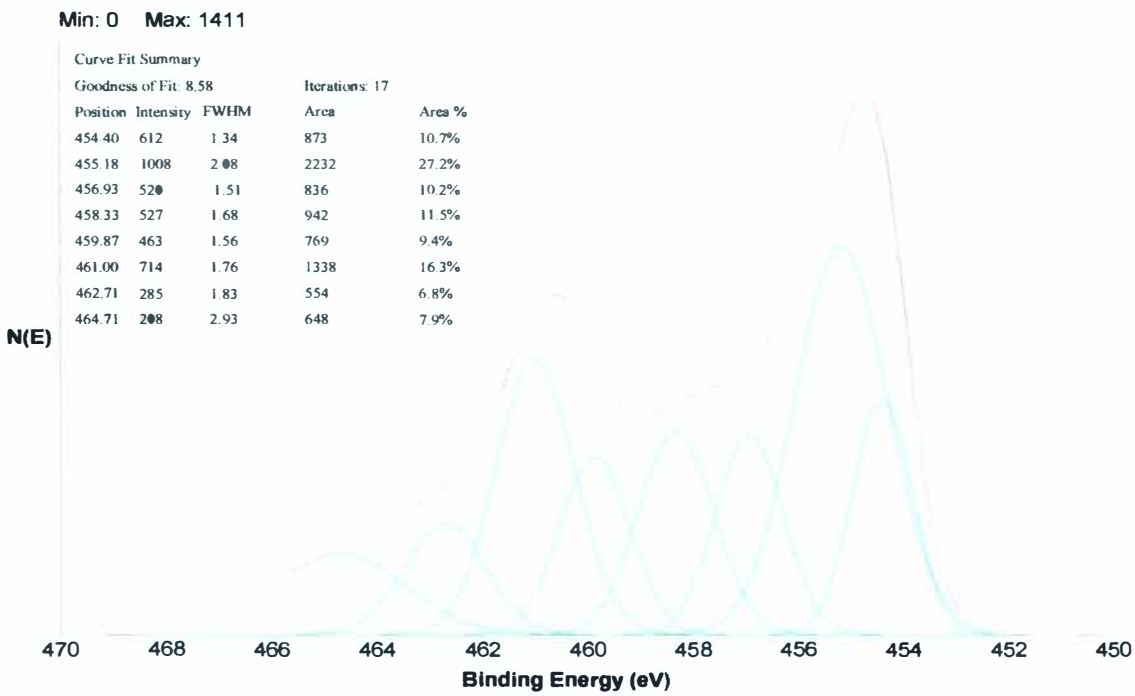

Figure B-11. Ti-1Month Sample after 20 Minutes Bombardment, Ti 2p

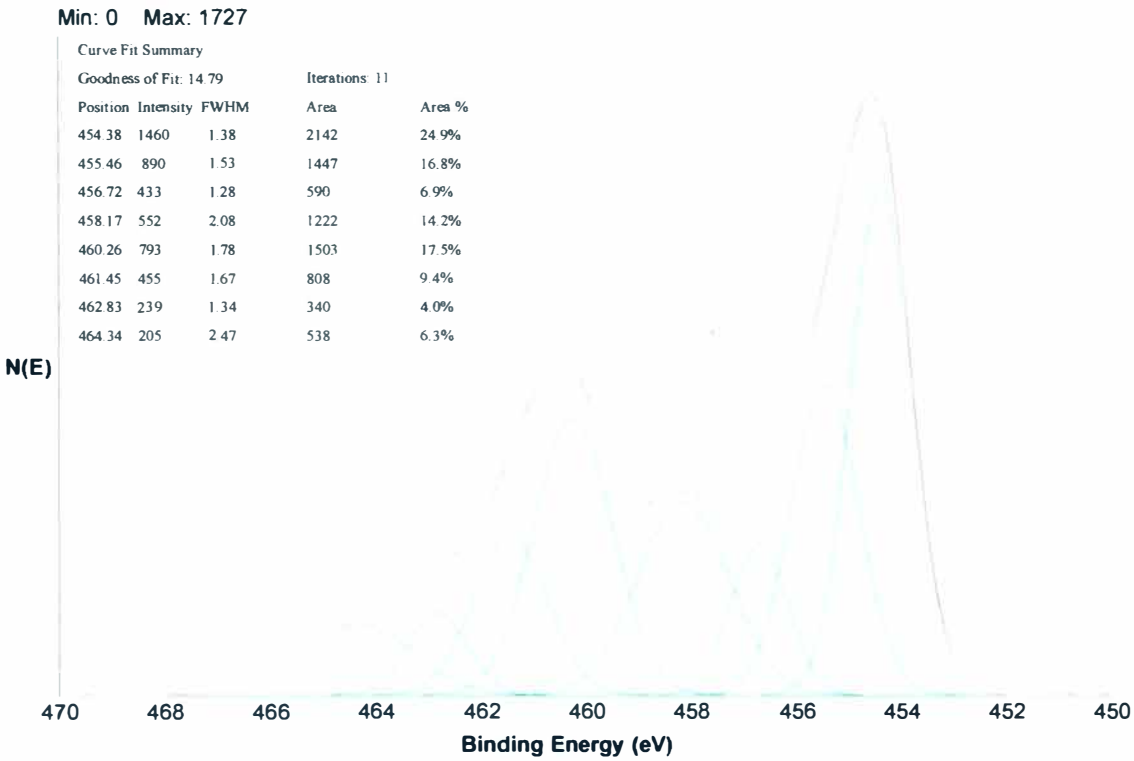

Figure B-12. Ti-1Month Sample after 30 Minutes Bombardment, Ti 2p

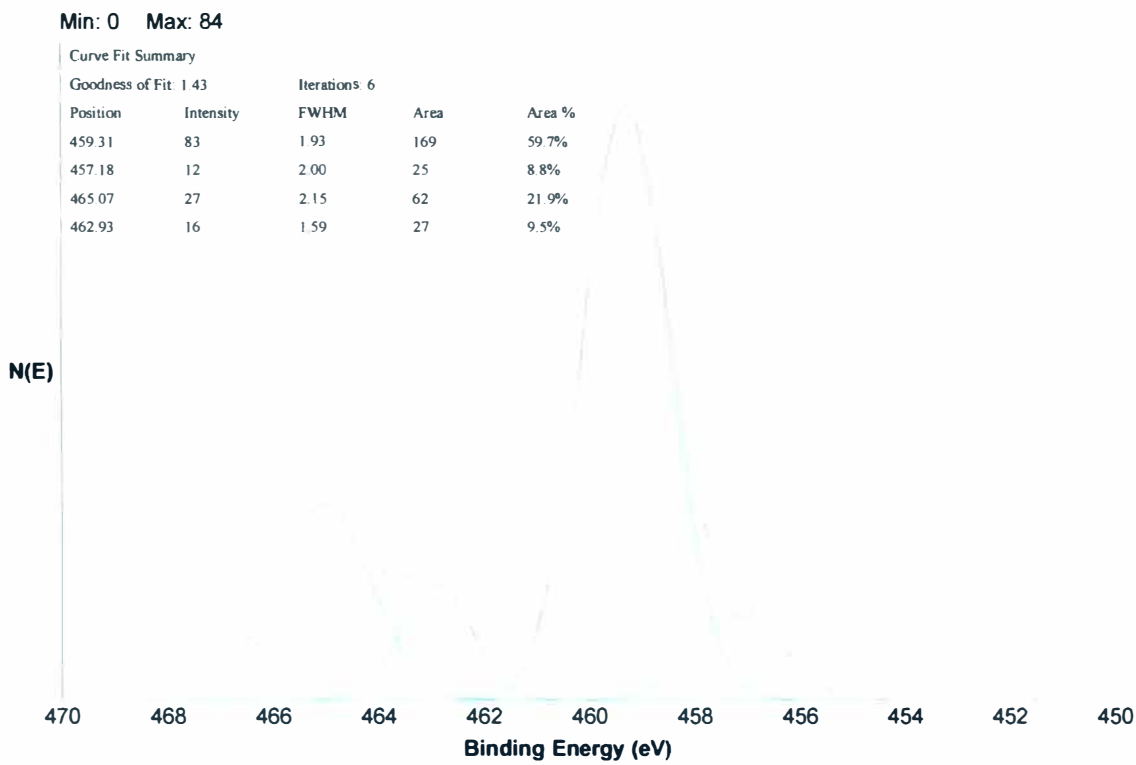

Figure B-13. Ti-2Months Sample after 30 Seconds Bombardment, Ti 2p

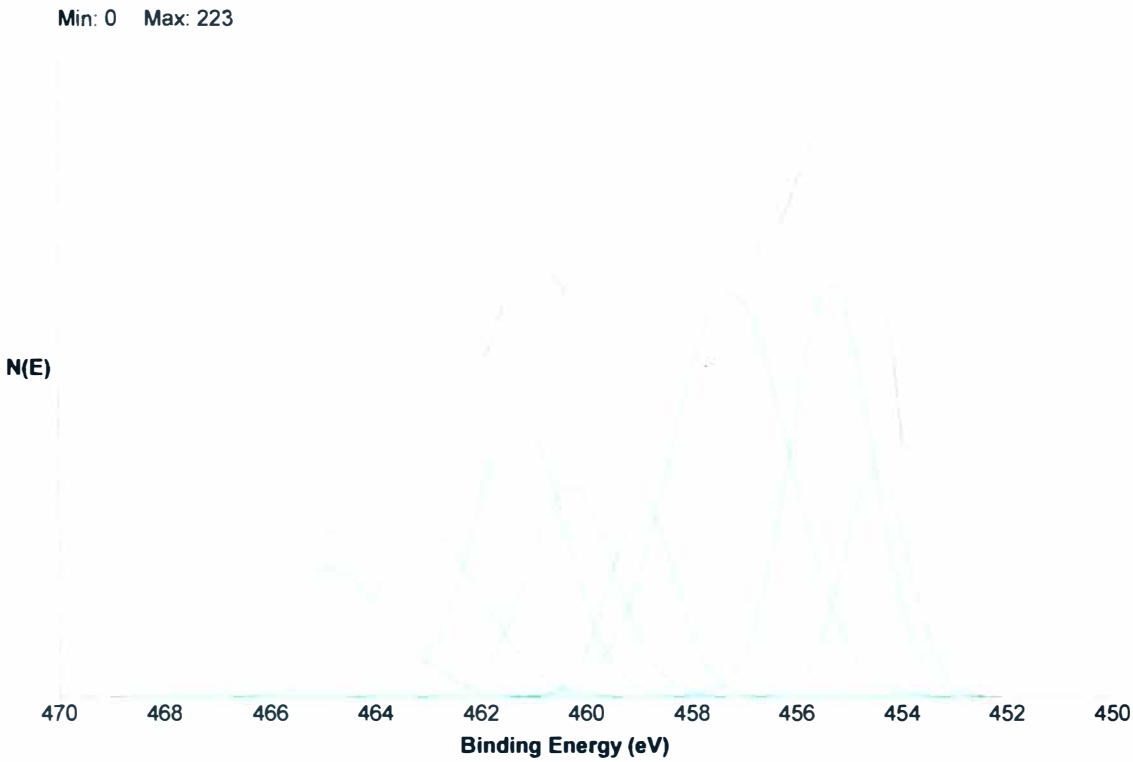

Figure B-14. Ti-2Months Sample after 10 Minutes Bombardment, Ti 2p

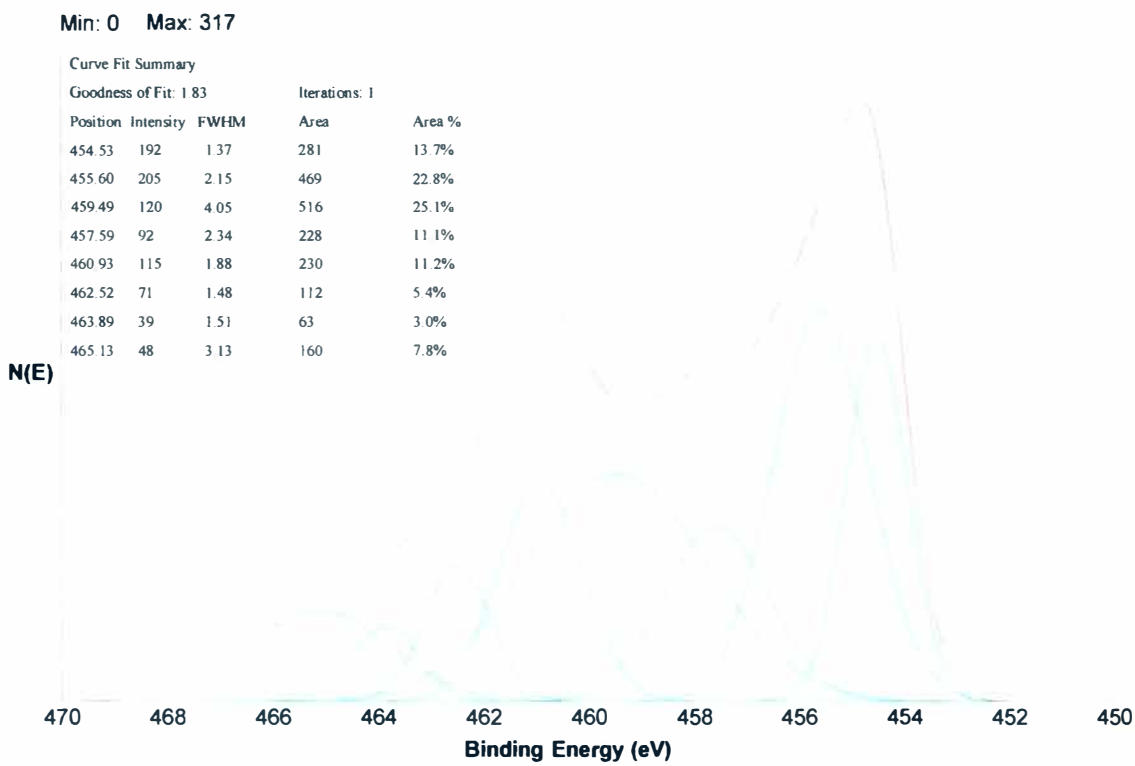

Figure B-15. Ti-2Months Sample after 20 Minutes Bombardment, Ti 2p

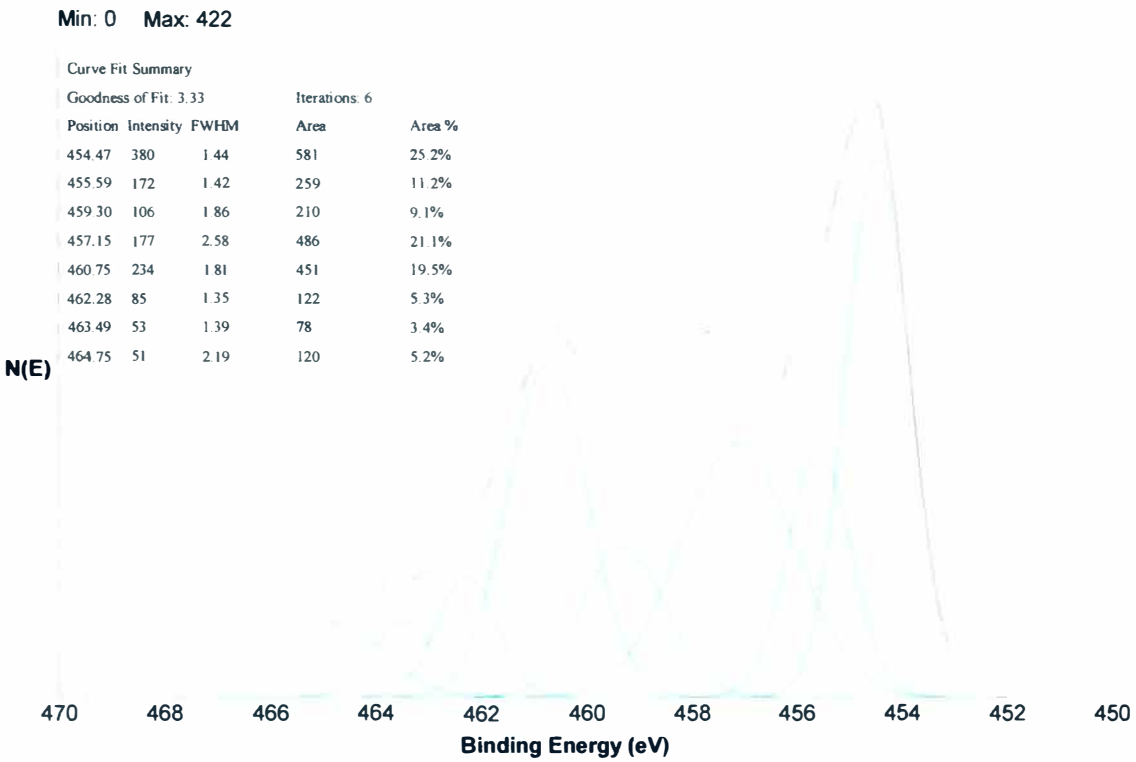

Figure B-16. Ti-2Months Sample after 30 Minutes Bombardment, Ti 2p

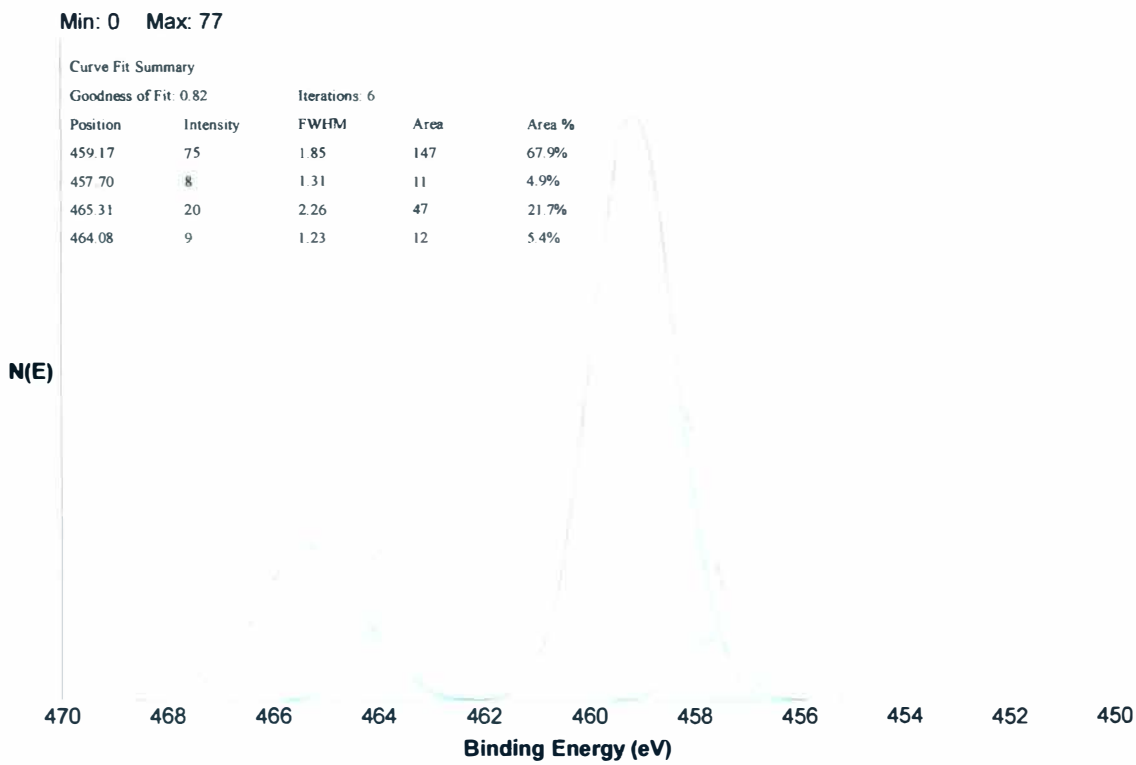

Figure B-17. Ti-3Months Sample after 30 Seconds Bombardment, Ti 2p

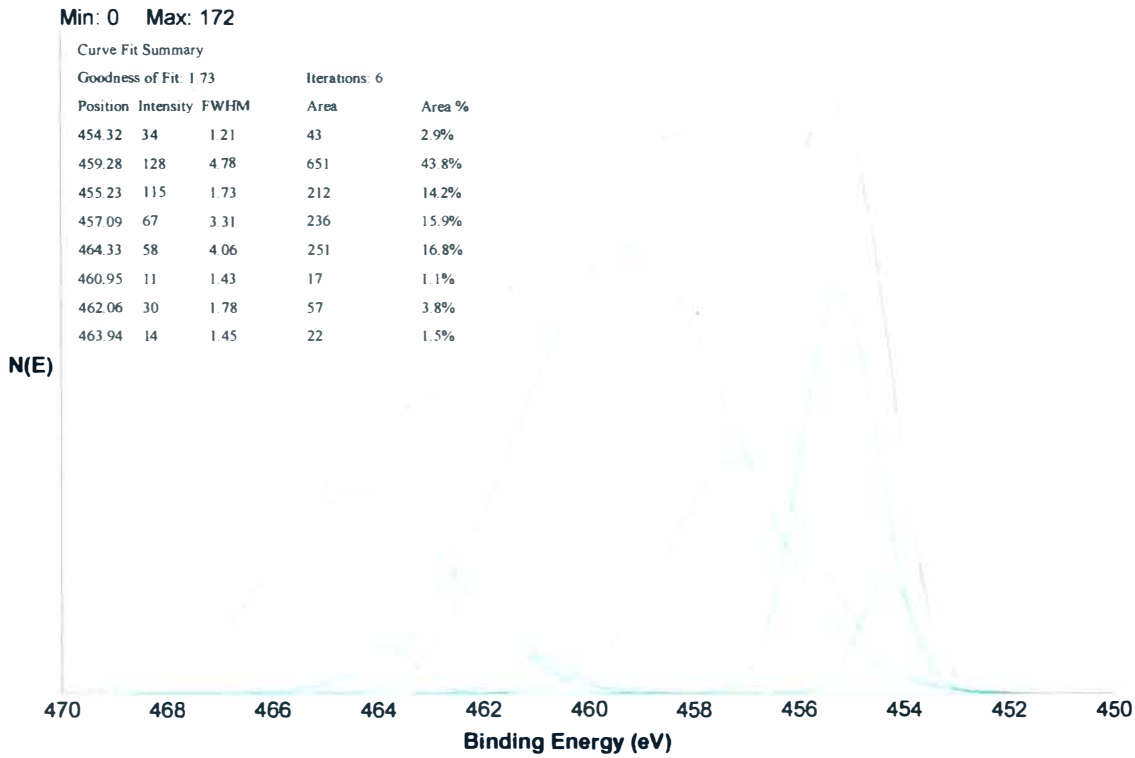

Figure B-18. Ti-3Months Sample after 10 Minutes Bombardment, Ti 2p

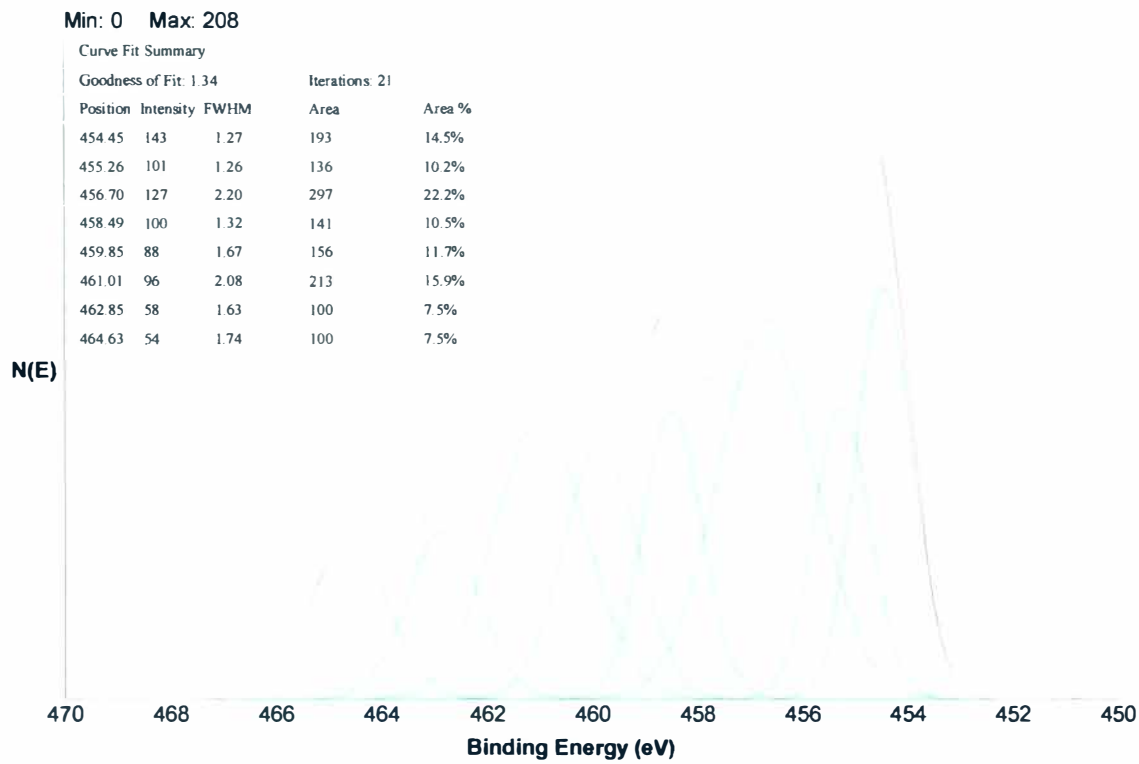

Figure B-19. Ti-3Months Sample after 20 Minutes Bombardment, Ti 2p

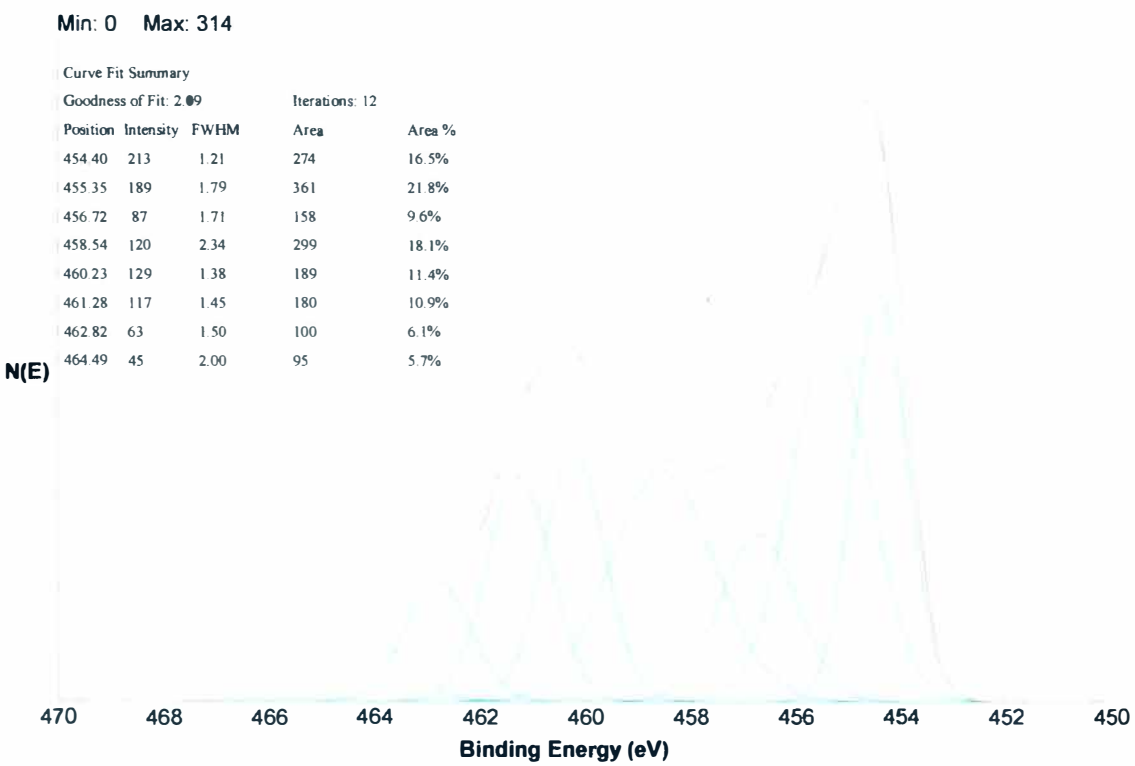

Figure B-20. Ti-3Months Sample after 30 Minutes Bombardment, Ti 2p

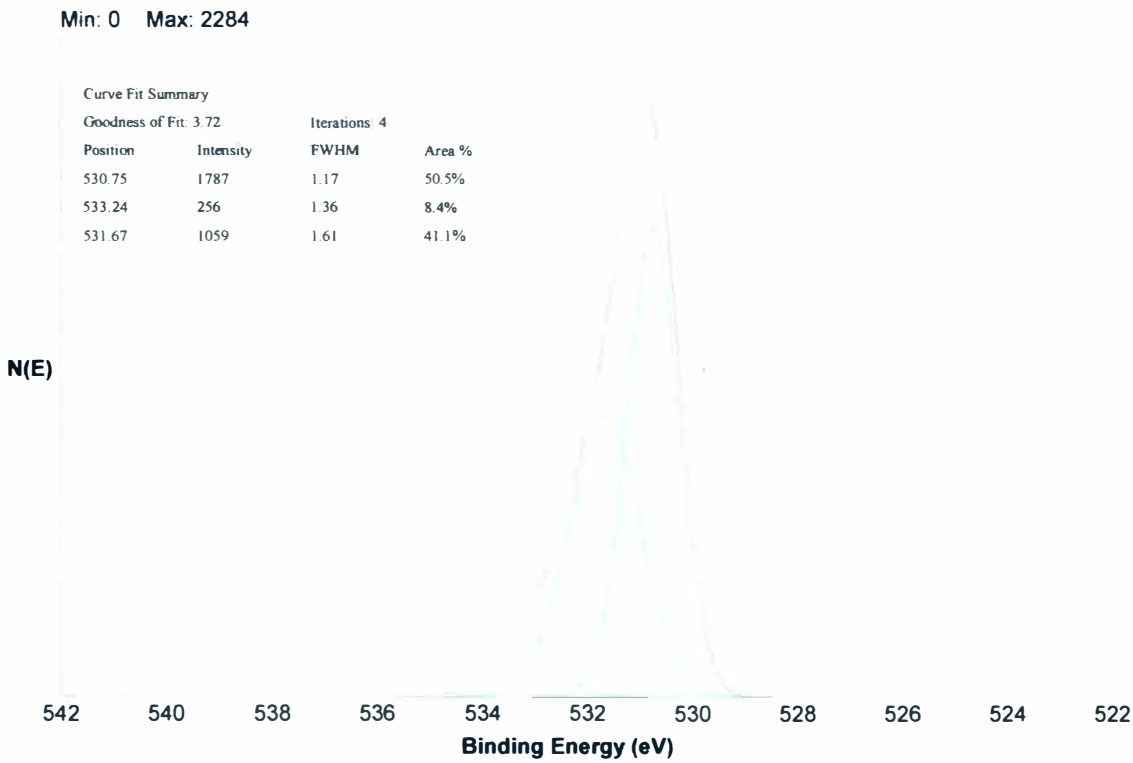

Figure B-21. Ti-Polished Sample after 30 Seconds Bombardment, O 1s

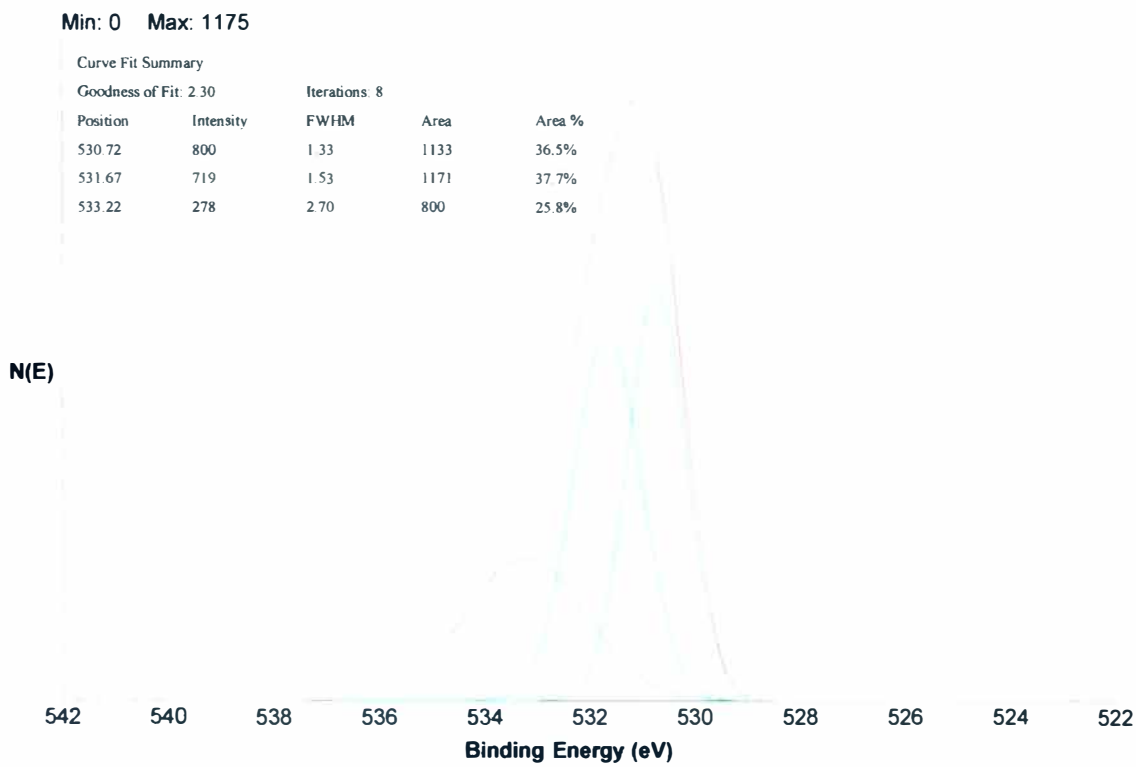

Figure B-22. Ti-Polished Sample after 10 Minutes Bombardment, O 1s

Min: 0 Max: 994

Curve Fit Summary

Goodness of Fit: 1.99 Iterations: 20

Position	Intensity	FWHM	Area	Area %
530.75	595	1.42	899	34.1%
531.67	634	1.57	1060	40.1%
533.24	241	2.66	681	25.8%

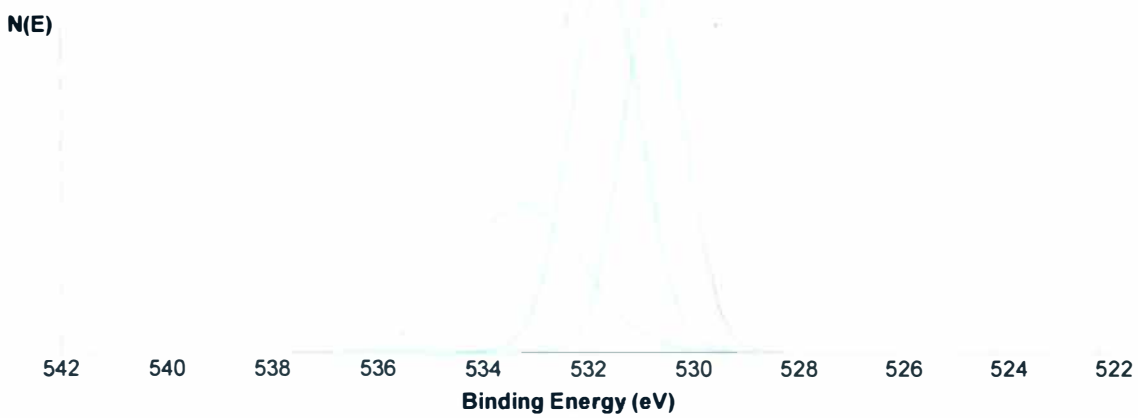

Figure B-23. Ti-Polished Sample after 20 Minutes Bombardment, O 1s

Min: 0 Max: 879

Curve Fit Summary

Goodness of Fit: 1.93 Iterations: 10

Position	Intensity	FWHM	Area	Area %
530.72	532	1.51	855	34.7%
531.67	559	1.66	988	40.1%
533.24	234	2.50	622	25.2%

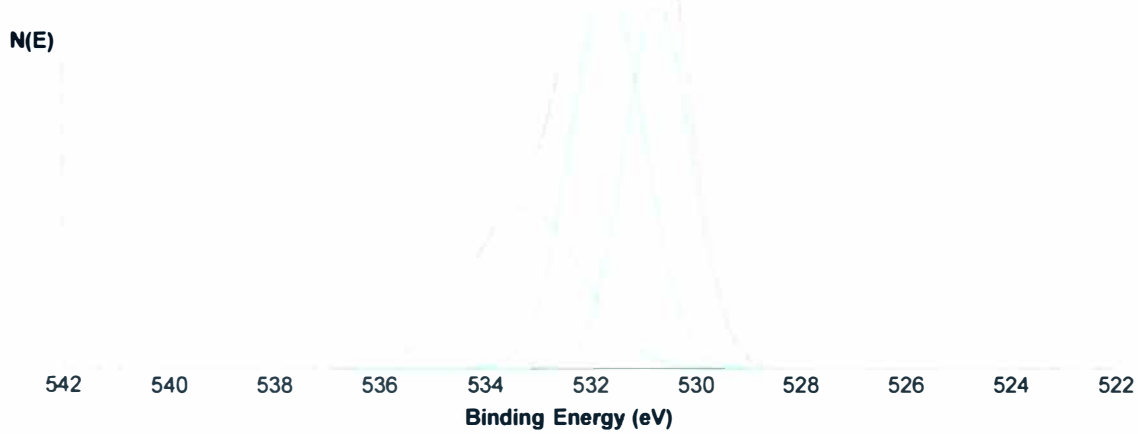

Figure B-24. Ti-Polished Sample after 30 Minutes Bombardment, O 1s

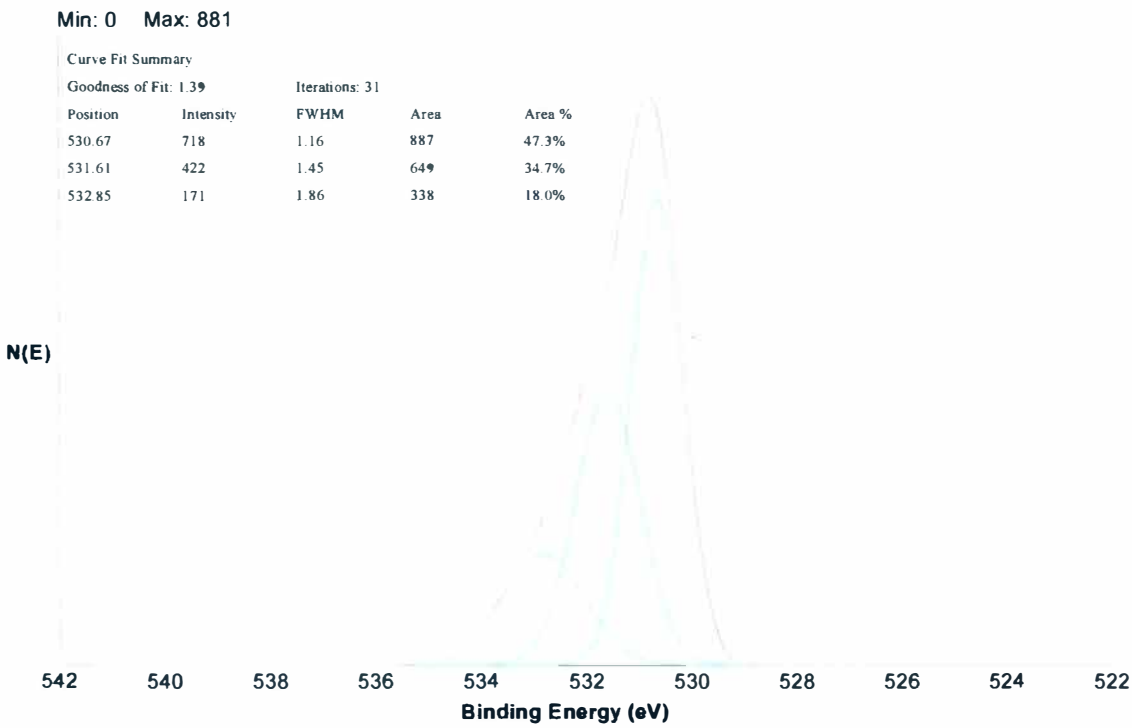

Figure B-25. Ti-2Weeks Sample after 30 Seconds Bombardment, O 1s

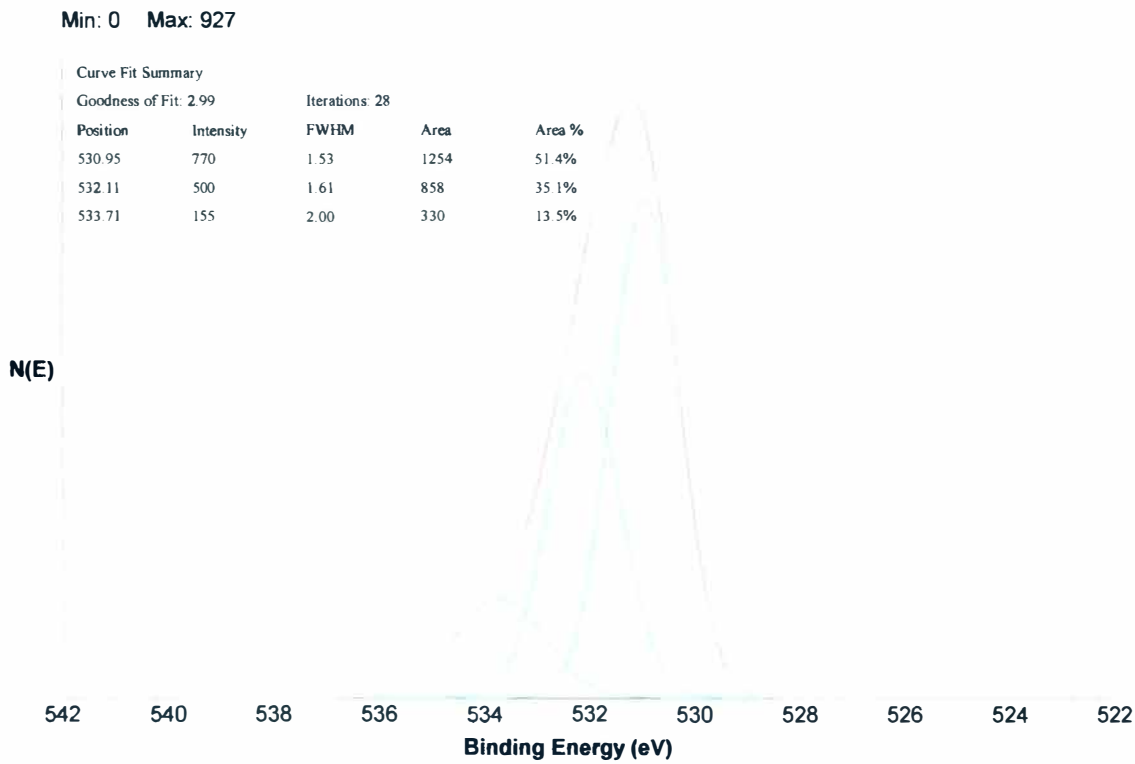

Figure B-26. Ti-2Weeks Sample after 10 Minutes Bombardment, O 1s

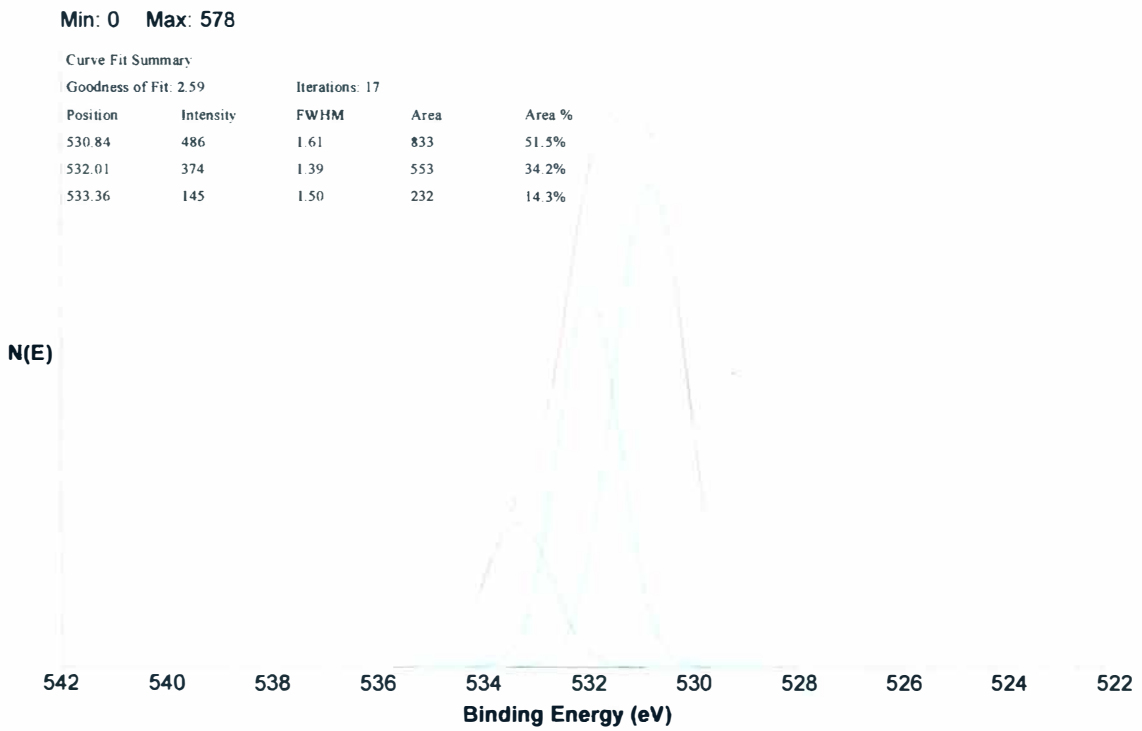

Figure B-27. Ti-2Weeks Sample after 20 Minutes Bombardment, O 1s

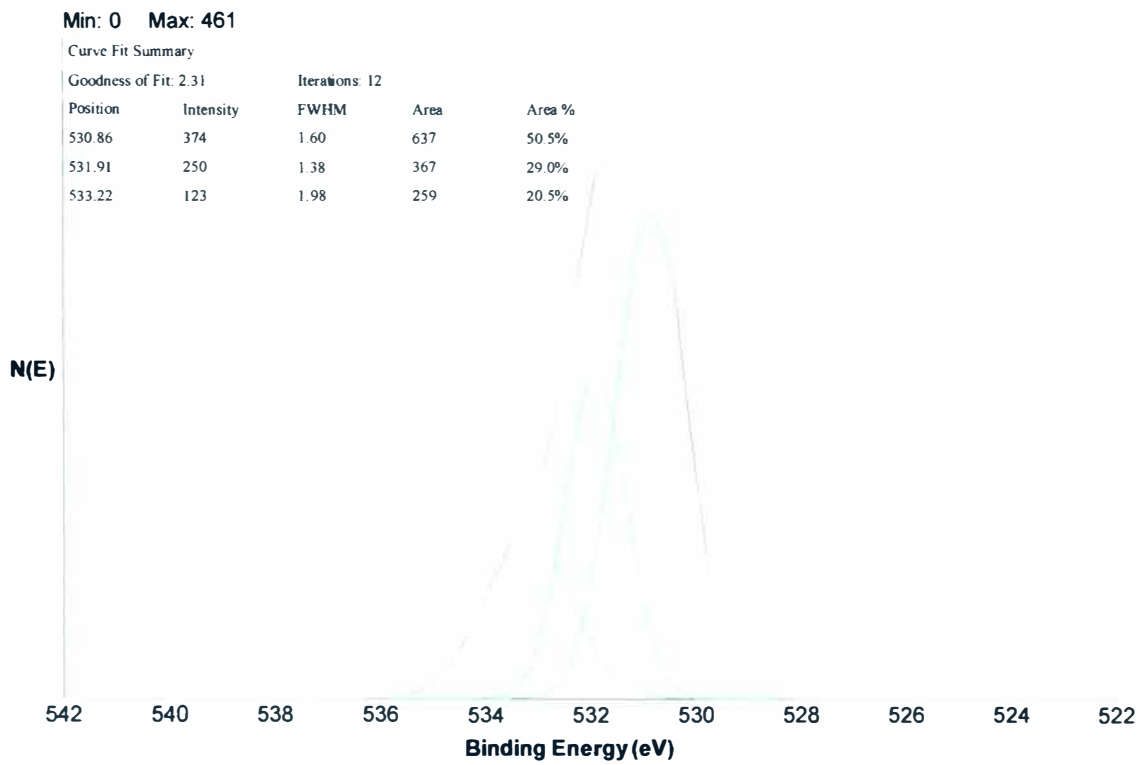

Figure B-28. Ti-2Weeks Sample after 30 Minutes Bombardment, O 1s

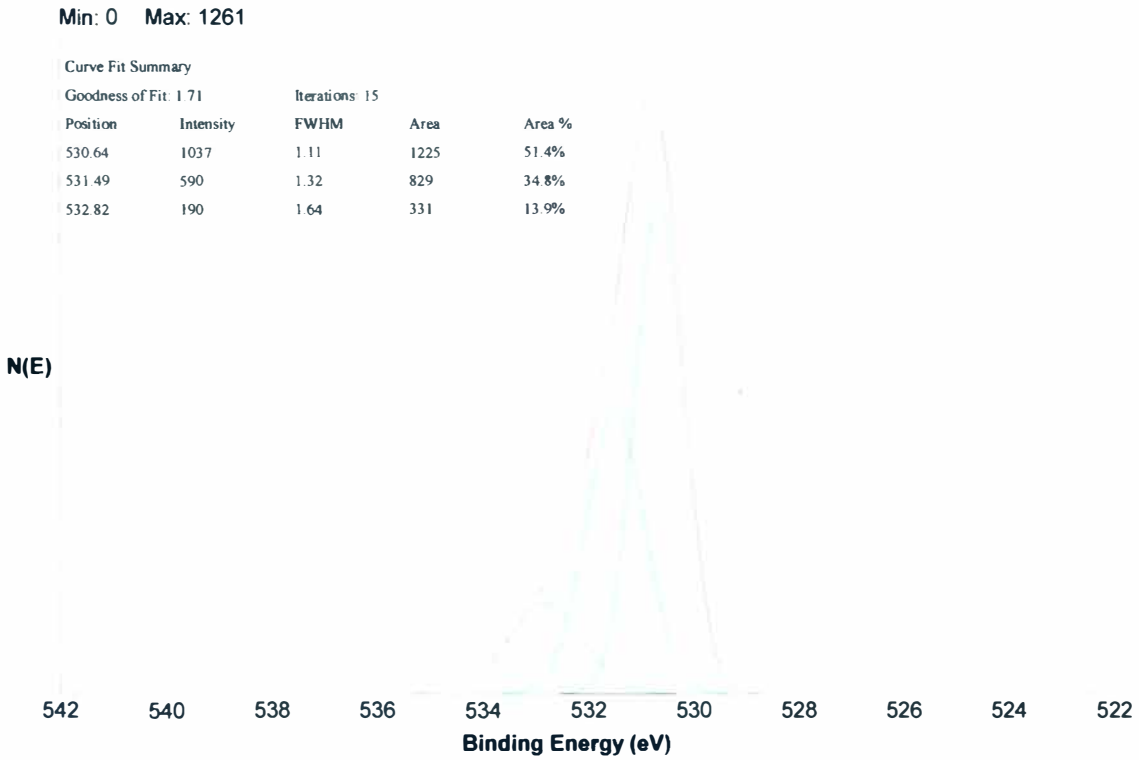

Figure B-29. Ti-1Month Sample after 30 Seconds Bombardment, O 1s

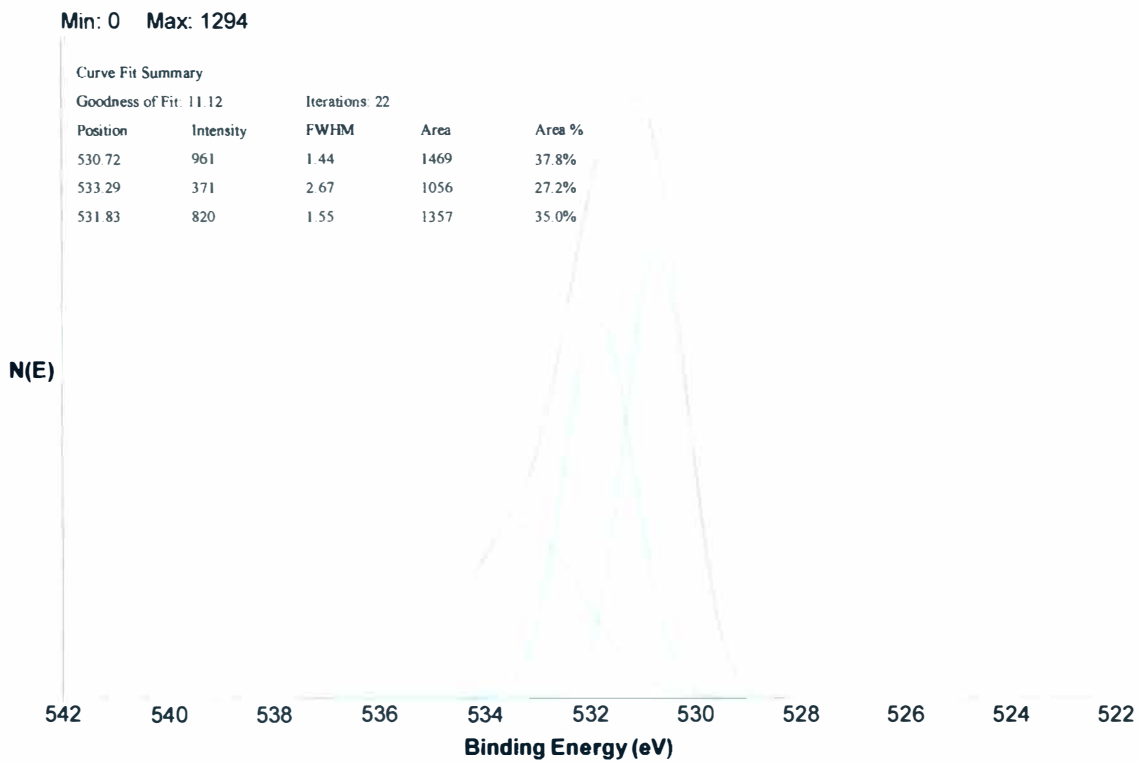

Figure B-30. Ti-1Month Sample after 10 Minutes Bombardment, O 1s

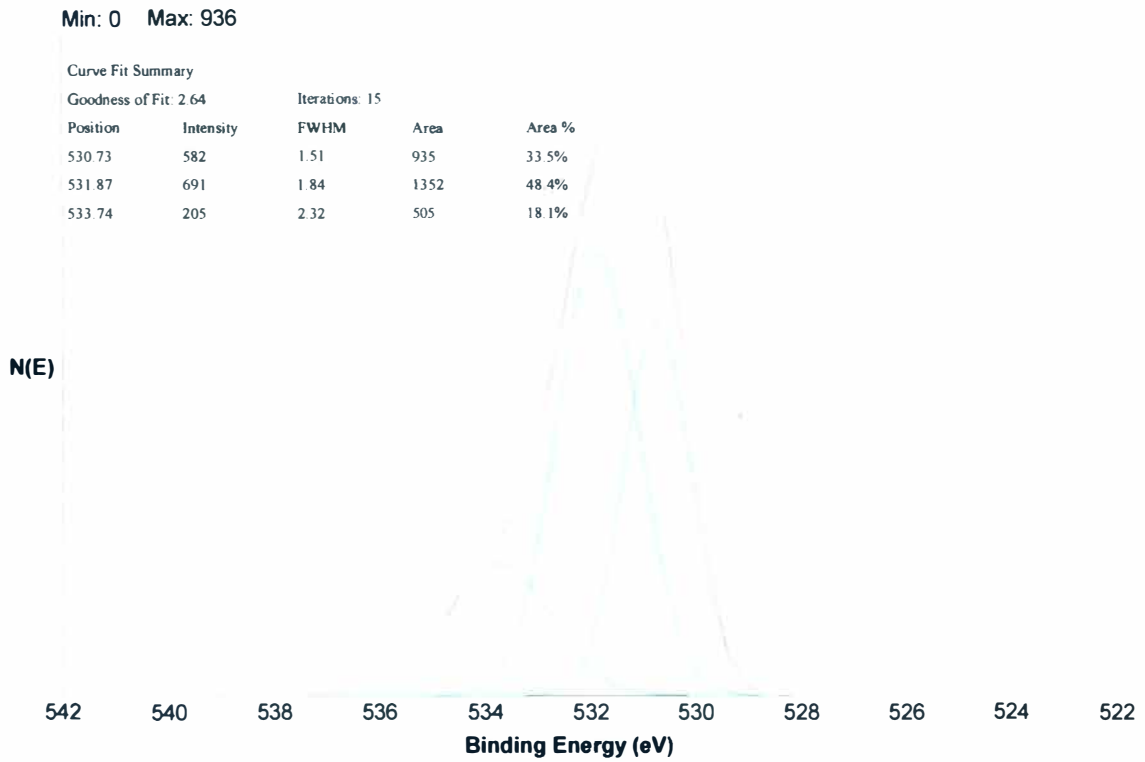

Figure B-31. Ti-1Month Sample after 20 Minutes Bombardment, O 1s

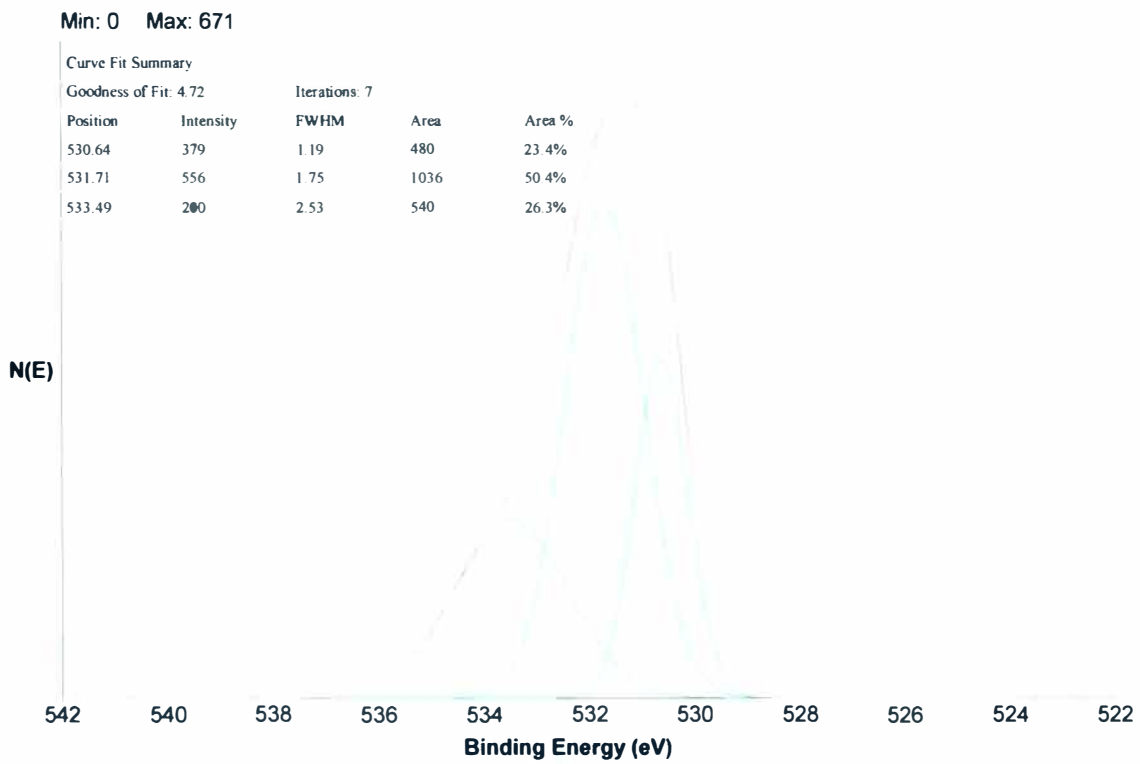

Figure B-32. Ti-1Month Sample after 30 Minutes Bombardment, O 1s

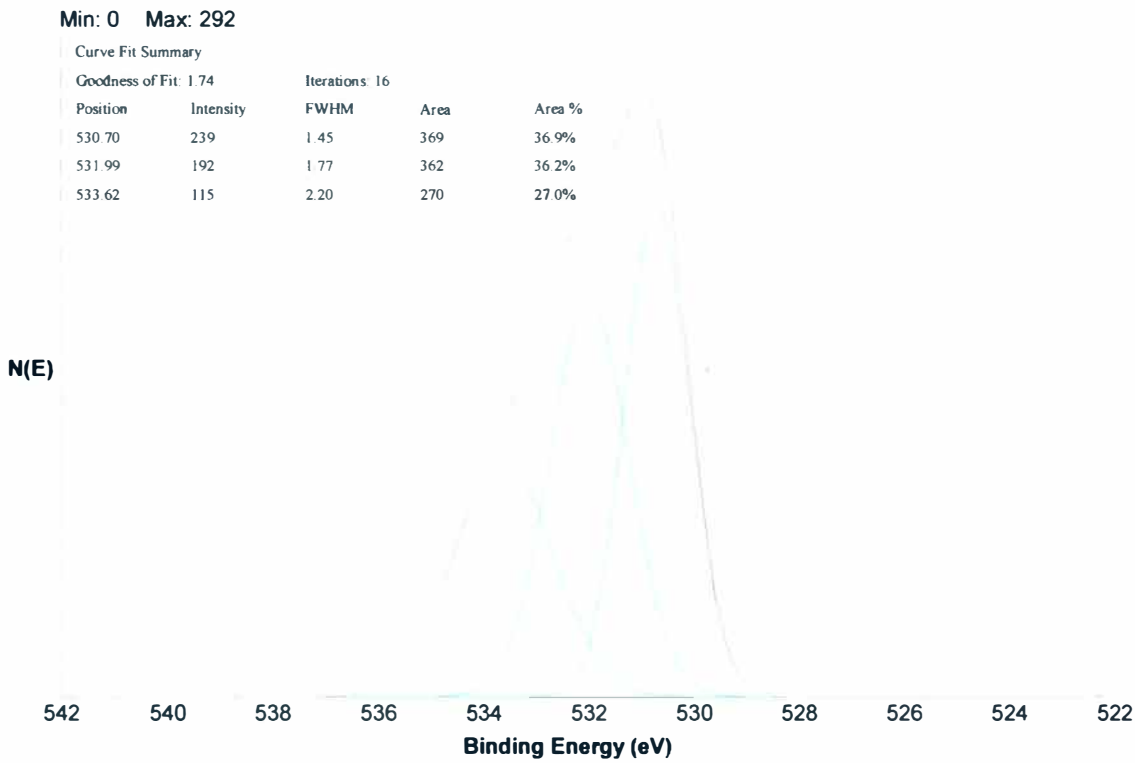

Figure B-33. Ti-2Months Sample after 30 Seconds Bombardment, O 1s

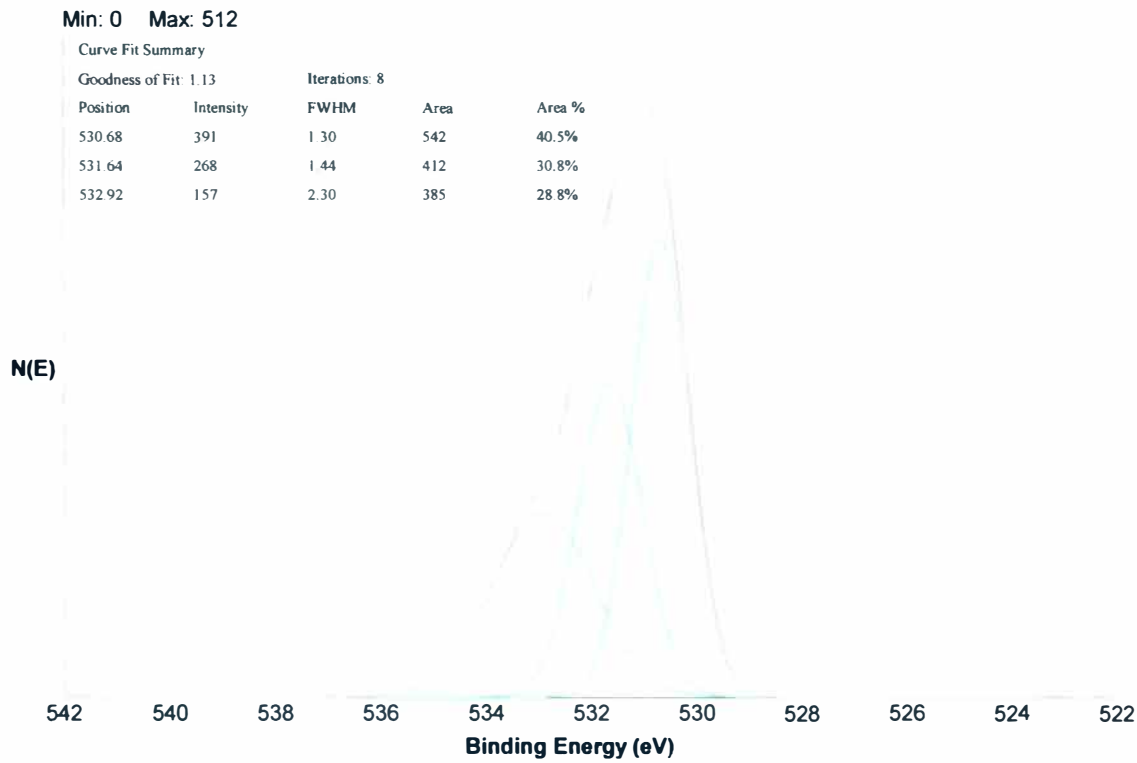

Figure B-34. Ti-2Months Sample after 10 Minutes Bombardment, O 1s

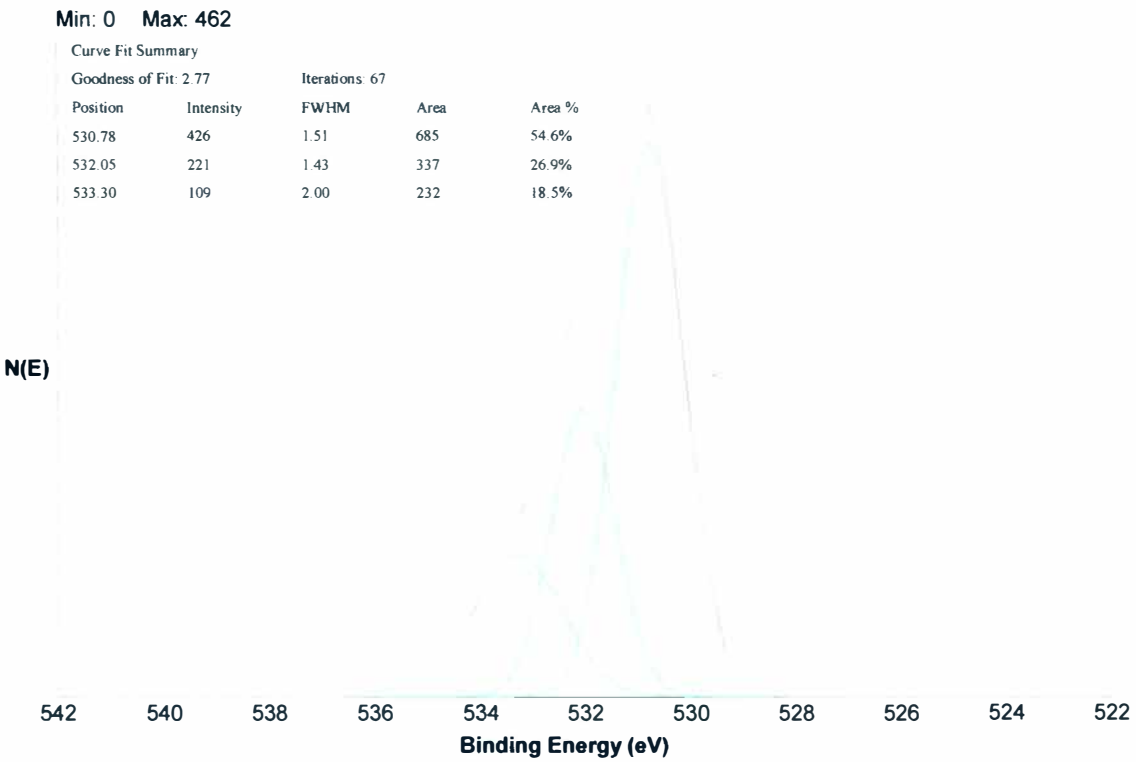

Figure B-35. Ti-2Months Sample after 20 Minutes Bombardment, O 1s

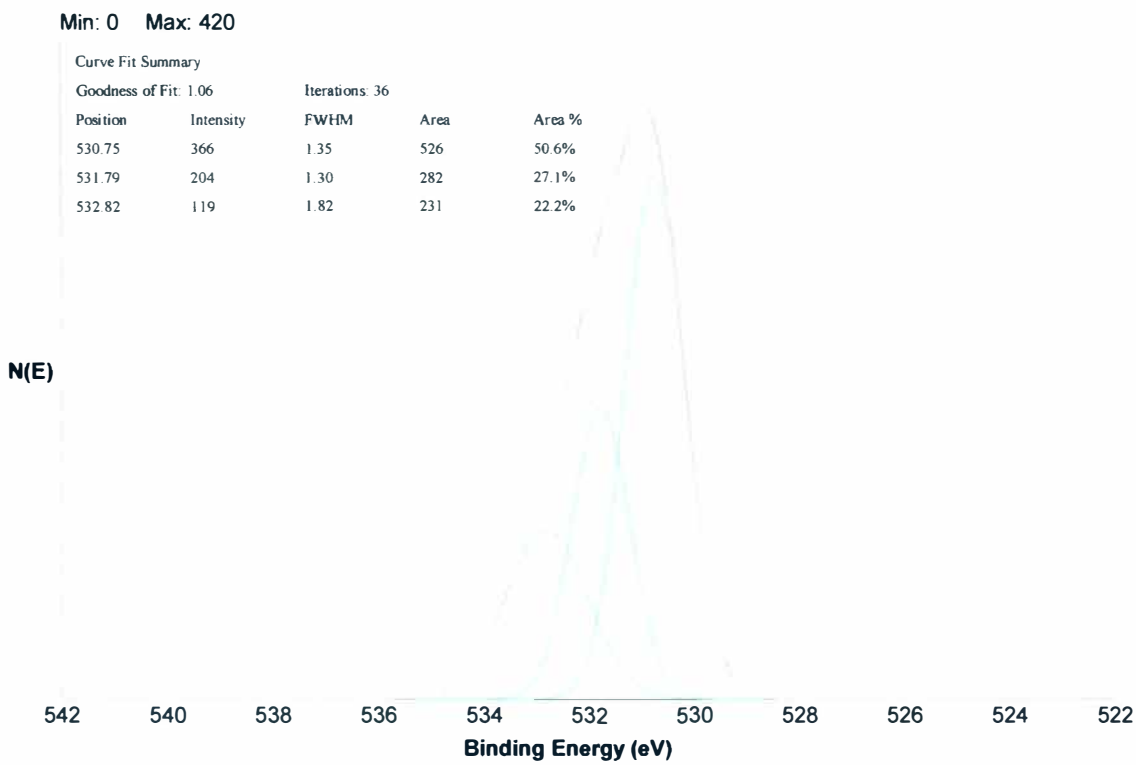

Figure B-36. Ti-2Months Sample after 30 Minutes Bombardment, O 1s

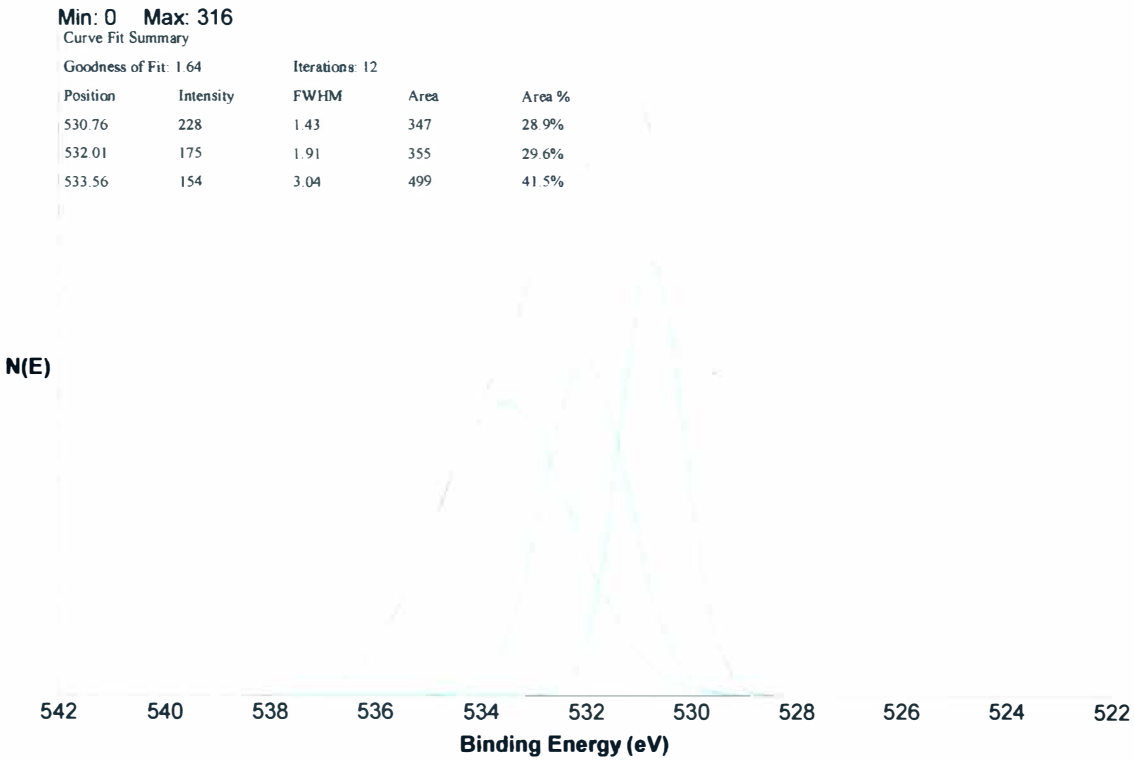

Figure B-37. Ti-3Months Sample after 30 Seconds Bombardment, O 1s

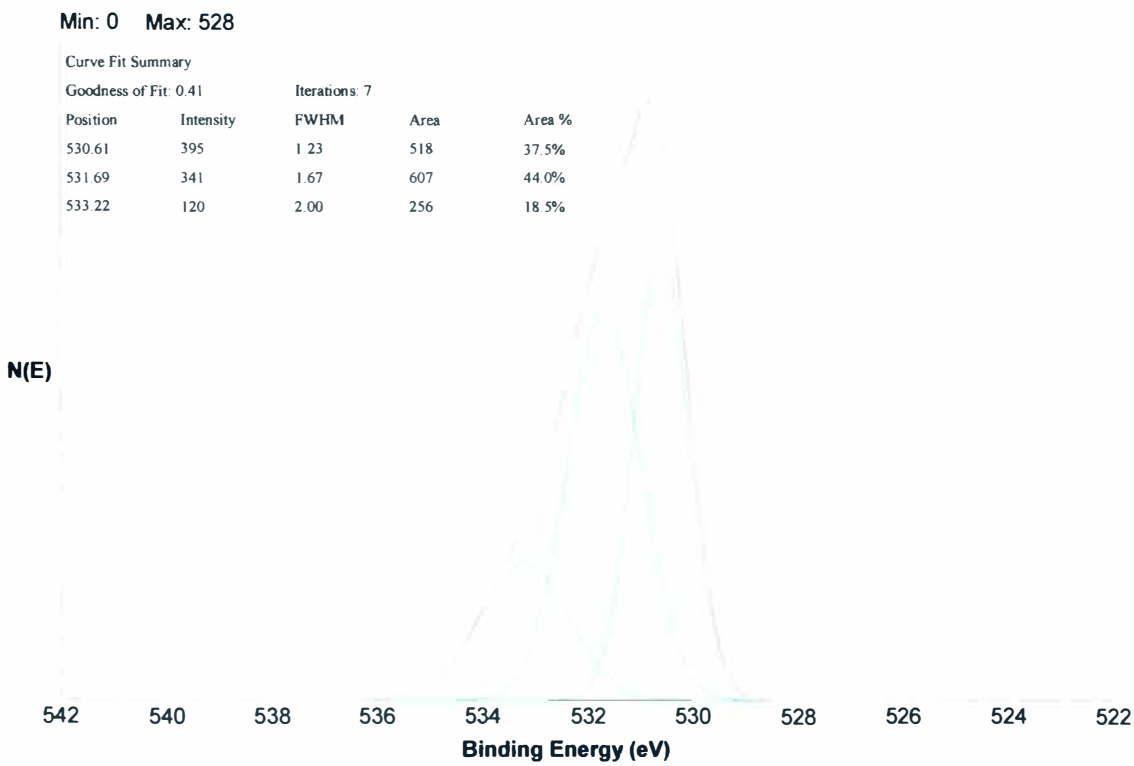

Figure B-38. Ti-3Months Sample after 10 Minutes Bombardment, O 1s

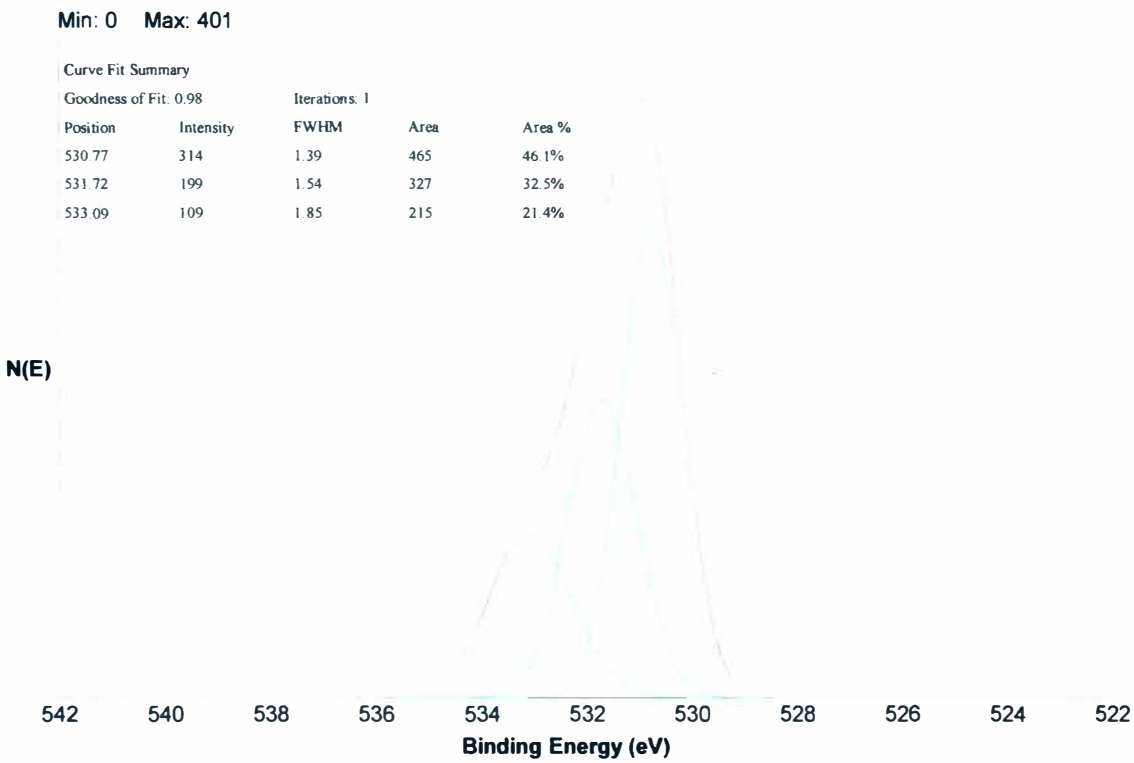

Figure B-39. Ti-3Months Sample after 20 Minutes Bombardment, O 1s

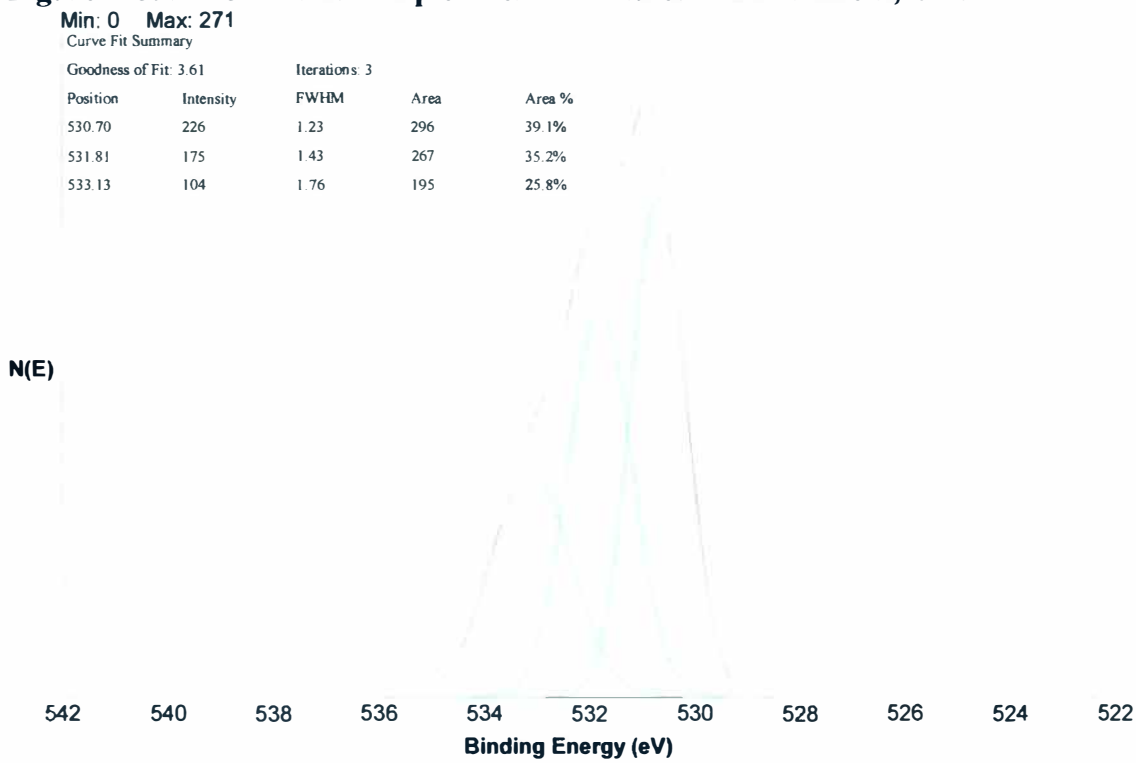

Figure B-40. Ti-3Months Sample after 30 Minutes Bombardment, O 1s

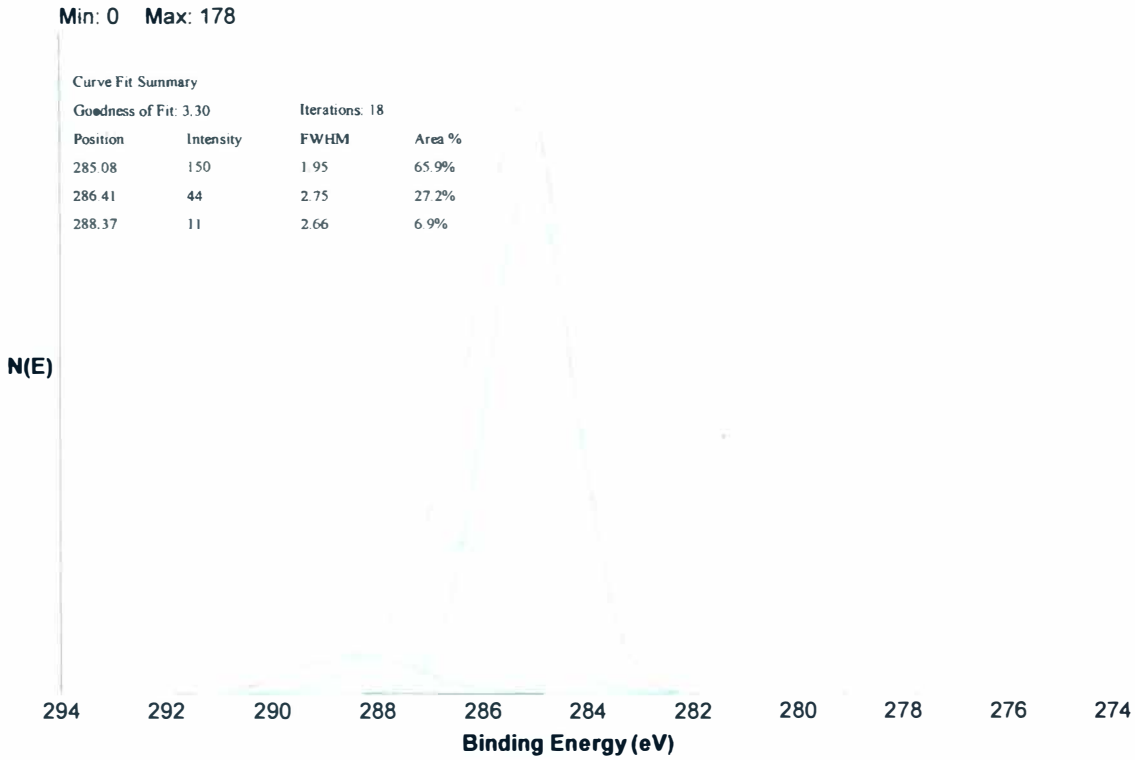

Figure B-41. Ti-Polished Sample after 30 Seconds Bombardment, C 1s

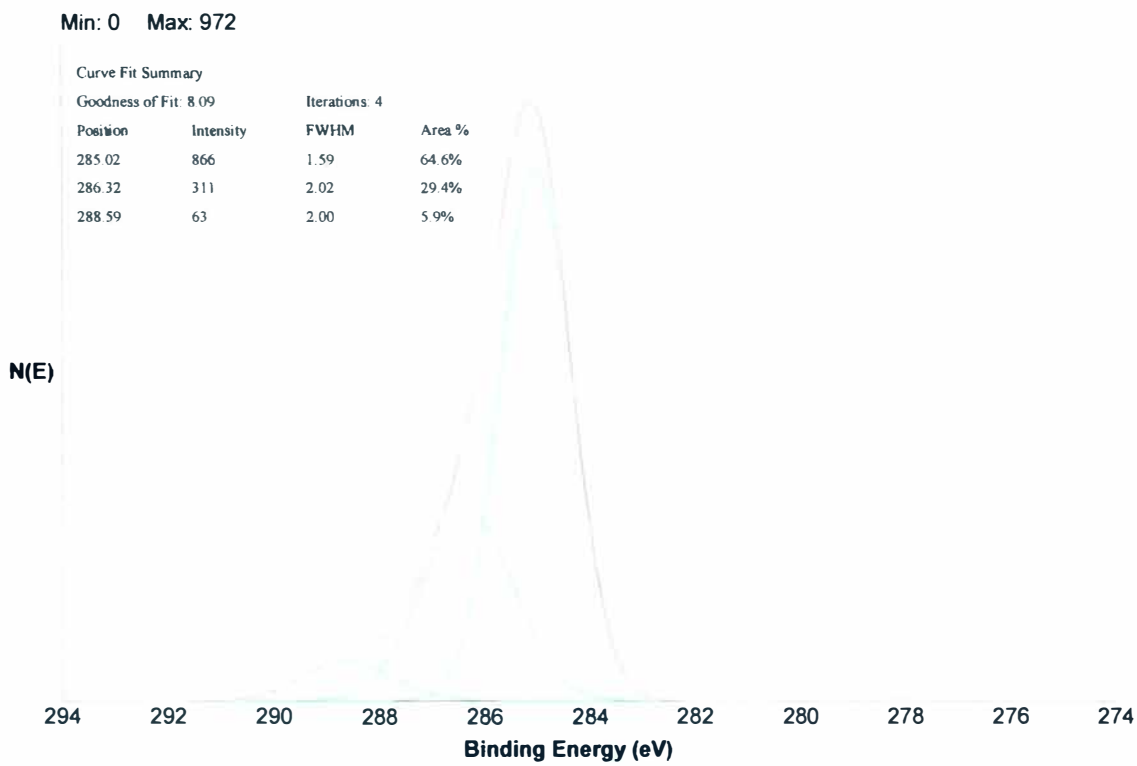

Figure B-42. Ti-2Weeks Sample after 30 Seconds Bombardment, C 1s

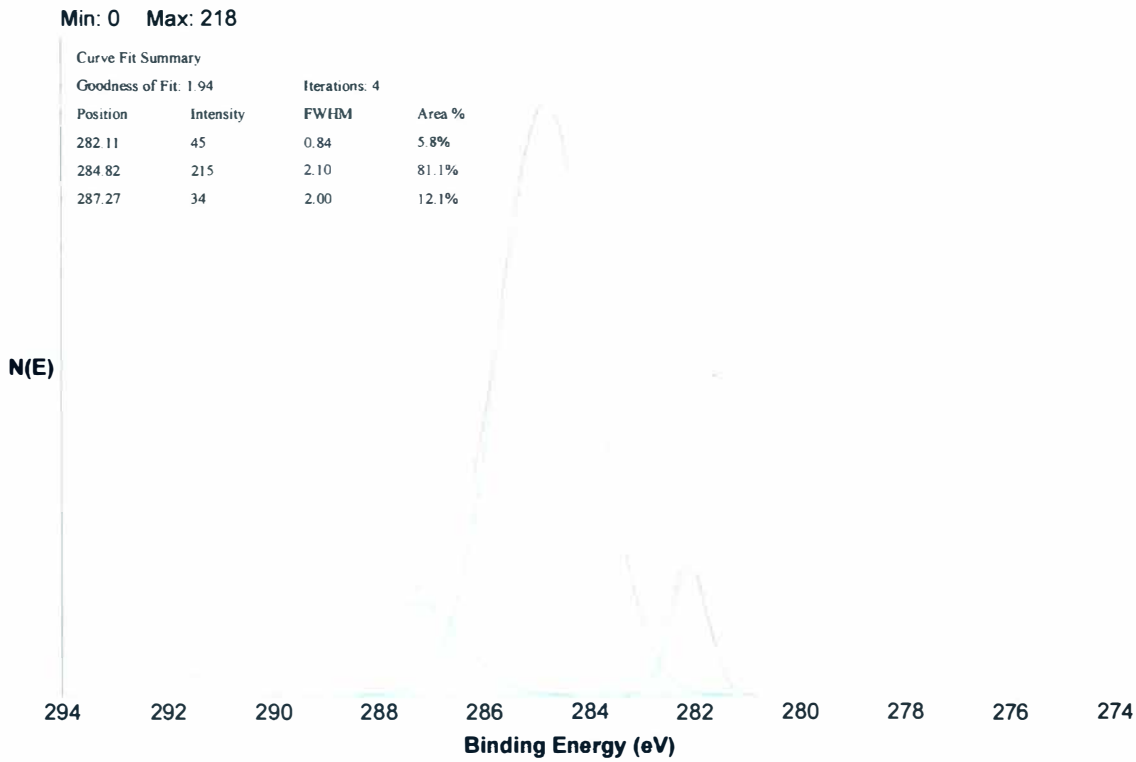

Figure B-43. Ti-2Weeks Sample after 10 Minutes Bombardment, C 1s

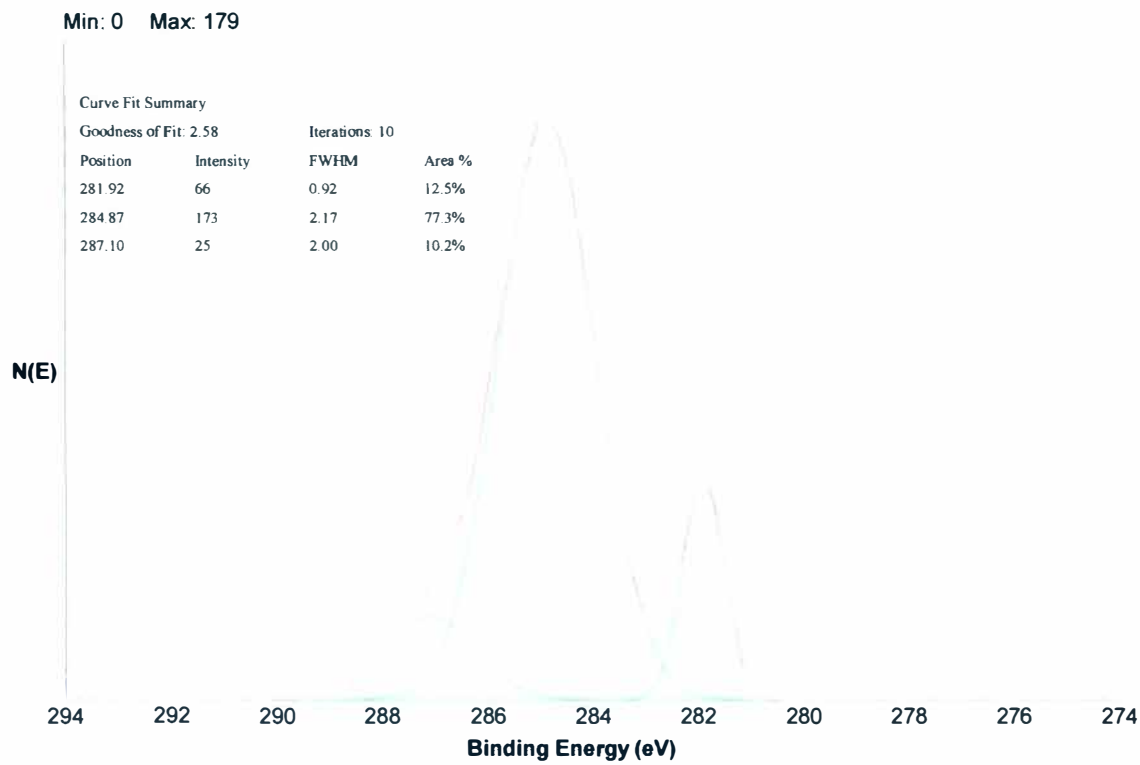

Figure B-44. Ti-2Weeks Sample after 20 Minutes Bombardment, C 1s

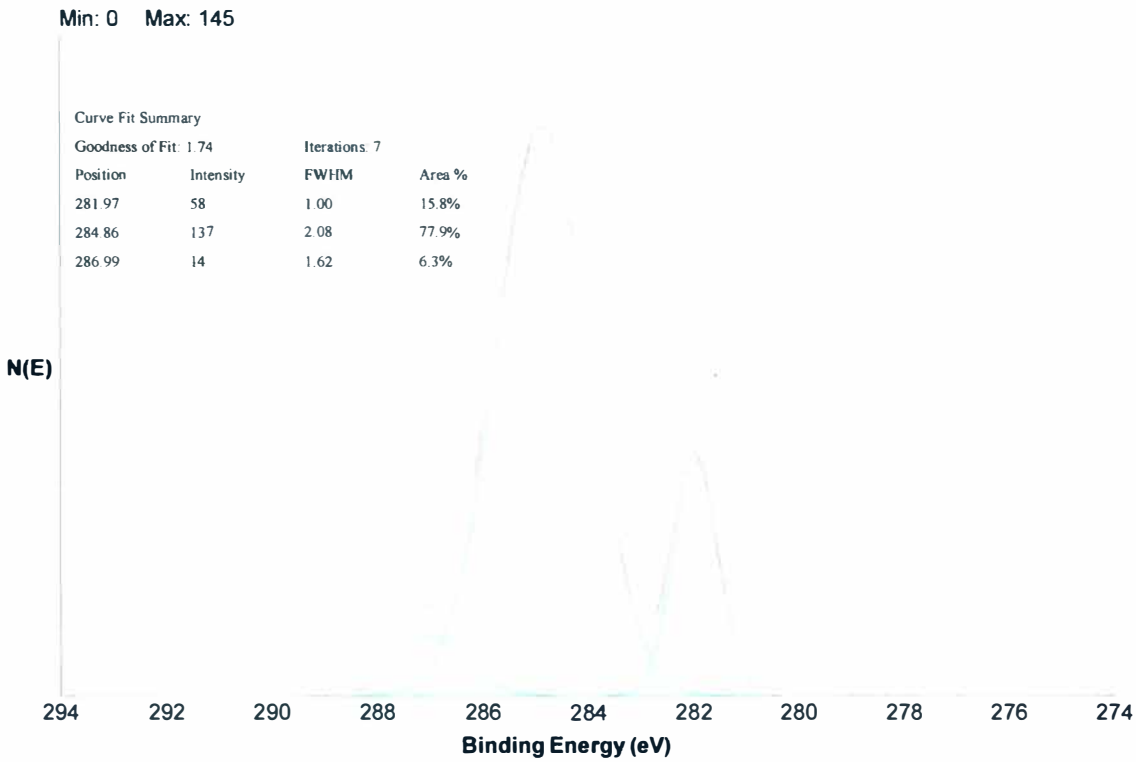

Figure B-45. Ti-2Weeks Sample after 30 Minutes Bombardment, C 1s

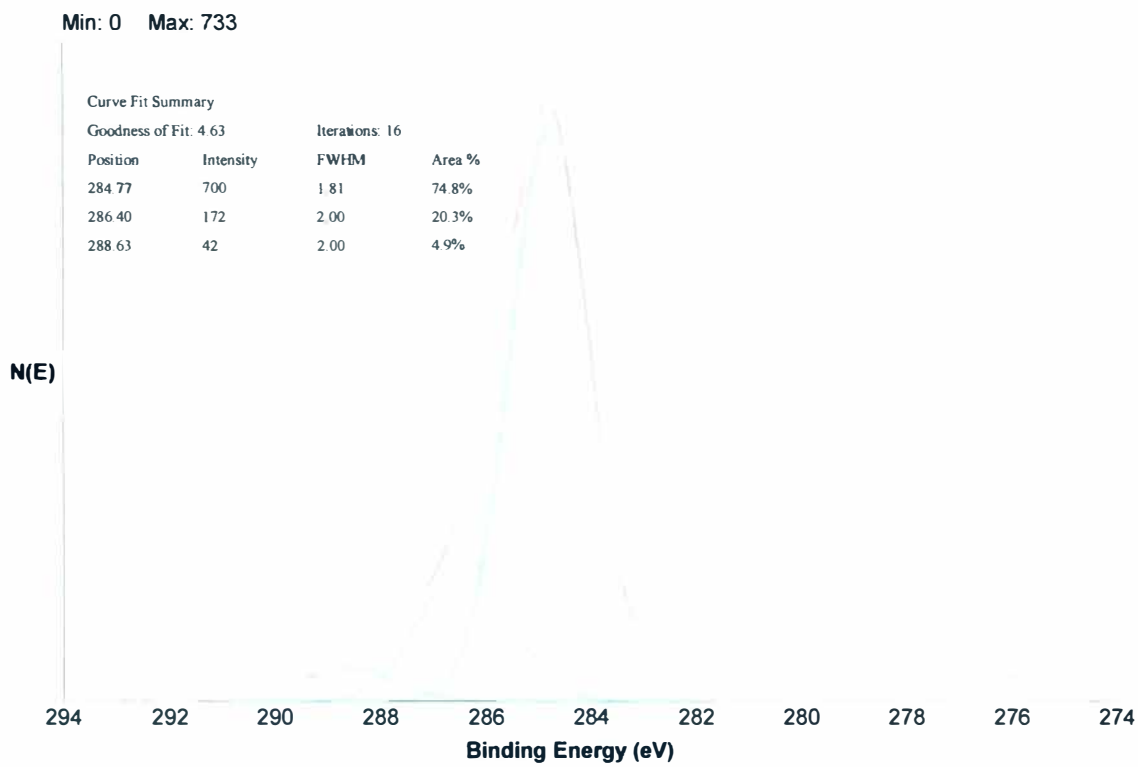

Figure B-46. Ti-1Month Sample after 30 Seconds Bombardment, C 1s

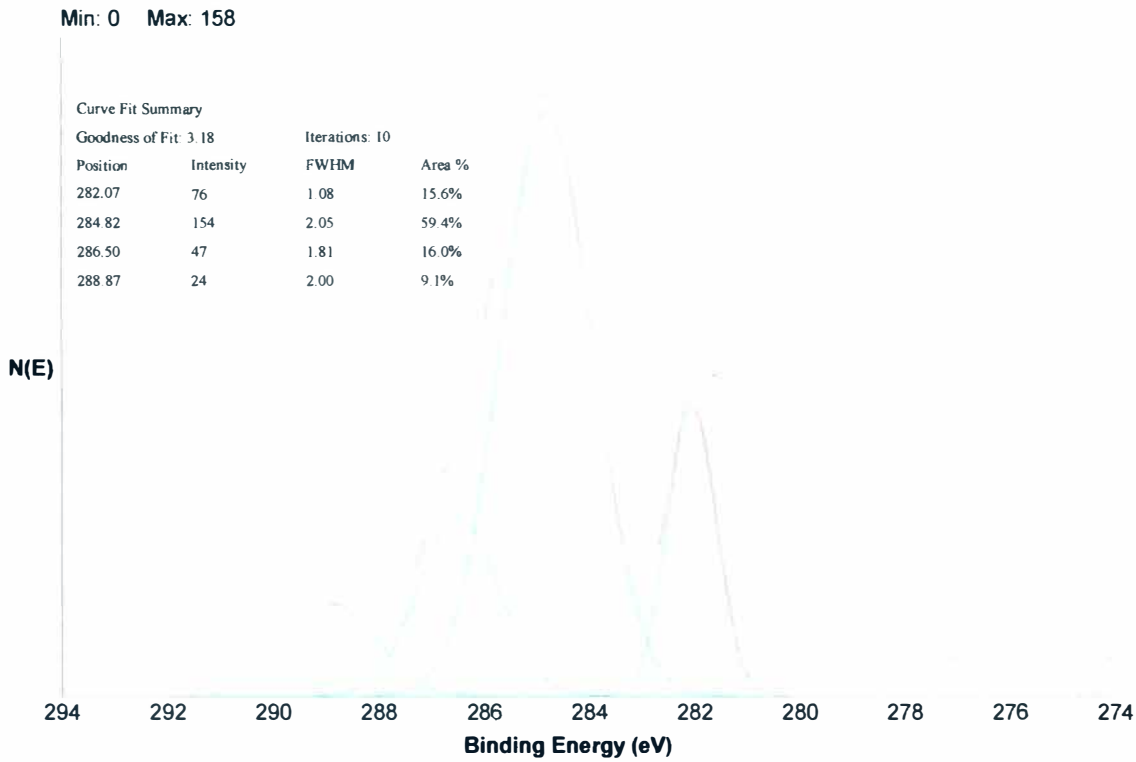

Figure B-47. Ti-1Month Sample after 10 Minutes Bombardment, C 1s

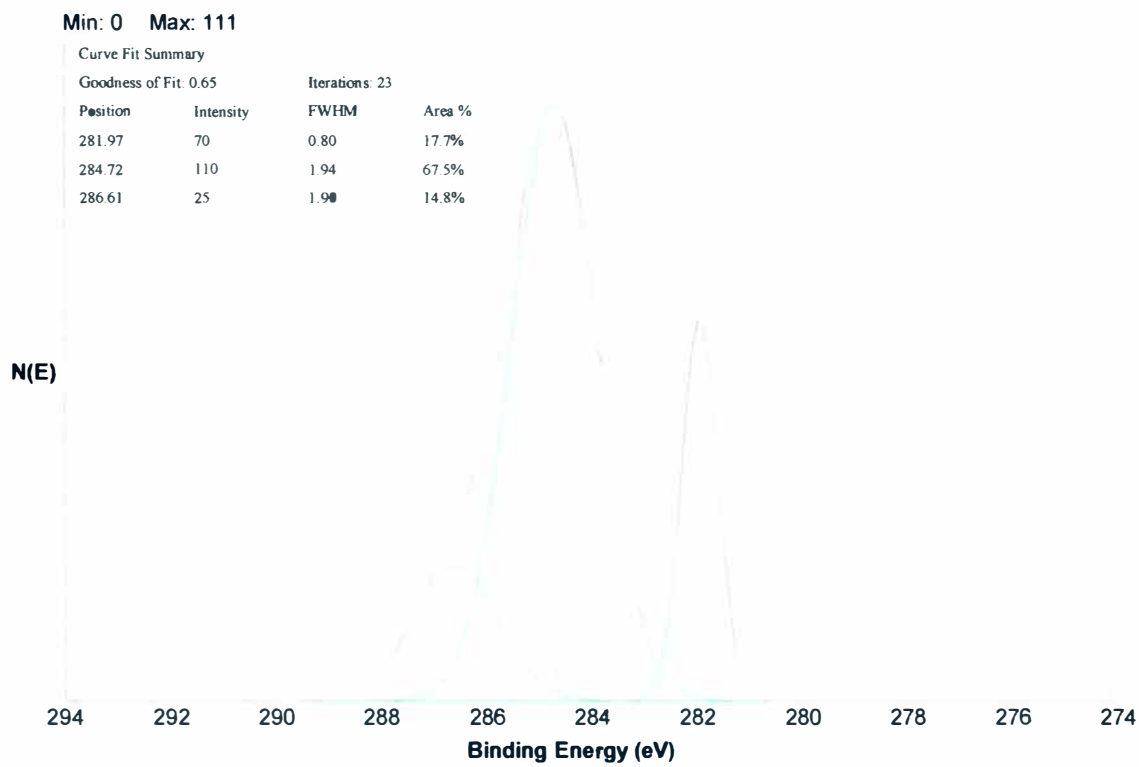

Figure B-48. Ti-1Month Sample after 20 Minutes Bombardment, C 1s

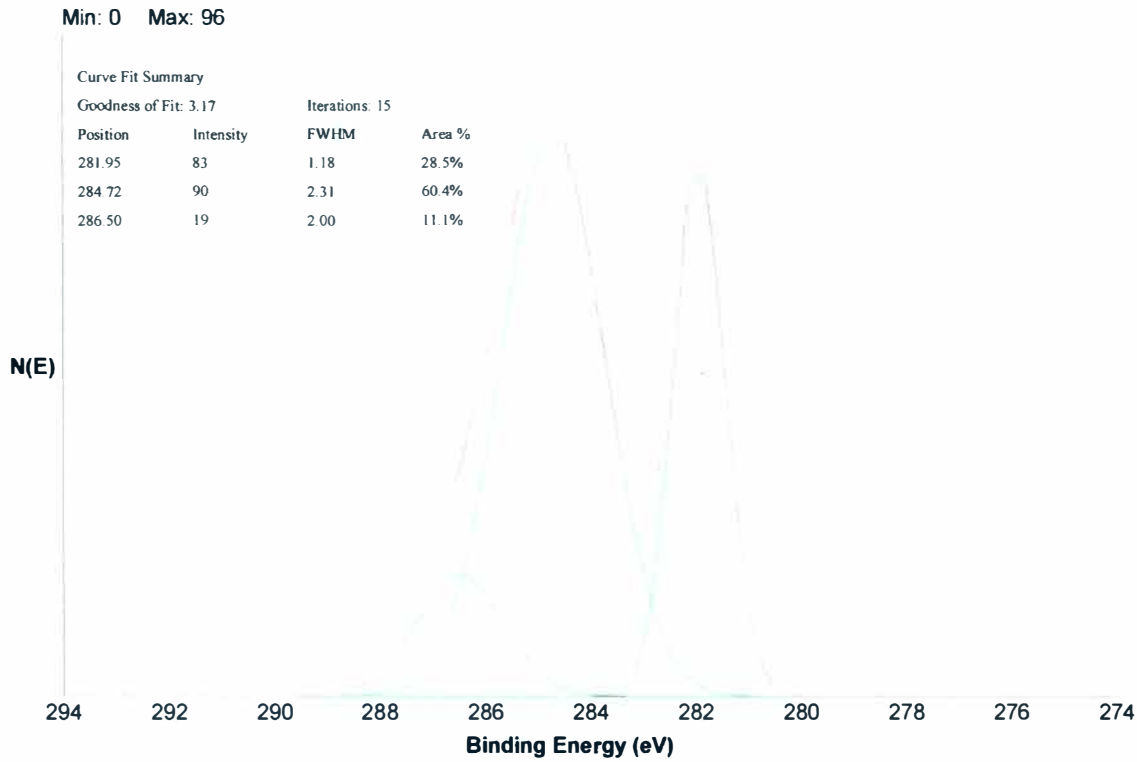

Figure B-49. Ti-1Month Sample after 30 Minutes Bombardment, C 1s

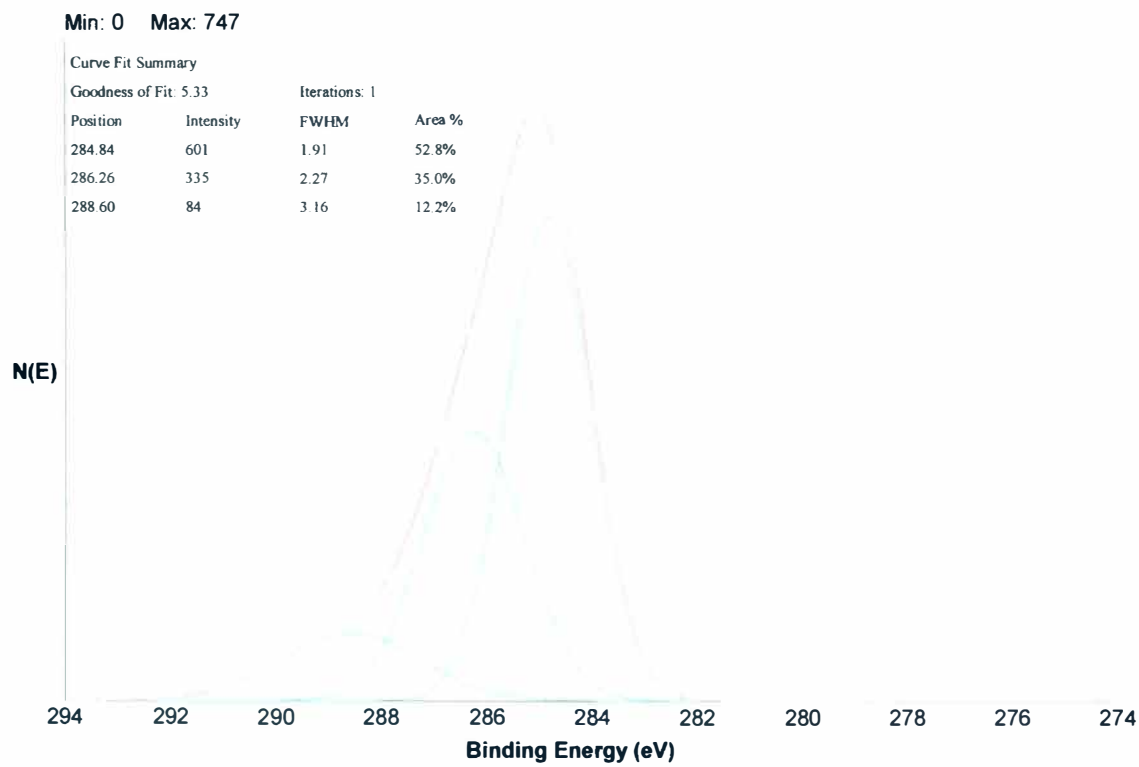

Figure B-50. Ti-2Months Sample after 30 Seconds Bombardment, C 1s

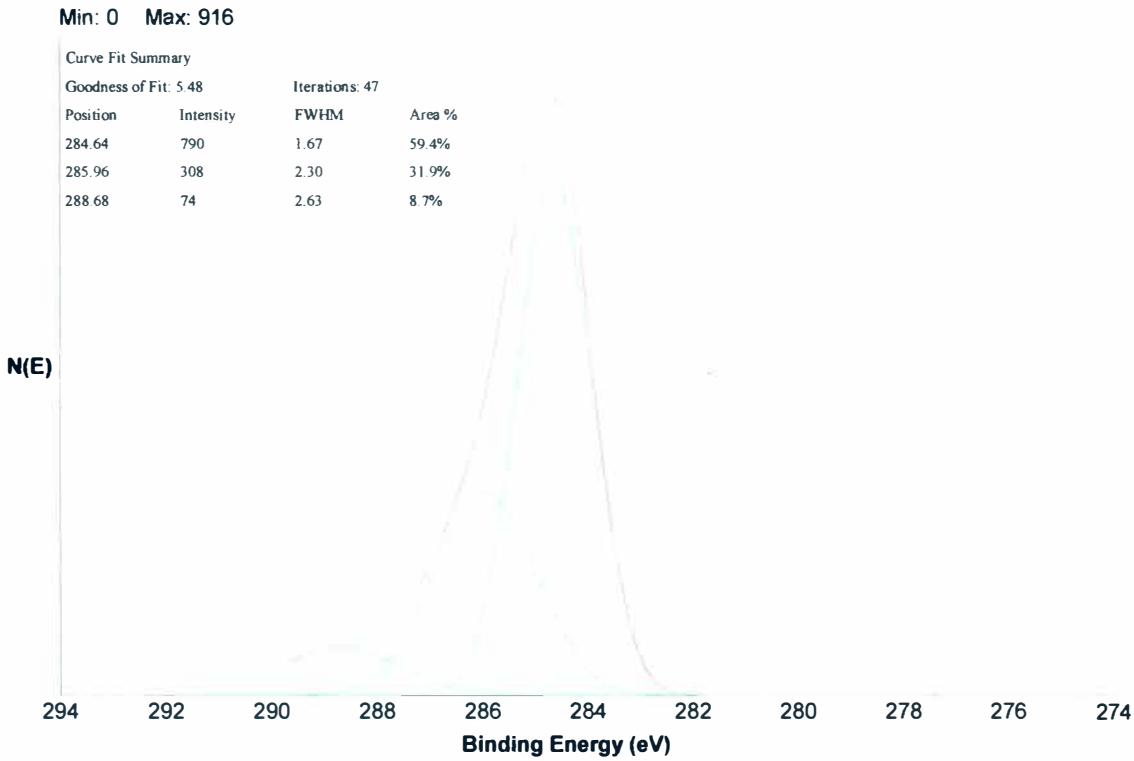

Figure B-51. Ti-2Months Sample after 10 Minutes Bombardment, C 1s

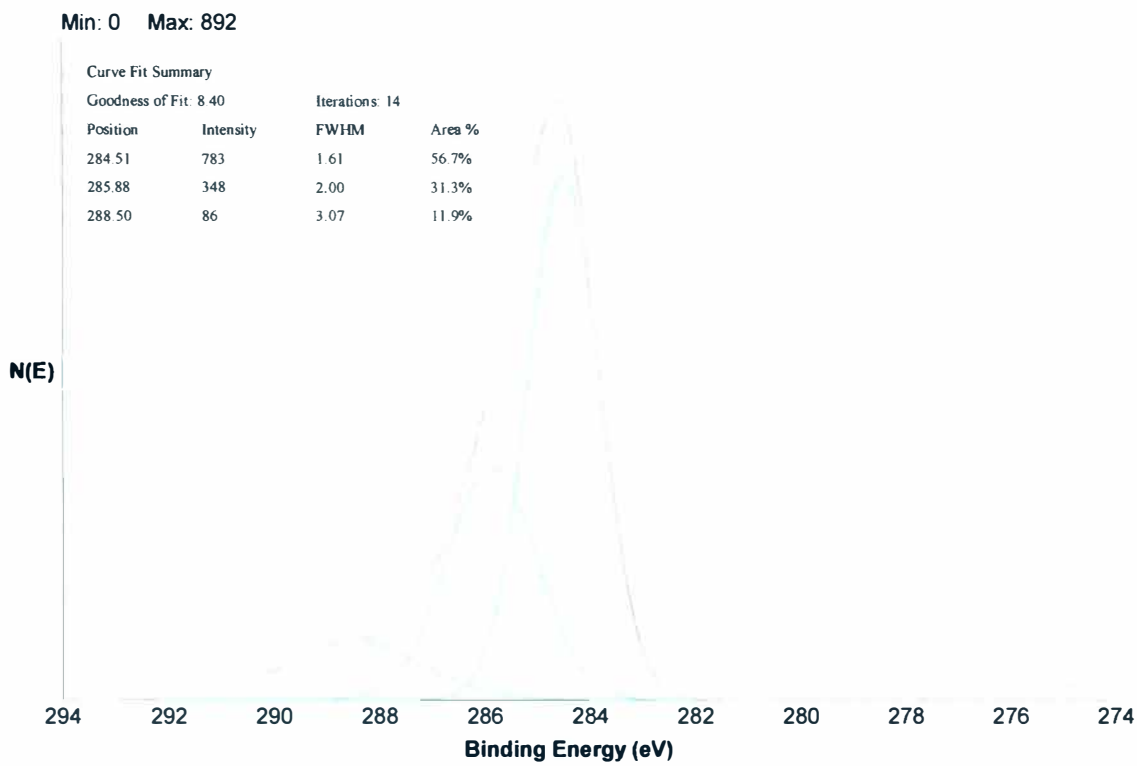

Figure B-52. Ti-2Months Sample after 20 Minutes Bombardment, C 1s

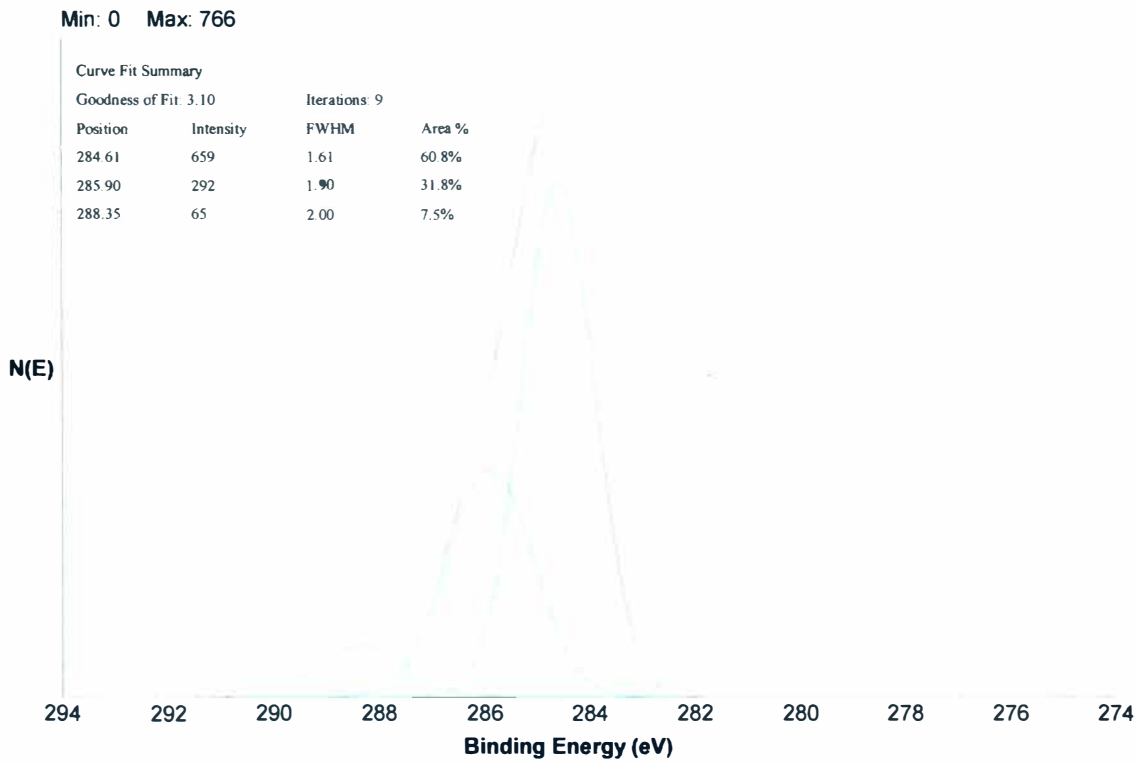

Figure B-53. Ti-2Months Sample after 30 Minutes Bombardment, C 1s

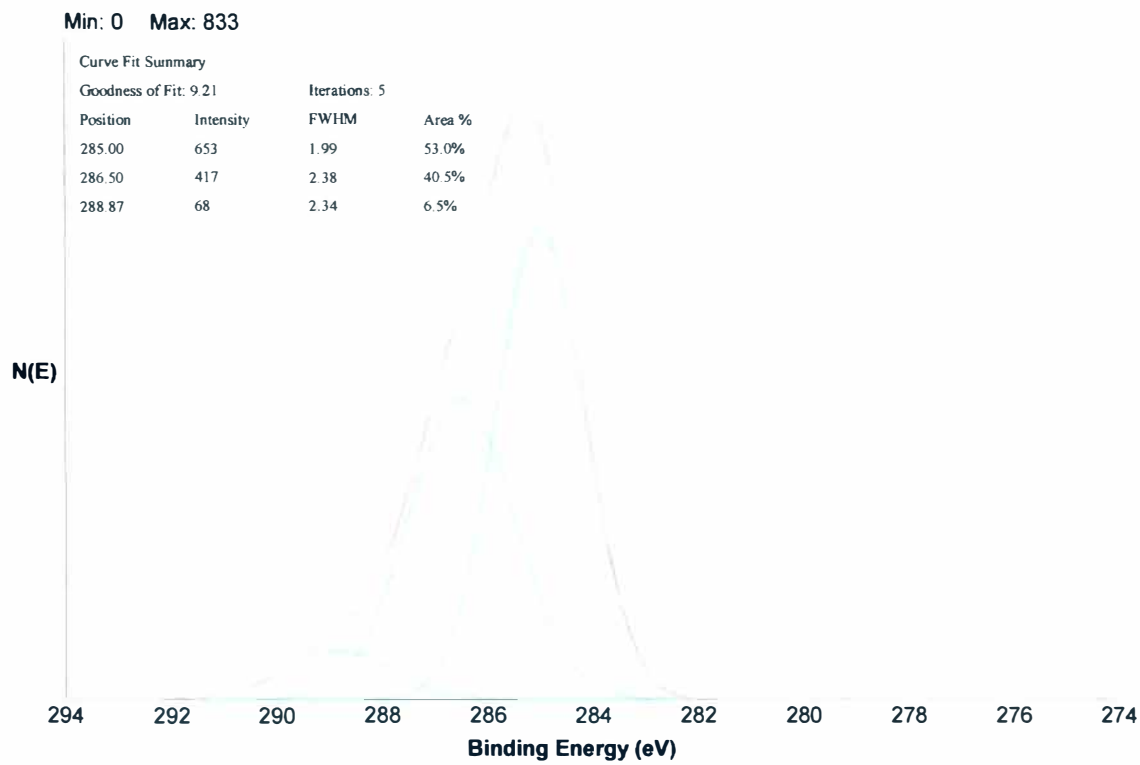

Figure B-54. Ti-3Months Sample after 30 Seconds Bombardment, C 1s

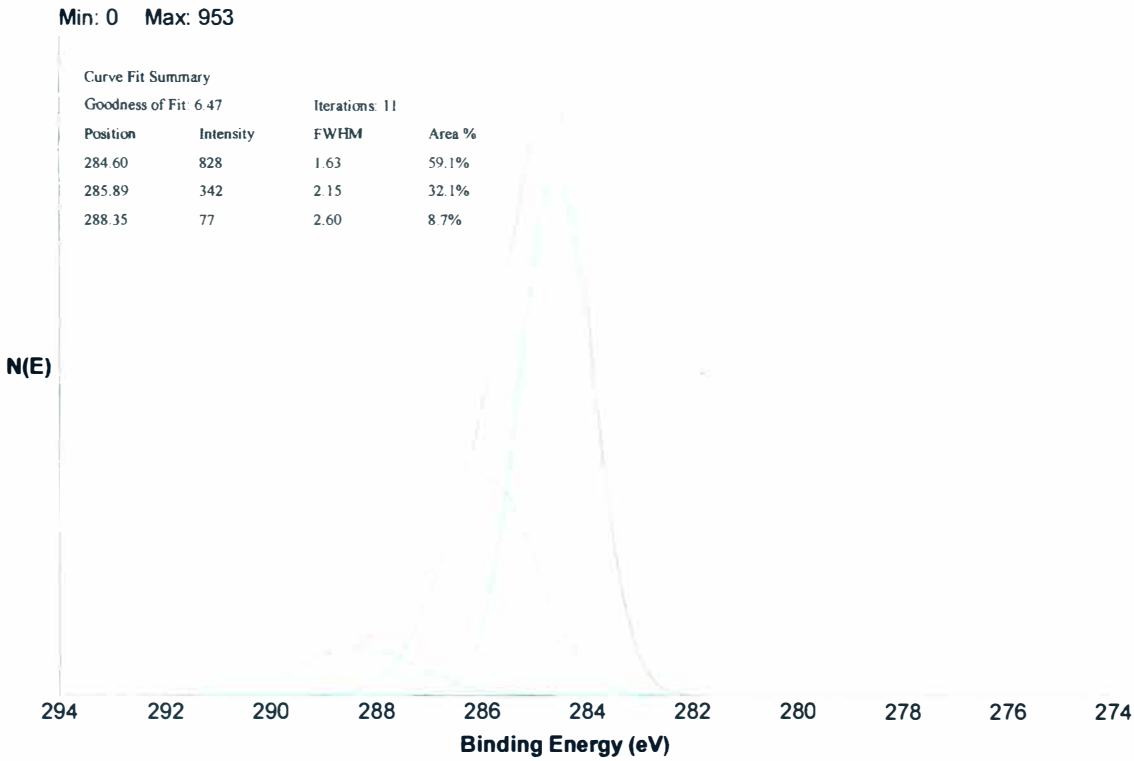

Figure B-55 Ti-3Months Sample after 10 Minute Bombardment, C 1s

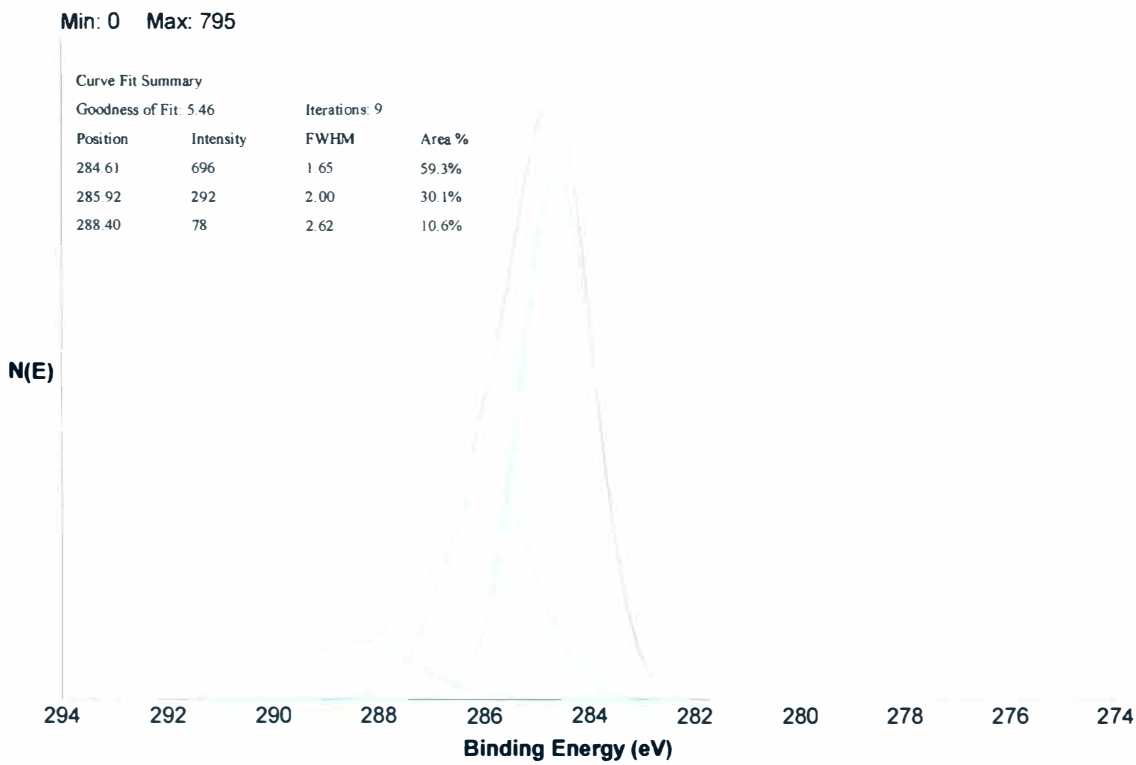

Figure B-56. Ti-3Months Sample after 20 Minute Bombardment, C 1s

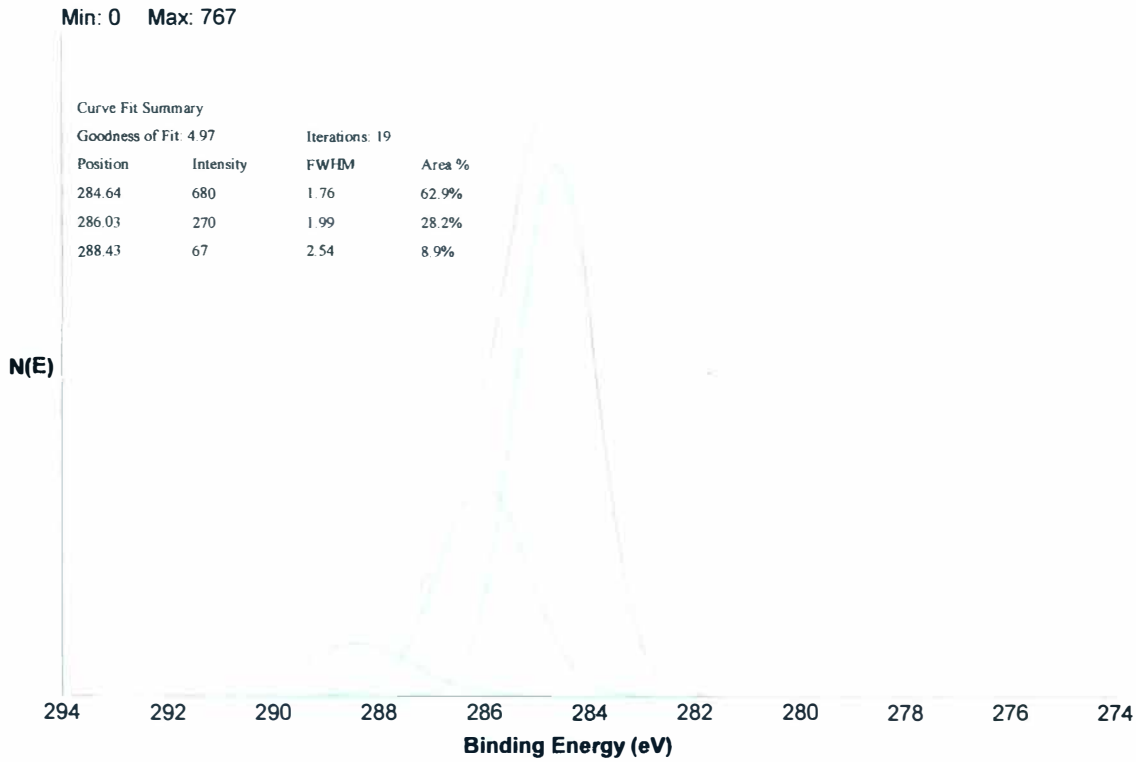

Figure B-57. Ti-3Months Sample after 30 Minutes Bombardment, C 1s

REFERENCES

1. Norma L., Hernandez de Gatica, Gary L. Jones and Joseph A. Gardella, Jr., "*Surface characterization of titanium alloys sterilized for biomedical applications*", Applied Surface Science 68, pp. 107-121, 1993.

2. David Hill, "*Design Engineering of Biomaterials for Medical Devices*" United Kingdom, John Wiley & Sons, 1998

3. Brunette, D. M., Tengvall, P., Textor, M., Thomsen, P., "*Titanium in Medicine*" New York, Springer, 2001.

4. MDA web page, http://www.medical-devices.gov.uk

5. M. Ask, J. Lausmaa, B. Kasemo, "*Preparation and surface spectroscopic characterization of oxide films on Ti6Al4V*", Applied Surface Science 35, pp. 283-301, 1988-89.

6. Helsen, J. A and Breme, H. J., "*Metals as Biomaterials*", West Sussex, England, John Wiley & Sons Ltd., 1998.

7. B. P. Bannon and E. E. Mild, "*Titanium Alloys for Biomaterial Application: An Overview*", American Society for Testing and Materials, pp. 7-15, 1983.

8. Gil, M. H., Mariz, M., Duarte, M. G., "*Polymeric biomaterials as drug delivery systems*", Boletim de Biotecnologia, 72, pp13-19, 2002.

9. Yan, L., Leng, Y., Weng, L., "*Characterization of chemical inhomogeneity in plasma-sprayed hydroxyapatite coatings*", Biomaterials, 24, pp. 2585-2592, 2003.

10. Geesink, R. G. T., Groot, K. D., Klein, C. P. A. T., "*Bonding of bone to apatite-coated implants*", J. Bone Jt. Surg, 70-B, pp. 17-22, 1988.

11. Oonishi, H., Yamamoto, M., Ishimaru, H., Tsuji, E., Kushitani, S., Anon, M., Ukon, Y., "*The effect of hydroxyapatite coating on bone growth into porous titanium alloy implants*", J. Bone Jt. Surg, 71-B, pp. 21-216, 1989.

12. Feng, B., Chen, J. Y., Zhang, X. D., "*Calcium phosphate coating on titanium induced by phosphating*", Bioceramics, 13, pp. 167-170, 2000.

13. Stoch, A., Jastrzebki, W., Brozek, A., Stoch, J., Szaraniec, J., Trybalska, B., Kmita, G., "*FTIR absorption-reflection study of biomimetic growth of*

phosphates on titanium implants", Journal of Molecular Structure, 555, pp. 375-382, 2000.

14. Sloten, J. V., Labey, L., Audekercke, R. V., Van der Perre, G., " *Materials selection and design for orthopaedic implants with improved long-term performance*", Biomaterials, 19, pp 1455-1459, 1998.

15. Wen, H. B., de Wijn, J. R., Cui, F. Z., de Groot, K., "*Preparation of calcium phosphate coatings on titanium implant materials by simple chemistry*", Journal of Biomedical Materials Research, 41, pp. 227-236, 1998.

16. Casaletto, M. P., Ingo, G. M., Kaciulis, S., Mattogno, G., Pandolfi, L., Scavia, G., "*Surface studies of in vitro biocompatibility of titanium oxide coatings*", Applied Surface Science, 172, pp. 167-177, 2001.

17. Frauchiger, V. M., Schlottig, F., Gasser, B., Textor, M., "*Anodic plasma-chemical treatment of CP titanium surfaces for biomedical applications*", Biomaterials, 25, pp. 593-606, 2004.
18. E. Czarnowska, T. Wierzchon, A. Maranda-Niedbala, "*Properties of the surface layers on titanium alloy and their biocompatibility in in-vitro tests*", Journal of Materials Processing Technology, 92-93, pp. 190-194, 1999.

19. D. F. Williams, "*Titanium: epitome of biocompatibility or cause for concern*", Journal of Bone Jt. Surg, 76, pp. 348, 1994

20. T. Wierzchon, A. Fleszar, "*Properties of surface layers on titanium alloy produced by thermo-chemical treatments under glow discharge condition*", Surface Coatings Technology, 96, pp. 205-209, 1997.

21. Feng, B., Weng, J., Yang, B.C., Chen, J. Y., Zhao, J. Z., He, L., Qi, S. K., Zhang, X. D., "*Surface characterization of titanium and adsorption of bovine serum albumin*", Materials Characterization, 49, pp. 129-137.

22. Van Noort R., "*Titanium: the implant materials today*", Journal of Materials Science, 22, pp. 3801-3811, 1987.

23. Zhu, X., Chen, J., Scheideler, L., Reichl, R., Geis-Gerstorfer, J., "*Effects of topography and composition of titanium surface oxides on osteoblast responses*" article in press.

24. Casaletto, M. P., Ingo, G. M., Kaciulis, S., Mattogno, G., Pandolfi, L., Scavia, G., "*Surface studies of in vitro biocompatibility of titanium oxide coatings*", Applied Surface Science, 172, pp. 167-177, 2001.

25. Sundgren, J. E., Bodo, P., Lundstrom, I., "*Auger electron spectroscopic studies of the interface between human tissue and implants of titanium and stainless steel*", Journal of Colloid and Interface Science, 110, No.1, pp. 9-21, 1995.

26. Kurado, D., Hanawa, T., Hiromoto, S., Katada, Y., Asami, K., "*Characterization of the surface oxide film of nickel-free austenitic stainless steel lacated in simulated body environments*", Materials Transactions, 43, No. 12, pp. 3093-3099, 2002.

27. Lampin, M., Warocquier-Clerout, R., Legris, C., Degrange, M., Sigot-Luizard, M. F., "*Correlation between substratum roughness and wettability, cell adhesion and cell migration*", J. Biomed Mater Res, 36, pp. 99-108, 1997.

28. Lim, Y. J., Oshida, Y., Andres, C. J., Barco, M. T., "*Surface characterization of variously treated titanium materials*", Int J Oral Maxillofac Implants, 16, pp. 333-342, 2001.

29. Hille, G. H., "*Titanium for Surgical Implants*", Journal of Materials, Vol. 1, No.2, June, 1966, pp. 373-383.

30. Donachie, M. J., Jr., "*Titanium, A Technical Guide*" Second Edition, Ohio, ASM International, 2000.

31. Wise, D. L., Trantolo, D. J., Lewandrowski, K., Gresser, J. D., Cattaneo, M. V., Yaszemski, M. J., "*Biomaterials Engineering and Devices, Human Applications*" Vol 2, New Jersey, Humana Press, 2000.

32. Okazaki, Y., Tateishi, T., Ito, Y, "*Corrosion resistance of implant alloys in pseudo physiological solution and role of alloying elements in passive films*", Materials Transactions, JIM, 38, pp. 78-84, 1997.

33. Sundararajan, T., Kamachi Mudali, U., Nair, K. G. M., "*Surface characterization of electrochemically formed passive film on nitrogen ion implanted Ti6Al4V alloy*", Materials Transactions, JIM, 39, pp. 756-761, 1998.

34. Zitter H., Plenk H. Jr., "*The electrochemical behavior of metallic implant materials as an indicator of their biocompatibility*" Journal of Biomed Mater Res., 21, pp. 881–896, 1987.

35. Imam, M. A. and Fraker, A. C., "*Titanium Alloys as Implant Materials*" *Medical Applications of Titanium and Its Alloys: The Material and Biological Issues, ASTM STP 1272*, S. A. Brown and J. E. Lemons, American Society for Testing and Materials, West Conshohocken, PA, 1996.

36. Steinemann, S. G., "*Titanium-the material of choice", Periodontology 2000, 17, pp. 7-21, 1998.*

37. Seagle, S. R., Bartlo, L. J., "*Physical metallurgy and metallography of titanium alloys*", Metals Engineering Quarterly, Vol. 8, pp. 1-10, 1968.
38. Lyman, T. (Metals handbook committee), "*Metals Handbook, Properties and selection of metals*", 8th Edition, Vol. 1, 1961.

39. Pan, J., Thierry, D., Leygraf, C., "*Electrochemical and XPS studies of titanium for biomaterial applications with respect to the effect of hydrogen peroxide*", Journal of Biomedical Materials Research, 28, pp. 113-122, 1994.

40. Bothe, T. R., Beaton, L. E., Davenport, H. A., "*Reaction of bone to multiple metallic implants*" Sur Gynecol Obst., 71, pp. 598-602, 1940.

41. Lausmaa, J., "*Surface spectroscopic characterization of titanium implant materials*", Journal of Electron Spectroscopy and Related Phenomena, 81, pp. 343-361, 1996.

42. Hiromoto, S., Hanawa, T., Asami, K., "*Composition of surface oxide film of titanium with culturing murine fibroblast L929*", Biomaterials, 25, pp. 979-986, 2004.

43. Hanawa, T., Ota, M., "*Calcium phosphate naturally formed on titanium in electrolyte solution*", Biomaterials, 12, pp. 767-774, 1991.

44. Hanawa, T., Ota, M., "*Characterization of surface film formed on titanium in electrolyte using XPS*", Applied Surface Science, 55, pp. 269-276, 1992.

45. Healy K. E., Ducheyne, P. D., "*Hydration and preferential molecular adsorption on titanium in vitro*", Biomaterials, 13, pp. 553-561, 1992.

46. Kasemo, B., Lausmaa, J., "*Surface properties and processes of the biomaterial-tissue interface*", Materials Science and Engineering, C1, pp. 115-119, 1994.

47. Vaquila, I., Vergara, L. I., Passeggi Jr., M. C. G., Vidal, R. A., Ferron, J., "*Chemical Reactions at Surfaces: titanium oxidation*", Surface and Coating Technology, 122, pp. 67-71, 1999.

48. Kasemo, B., "*Biocompatibility of titanium implants: Surface science aspects*" J Prosthet Dent, 49, pp. 832, 1983.

49. McCafferty, E., Wightman, J. P., "*An X-ray photoelectron spectroscopy sputter profile study of the native air-formed oxide film on titanium*", Applied Surface Science, 143, pp. 92-100, 1999.

50. Cacciafesta, P., Hallam, K. R., Oyedepo, C. A., Humphris, A. D. L., Miles, M. J., Jandt, K. D., "*Characterization of ultraflat titanium oxide surfaces*", Chem. Mater., 14, pp. 777-789., 2002.

51. Kumar, M. P., Badrinarayanan, S., Sastry, M., "*Nanocrystalline TiO_2 studied by optical, FTIR and X-ray photoelectron spectroscopy: correlation to presence of surface states*", Thin Solid Films, 358, pp.122-130, 2000.

52. Milosev, I., Metikos-Hukovic, M., Strehblow, H.-H., "*Passive film on orthopaedic TiAlV alloy formed in physiological solution investigated by X-ray photoelectron spectroscopy*", Biomaterials 21, pp. 2103-2113, 2000.

53. Lide, D. R., "*Hand Book of Chemistry and Physics*", 77th Edition,CRC Press, London, 1996-1997.

54. Aarik, J., Aidla, A., Uustare, T., Sammelselg, V., "*Morphology and structure of TiO_2 thin films grown by atomic layer deposition*", Journal of Crystal Growth, 148, pp. 268-275, 1995.

55. Sitting, C., Textor, M., Spencer, N. D., Wieland, M., Vallotton, P. H., "*Surface characterization of implant materials CP Ti, Ti-6Al-7Nb, and Ti-6Al-4V with different parameters*", J. Mater. Sci., pp.35-46, 1999.

56. Browne, M., Gregson, P. J., "*Surface modification of titanium-alloy implants*", Biomaterials 15, 11, pp. 894-898, 1994.

57. Motte, F., Coddet, C., Sarrazin, P., Azzopardi, M., Besson, J., "*A comparitive study of the ozidation with water vapor of pure titanium and Ti-6Al-4V*", Oxidation of Metals, 10, pp. 113-126, 1976.

58. Schniedgen, M., Graart, P. C. J., Baretzky, B., Mittemiejer, E. J., "*The initial stages of oxidation of γ-TiAl: an X-ray photoelectron study*", Thin Solid Films 415, pp. 114-122, 2002.

59. Bearinger, J. P., Orme, C. A., Gilbert, J. L. "*Direct observation of hydration ot TiO_2 on Ti using electrochemical AFM: freely corroding versus potentiostatically help*", Surface Science, 491, pp. 370-387, 2001.

60. Healy, K. E., Ducheyne, P., "*Oxidation kinetics of titanium thin films in model physiologic environments*", Journal of Colloid and Interphase Science, 150, pp. 404-417, 1992.

61. Hanawa, T., Hiromoto, S., Asami, K., Okuno, O., Asaoka, K., "*Surface oxide films on titanium alloys regenerated in Hanks' solution*" Materials Transaction, 43, pp. 3000-3004, 2002.

62. Tengvall, P., Lundstrom, I., Sjoqvist, L., Elwing, H., Bjursten, L. M., "*Titanium-hydrogen peroxide interaction-model studies of the influence of the inflammatory response on titanium implants*", Biomaterials, 10, pp.166-175, 1989.

63. Lu,G., Bernasek, L., Schwartz, J., "*Oxidation of polycrystalline titanium surface by oxygen and water*", Surface Science, 458, pp. 80-90, 2000.

64. Aragob, P. J., Hulbert, S. F., "*Corrosion of Ti-6Al-4V in simulated body fluids and bovine plasma*", J. Biomed. Mater. Res., 6, pp-155-164, 1972.

65. Deligianni, D. D., Katsala, N., Ladas, S., Sotiropoulou, D., Amedee, J., Missirlis, Y. F., "*Effect of surface roughness of the titanium alloy Ti-6Al-4V on human bone marrow cell response and on protein adsorption*", Biomaterials, 22, pp. 1241-1251, 2001.

66. *Certificate of Analysis of Alpha Calf™ Fraction*, HyClone, A Prebio Company.

67. Watts, J. F., Wolstenholme, J., "*An Introduction to Surface Analysis by XPS and AES*", West Sussex, England, John Wiley & Sons, 2003.

68. Riviere, J. C., Myhra, S., "*Handbook of Surface and Interface Analysis*", New York, Marcel Dekker Inc., 1998.

69. Woodruff, D. P., Delchar, T. A., "*Modern techniques of surface science*", Cambridge, Cambridge University Press, 1989.

70. XPS Handbook, http://emalwww.engin.umich.edu/handbooks/pdfs/xps.pdf

71. Miller, M. K., "*Atom probe topography, analysis at the atomic level*", Oak Ridge National Laboratory, Tennessee, Kluwer Academic/Plenum Publishers, 2000.

72. Morant, C., Lopez, M. F., Gutierrez, A., Jimenez, J. A., "*AFM and SEM characterization of non-toxic vanadium-free Ti alloys used as biomaterials*", Applied Surface Science, 220, pp. 79-87, 2003.

73. Digital Instruments, "*Scanning Probe Microscopy Training Book*", Version 3.0, 2000.

74. Binning, G., Rohrer, H., Gerber, Ch., Weibel, E., "*Surface studies by scanning tunneling microscopy*", Phys. Rev. Lett, 49, pp. 57-61, 1982.

75. West, P., Starostina, N., "*Atomic Force Microscopy*", Advance Materials & Processes, vol. 162, i. 2, p. 35(3), 2004.

76. Smith, B., "*Infrared Spectral Interpretation, A Systematic Approach*", Boca Raton, CRC Press, 1998.

77. Smith, B., "*Fourier Transform Infrared Spectroscopy*", Boca Raton, CRC Press, 1995.

78. Xiao,Z., Su, L. Gu. N., Lu, Z. Wei, Y., "*The growth of TiO_2 thin films on mixed self-assembly monolayers from solution*", Thin Solid Films, 333, pp. 25-28, 1998.

79. BCA Protein Assay Kit Instructions, PIERCE number 23227. http://www.piercenet.com/files/ACF1719.pdf

80. Botha, S. J., "*Surface properties and bio-acceptability of Ti_2O_3 surfaces*", Materials Science and Engineering, A243, pp. 221-230, 1998.